The Thesis Committee for Ioannis Tsiapas
Certifies that this is the approved version of the following thesis:

Pore Pressure Response of Liquefiable Soil Treated with Prefabricated Vertical Drains: Experimental Observations and Numerical Predictions

APPROVED BY
SUPERVISING COMMITTEE:

Supervisor: _____
Ellen M. Rathje

_____
Chadi El Mohtar

Pore Pressure Response of Liquefiable Soil Treated with Prefabricated Vertical Drains: Experimental Observations and Numerical Predictions

by

Ioannis Tsiapas, Dipl.

Thesis

Presented to the Faculty of the Graduate School of

The University of Texas at Austin

in Partial Fulfillment

of the Requirements

for the Degree of

Master of Science in Engineering

The University of Texas at Austin

May, 2012

Acknowledgements

I would like to express my sincere gratitude to Dr. Ellen M. Rathje for her continuous guidance and cooperation. Without her constant support, her interest and the time she spent for me, I would not be able to complete this thesis. The last two years that I had to opportunity to work under her supervision, I gained valuable knowledge and inspiration for my career.

I would like to thank Dr. Chadi El Mohtar for reading my thesis and for his useful comments. In addition, I am very grateful for the knowledge I gained from my professors: Dr. Kenneth Stokoe II, Dr. Robert Gilbert, Dr. Jorge Zornberg, Dr. Lance Manuel and Dr. John Tassoulas. I want also to acknowledge the support of Rachelle Howell, who provided me with very essential information for my research.

I am feeling very lucky that, during my studies, I made two very good friends: George Zalachoris and Iraklis Koutrouvelis. Their support and "tolerance" the last two years were vital for me and I will be always grateful for that.

Last but not least, I would like to thank my parents Zikos Tsiapas and Georgia Kostara for their invaluable guidance and support. Without them, I would never be, in all terms, able to live this lifetime experience, to study at The University of Texas at Austin.

May 4, 2012

Abstract

Pore Pressure Response of Liquefiable Soil Treated with Prefabricated Vertical Drains: Experimental Observations and Numerical Predictions

Ioannis Tsiapas, M.S.E.

The University of Texas at Austin, 2012

Supervisor: Ellen M. Rathje

Prefabricated vertical drains represent a soil improvement technique that achieves liquefaction mitigation by decreasing the drainage path length and hence expediting the dissipation of excess pore pressures. When evaluating the required spacing between vertical drains to achieve the desired reduction in pore pressure response, simplified design charts or more sophisticated finite element analyses are used to predict the pore pressure response. These charts and programs have not been evaluated in terms of their accuracy because there exists little data with which to compare the numerical predictions. More recently, the effectiveness of prefabricated vertical drains for liquefaction mitigation has been evaluated via small – scale centrifuge testing performed on untreated soil deposits and on soil deposits treated with vertical drains. In particular, the performance of the soil deposits subjected to sinusoidal motions and actual earthquake recordings was tested.

The main goal of this research is to compare the experimental observations of pore pressure response from the centrifuge experiments with the numerical predictions. The comparison focuses on the average excess pore pressure ratio ($r_{u,avg}$) that was developed in the location of a vertical pore pressure array in both the untreated and drain – treated sides of the models. In parallel, a parametric study is performed for the numerical predictions in order to study the effect of each input parameter that influences the pore pressure prediction, namely the effect of soil properties, ground motion characteristics and drain parameters.

The numerical predictions are found to provide reliable predictions of the pore pressure response despite the simplicity of the constitutive model employed. The numerical predictions of $r_{u,avg}$ time – histories are generally in good agreement with the recorded values in the centrifuge experiments. In most of the cases, the numerical model managed to predict the same maximum average excess pore pressure ratio, which is the parameter that is used in drain design. To incorporate any uncertainty on the soil properties or on the characteristics of shaking, the use of a smaller pore pressure threshold for drain design is recommended.

Table of Contents

List of Tables

List of Figures

Chapter 1

Introduction

1.1 Research Significance

Liquefaction is a phenomenon that can occur in saturated, loose granular soils subjected to rapid cyclic loading (e.g. earthquake shaking). Despite the relatively high hydraulic conductivity of granular soils, earthquakes induce an undrained type of loading due to the short duration of shaking and hence excess pore pressures are developed. Loose soils typically tend to compress when loaded (contractive behavior), which results in the development of positive excess pore pressures. As the total stresses are not altered by the earthquake shaking, the increase in pore pressure will cause a decrease in effective stresses and hence a reduction in the shear strength and stiffness of the soil. In the case that the pore pressure becomes equal to the total vertical stress, the effective stress drop to zero and liquefaction occurs.

Liquefaction damage can occur either during the earthquake shaking or after it ends, when the excess pore pressures are dissipated. The total reduction of effective stresses to zero is not required for liquefaction damage to occur, as the development of significant pore pressures can also have devastating results. The consequences of liquefaction include sand ejecta, loss of bearing capacity, vertical settlements, lateral spreading, floating of buried structures, retaining wall failures, ground oscillations and stability failures in level-ground sites. The first

documentation of extensive liquefaction damage in man-made structures occurred in the Niigata earthquake (Japan, 1964) and since then liquefaction is considered to be one of the most important phenomena in geotechnical earthquake engineering. Severe liquefaction damage has occurred in almost every large earthquake, including the Loma Prieta earthquake (USA, 1989), Kobe earthquake (Japan, 1995), Kocaeli earthquake (Turkey, 1999), Canterbury earthquake (New Zealand, 2010) and Tohoku earthquake (Japan, 2011).

To prevent earthquake induced liquefaction, engineers rely on a wide range of soil improvement techniques that focus either on increasing the soil's strength and stiffness (i.e. densification, soil mixing and reinforcement techniques) or accelerating the excess pore pressure dissipation (i.e. drainage techniques). Many soil improvement methods, such as vertical drains, can achieve both faster dissipation and improved soil properties. Vertical drains prevent liquefaction by decreasing the drainage path length and hence expediting the dissipation of excess pore pressures. The design of vertical drains focuses on selecting a drain spacing that keeps the excess pore pressures below a threshold value. Gravel drains are a common type of vertical drain and they have the added advantage of densifying the surrounding soil during the installation process. However, the long – term drainage capacity of gravel drains is limited due to soil clogging in the gravel voids.

Prefabricated vertical drains are a new type of vertical drains which consist of a perforated plastic pipe encased in a geosynthetic fabric. The presence of the geosynthetic fabric prevents clogging and guarantees satisfactory drainage capacity in long – term conditions. However, prefabricated vertical drains provide limited densification of the surrounding soil during installation and hence engineers rely mainly on their drainage benefits. The effectiveness of prefabricated vertical drains

for liquefaction mitigation has been recently evaluated via small – scale centrifuge testing performed on untreated soil deposits and on soil deposits treated with vertical drains. In particular, their performance in soil deposits subjected to sinusoidal motions and actual earthquake recordings was tested by Marinucci et al. (2008) and Howell (2008) respectively.

The main goal of this research is to compare the experimental results of Marinucci et al. (2008) and Howell (2008) with the numerical predictions of the finite element program "FEQDrain" developed by Pestana et al. (1997).

1.2 Organization of the Thesis

This thesis is organized into six chapters:

Chapter 1 discusses the significance of the research and outlines the thesis.

Chapter 2 provides the required theoretical background and describes the program FEQDrain, the most common numerical code used in drain design. The prediction of pore pressure response in drain – treated sites using design charts is also discussed.

Chapter 3 investigates the effect of model parameters on developed excess pore pressure for treated and untreated sites.

Chapter 4 presents the comparison between the numerical results and the experimental data of the centrifuge tests of Marinucci et al. (2008), concerning untreated and treated with PVDs soil deposits subjected to sinusoidal motions.

Chapter 5 compares the experimental results of the centrifuge test, conducted by Howell (2008), on untreated and treated with PVDs soil deposits subjected to actual ground motion recordings with the numerical predictions.

Chapter 6 provides a summary of the main points along with the conclusions of the work.

Chapter 2

Theoretical Predictions of Pore Pressure Response

2.1 Introduction

Liquefaction mitigation can be achieved by a wide range of soil improvement techniques. These techniques can be organized in four major categories depending on the mechanism of improvement: (1) densification, (2) drainage, (3) mixing, and (4) reinforcement. As for drainage, the conventional technique involves the installation of gravel drains, typically 0.80m – 1.20m in diameter. The shorter drainage distances introduced by lateral drainage to the drains along with the larger hydraulic conductivity of gravel than the liquefiable sand imply that the excess pore water pressure will dissipate quickly relative to the rate of pore pressure generation, and hence liquefaction will be prevented. An additional advantage of gravel drains is the densification of the surrounding soil that is achieved during the installation process. However, the long-term performance of a gravel drain is restricted by the clogging of the sand in the voids of gravel, which reduces the hydraulic conductivity of the drain and slows down the dissipation of pore pressures. For this reason, recently there has been new interest in using prefabricated vertical drains as a drainage soil improvement technique, even though the additional benefits from densification are limited.

The success of a drainage system relies on the determination of the appropriate drain spacing so that the excess pore pressures will be dissipated

adequately during earthquake shaking. This chapter discusses the most common analytical and numerical methodologies that are used in practice for the prediction of pore pressure response in the case of radial drainage and the adequate drain design in order to achieve liquefaction mitigation.

2.2 Chart Solutions

Seed and Booker (1977) were the first who proposed an analytical method for the evaluation of radial drainage on earthquake induced excess pore pressures, for the case of drain-treated uniform ground. It was assumed that the gravel drains, which have diameter of "2a", are equally spaced in a center-to-center distance of "2b" and have infinitely large permeability (Figure 2.1). Analyses are performed for a unit cell that represents the zone of influence around a single drain.

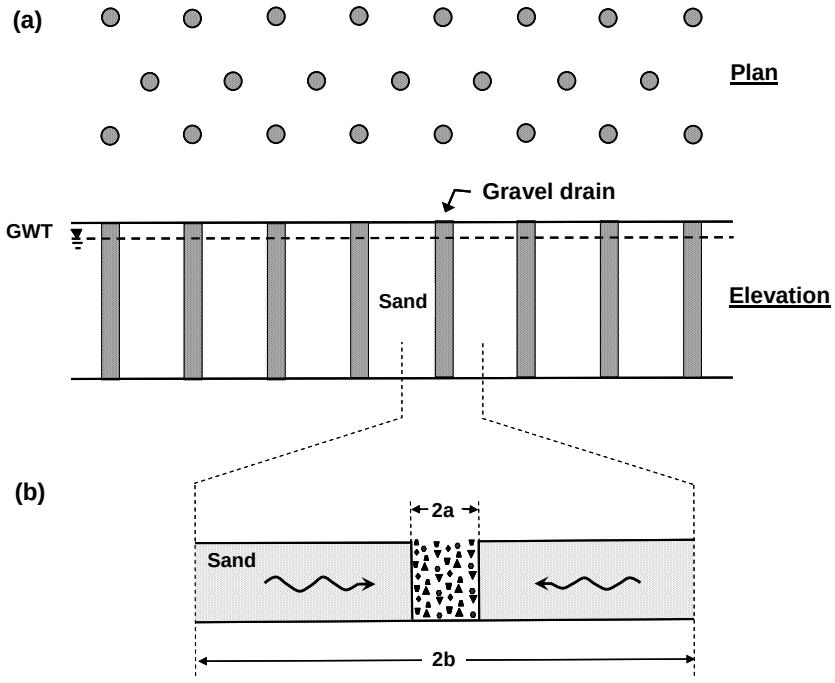

Figure 2.1: (a) Arrangement of gravel drain system, (b) Gravel drain with radial drainage only (Seed and Booker, 1977)

Assuming that the flow of the pore water is governed by Darcy's Law, Seed and Booker (1977) expressed the continuity of flow through the ground using:

$$\frac{\partial}{\partial x}\left(\frac{k_h}{\gamma_w}\frac{\partial u}{\partial x}\right)+\frac{\partial}{\partial y}\left(\frac{k_h}{\gamma_w}\frac{\partial u}{\partial y}\right)+\frac{\partial}{\partial z}\left(\frac{k_v}{\gamma_w}\frac{\partial u}{\partial z}\right)=\frac{\partial \varepsilon}{\partial t} \tag{2.1}$$

where u is the excess pore pressure, k_v and k_h are the hydraulic conductivity in the vertical and the horizontal direction respectively, γ_w is the unit weight of water and ε is the volumetric strain. Neglecting the change in bulk stress, the volume change ($d\varepsilon$) of a soil element in time dt is related to the change in the pore water pressure (du) of the element in the same time by the coefficient of volumetric compressibility (m_{v3}). In the same period of time (dt) the pore pressure are also increased due to the dt earthquake cycles of alternating shear stress.

$$d\varepsilon = m_{v3}\left(du-\frac{\partial u_g}{\partial N}dN\right) \tag{2.2}$$

where u_g is the pore pressure generated by the seismic loading. Seed and Booker (1977) assumed that m_{v3} is constant and that the drainage is purely radial (no vertical flow: $\partial u/\partial z$ = 0). Taking into account these assumptions and combining Equations 2.1 and 2.2, the dissipation of earthquake induced excess pore pressure in drain-treated ground is described by the Equation 2.3:

$$\frac{k_h}{\gamma_w m_{v3}}\left(\frac{\partial^2 u}{\partial r^2}+\frac{1}{r}\frac{\partial u}{\partial r}\right)=\frac{\partial u}{\partial t}-\frac{\partial u_g}{\partial N}\frac{\partial N}{\partial t} \tag{2.3}$$

The term $\partial N/\partial t$ is assumed to be equal to an equivalent number of uniform stress cycles (N_{EQ}) occurring during the time of earthquake shaking (t_d):

$$\frac{\partial N}{\partial t}=\frac{N_{EQ}}{t_d} \tag{2.4}$$

To evaluate the rate of pore pressure generation ($\partial u_g/\partial N$), the pore pressure generation function of Seed et al. (1975) was adopted. Based on the results of both cyclic triaxial tests (Lee and Albaisa, 1974) and cyclic simple shear tests (De Alba et al., 1975), Seed et al. (1975) found that u_g can be expressed as a function of the cyclic ratio N/N_L, where N_L is the number of cycles required to cause liquefaction:

$$\frac{u_g}{\sigma_0'} = \frac{2}{\pi}\sin^{-1}\left(\frac{N}{N_L}\right)^{1/2A} \tag{2.5}$$

The term σ'_0 represents the initial vertical effective stress, while "A" is an empirical constant that controls the shape of the curve. Seed and Booker (1977) found that the value A = 0.7 is in good agreement for most experimental data, as presented in Figure 2.2 for the tests of De Alba et al. (1975), and this value is adopted in their charts.

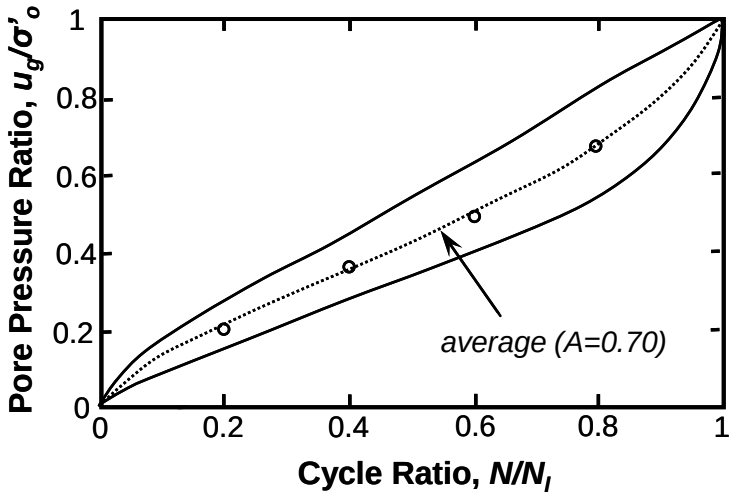

Figure 2.2: Rate of excess pore pressure build-up in cyclic simple shear tests (De Alba et al, 1975)

Equation (2.5) represents the earthquake induced excess pore water pressures in terms of an excess pore pressure ratio ($r_u = u/\sigma_0'$), where r_u = 1.0

indicates initial liquefaction and a condition of zero effective stress. The level of r_u generated in drain-treated ground during an earthquake is a function of three parameters: (i) the gravel drain spacing ratio a/b, (ii) the ratio N_{EQ}/N_L, which represents the intensity of earthquake shaking relative to the liquefaction resistance of the soil and (iii) the dimensionless time factor T_{ad}, which relates the duration of shaking to the consolidation properties of the sand using:

$$T_{ad} = \frac{k \cdot t_d}{m_{v3}\gamma_w a^2} \tag{2.6}$$

Seed and Booker (1977) performed a parametric study in which they computed the pore pressure field around a drain for different input parameters. The results of the parametric study were portrayed in various design charts. Figure 2.3 shows the developed design charts that relate the spacing ratio (a/b) with the maximum r_u in any location and at any time (r_g in the charts) for different values of the time factor T_{ad} and for N_{EQ}/N_L = 1 – 4. The design charts in Figure 2.3 indicate that the induced r_g increases as the spacing ratio (a/b) decreases (i.e., the drain spacing, b, increases for a constant drain radius, a), the time factor T_{ad} decreases, and the cycle ratio N_{EQ}/N_L increases. Large values of drain spacing indicate a longer drainage distance, which leads to larger pore pressures. Smaller values of T_{ad} indicate that the permeability of the soil (k) is smaller, the compressibility of the soil (m_v) is larger, or the duration of shaking (t_d) is shorter, all of which decrease the rate of pore pressure dissipation. Large values of N_{EQ}/N_L indicate a more liquefiable condition (i.e. smaller factor of safety against liquefaction), which leads to larger pore pressures. Seed and Booker (1977) also developed design charts in terms of the maximum average (over space) r_u at any time ($\overline{r_g}$ in the charts) for the same T_{ad} and N_{EQ}/N_L values (Figure 2.4). Values of $\overline{r_g}$ better represent the overall pore

pressure field within the unit cell surrounding the drain. The design charts can be used to specify an appropriate spacing ratio that maintains $\overline{r_g}$ below a design threshold (e.g., 0.5) for a given T_{ad} and N_{EQ}/N_L.

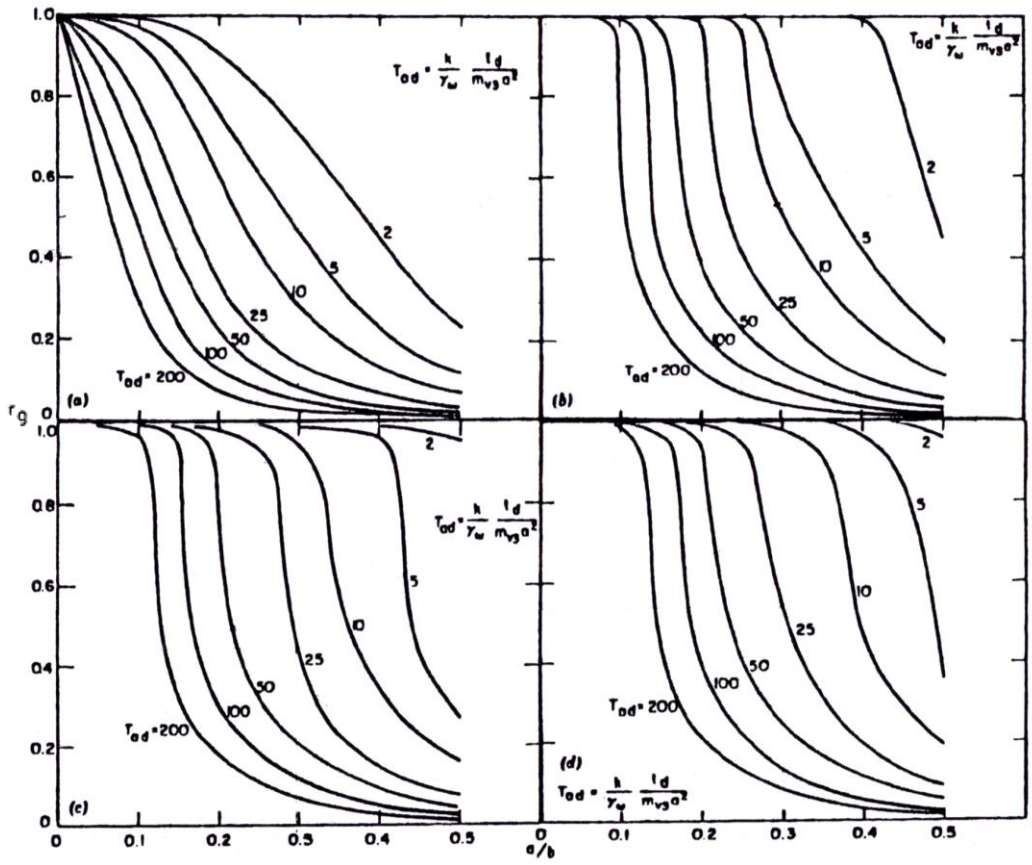

Figure 2.3: Maximum pore pressure ratio versus drain spacing a/b for (a) N_{EQ}/N_L=1, (b) N_{EQ}/N_L=2, (c) N_{EQ}/N_L=3, (d) N_{EQ}/N_L=4 (Seed and Booker, 1977)

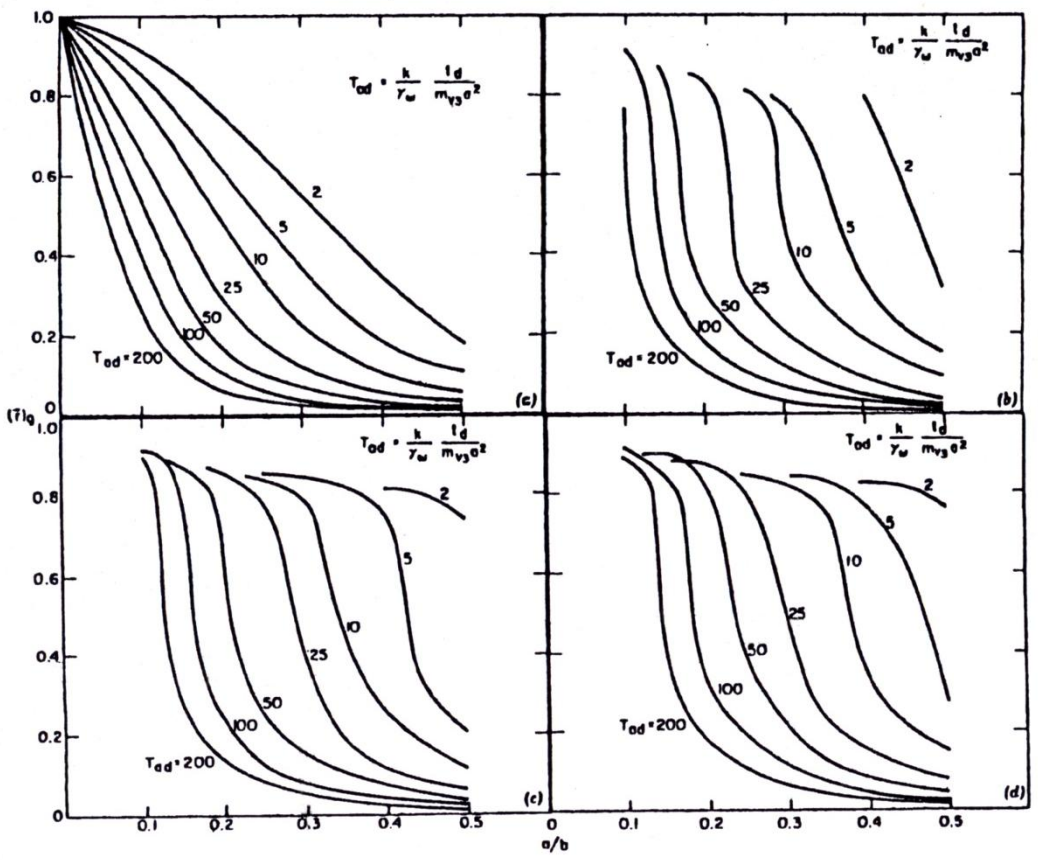

Figure 2.4: Maximum average pore pressure ratio versus drain spacing a/b for (a) N_{EQ}/N_L=1, (b) N_{EQ}/N_L=2, (c) N_{EQ}/N_L=3, (d) N_{EQ}/N_L=4 (Seed and Booker, 1977)

The approach of Seed and Booker (1977) is based on major assumptions regarding the type of drainage, the material properties and the buildup of excess pore pressure. The proposed method considers only radial drainage, neglecting thus any beneficial effect of the vertical drainage. As for the permeability of the drain (k_{dr}), Seed and Booker (1977) found that when $k_{dr}/k > 200$ it is reasonable to assume that is infinite, which means that there is no excess pore pressure inside the drain. Additionally, the coefficient of compressibility (m_{v3}) was considered to be constant regardless of the increase in r_u. As proved by the experimental results of

Lee and Albaisa (1974), the coefficient of compressibility is constant for small values of r_u and then it increases exponentially with increasing pore pressure ratio (Figure 2.5). Keeping in mind that the design values of r_u do not usually exceed 0.5, the increase in m_v is negligible and hence this assumption is reasonable. Finally, the generation of excess pore pressure is based on Equation 2.5, which is empirically based on laboratory tests, and the exponent A is regarded as constant and equal to 0.70. Recent experimental results and numerical studies (Bouckovalas et al, 2011) indicated that 0.70 is not a representative value for most of the ground materials and the value of A must be considered as an additional variable to the problem.

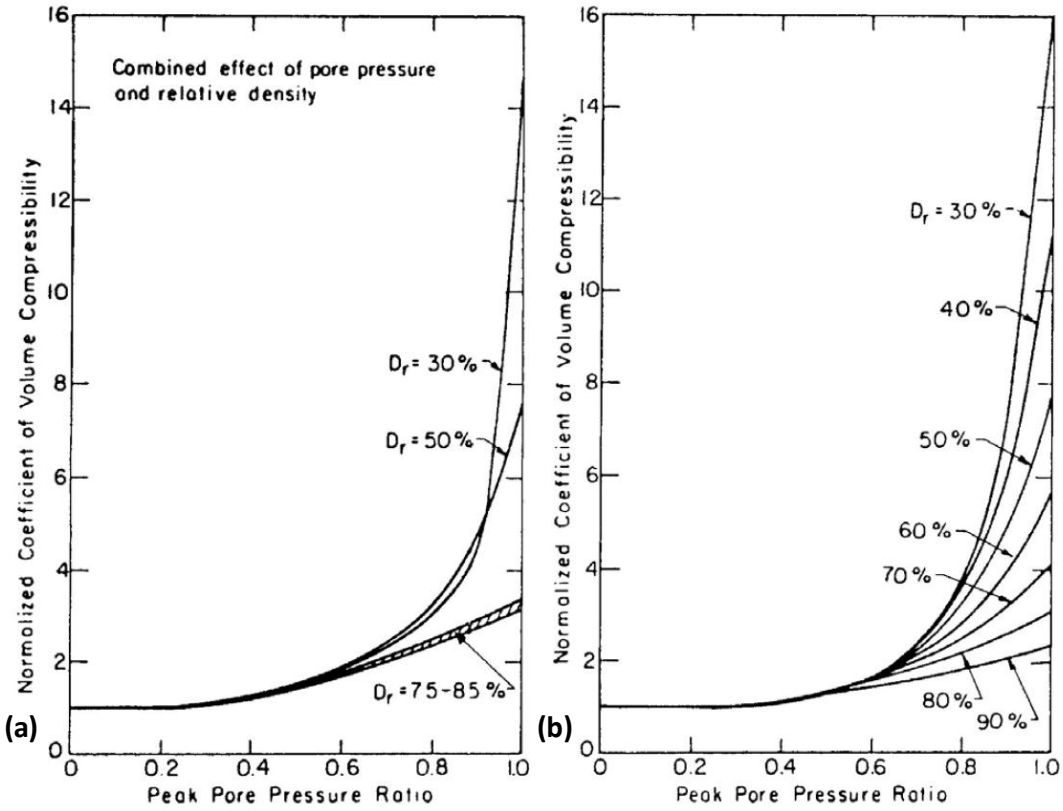

Figure 2.5: (a) Measured m_v values of saturated sands versus r_u (Lee and Albaisa, 1974), (b) theoretical relationships between m_v and r_u (Seed et al., 1975)

Onoue (1988) examined the effect of the permeability of the gravel drain ("well resistance") on the radial dissipation of earthquake induced excess pore pressures. To evaluate this effect, Onoue et al. (1987) performed in-situ experiments on gravel drains of 300 – 500 mm diameter (d_w) and 11m length (H), surrounded by liquefiable sand deposits. The predicted $r_{u,max}$ values from Seed and Booker (1977) were significantly smaller than the values measured in the experiments (Figure 2.6). Consequently, Onoue et al. (1987) concluded that the effect of the well resistance on the dissipation rate of excess pore pressures cannot be neglected.

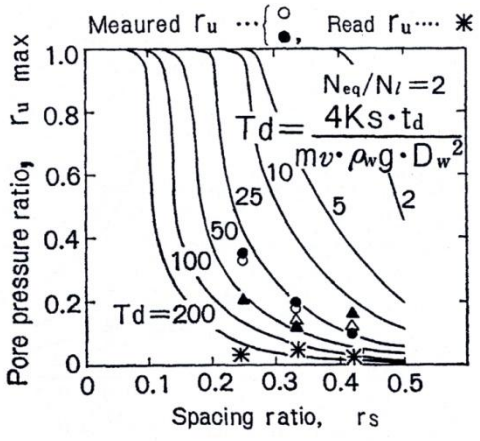

Figure 2.6: Comparison between the design charts proposed by Seed and Booker (1977) and the experimental results (Onoue, 1988)

To deal with the variance of the well resistance, Onoue (1988) inserted in the basic equations of Seed and Booker (1977) an additional continuity condition along the drain perimeter:

$$\left(\frac{\partial u}{\partial r}\right)_{r=r_w} + \frac{r_w}{2}\frac{k_w}{k_s}\left(\frac{\partial^2 u}{\partial z^2}\right)_{r=r_w} = 0 \qquad (2.7)$$

where r_w the well radius, k_s and k_w are the hydraulic conductivities of the soil and the well (i.e., drain), respectively. Differences in vertical and horizontal hydraulic

conductivities were not modeled. The boundary conditions of the developed model are presented in Figure 2.7. Based on this model, Onoue (1988) provided revised predictions of the maximum average r_u ($\bar{r}_{u,max}$, which is the same as $\overline{r_g}$ from Seed and Booker 1977), in which the finite permeability of the drain is incorporated via the dimensionless coefficient of well resistance L_w:

$$L_w = \frac{32}{\pi^2}\frac{k_s}{k_w}\left(\frac{H}{d_w}\right)^2 \tag{2.8}$$

The experimental results of Onoue et al. (1987), are in good agreement with the analytical predictions of $\bar{r}_{u,max}$ based on the model of Onoue (1988), which proves the improvement of the revised approach (Figure 2.8). Additionally, the analytical predictions indicated the effect of the vertical drainage on the dissipation of excess pore pressure. More specific, for N_{EQ}/N_L = 1 the assumption of both vertical and radial flow through the ground affects considerably the developed r_u whereas there is practically no effect for $N_{EQ}/N_L \geq 2$.

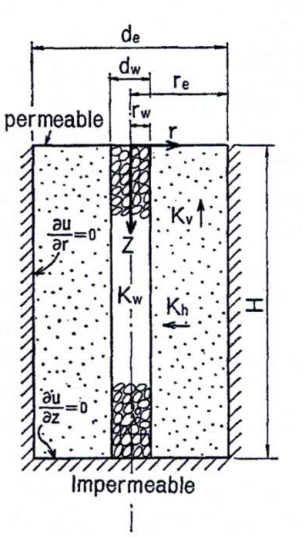

Figure 2.7: Drain well and boundary conditions (Onoue, 1988)

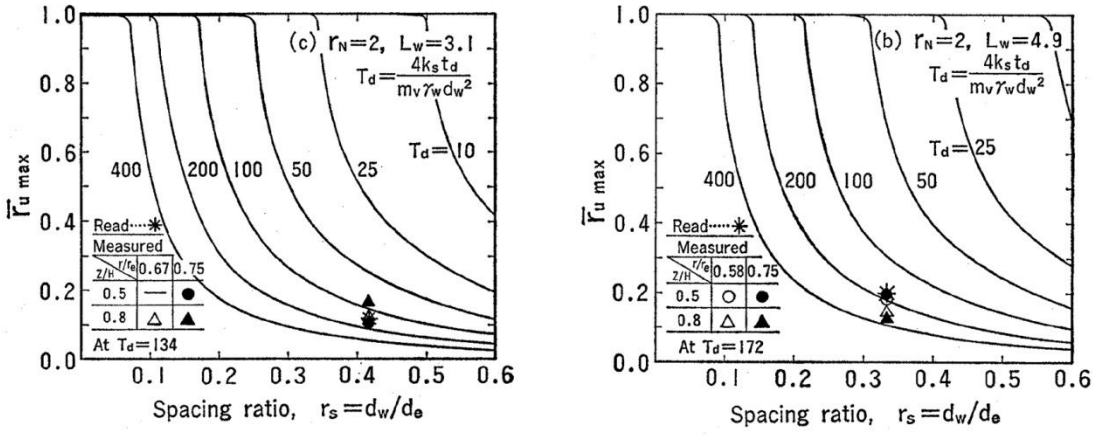

Figure 2.8: Relationship between spacing ratio and maximum $\bar{r}_{u,max}$ (Onoue, 1988)

Finally, Onoue (1988) proposed revised design charts, which relate the spacing ratio $r_s = r_w/r_e$ (same as a/b) with the coefficient of well resistance L_w and the time factor T_d for a specific design value of $\bar{r}_{u,max}$ (0.3, 0.4, 0.5 and 0.6) and for N_{EQ}/N_L = 1 – 4. The time factor T_d is equivalent to T_{ad} and is given by:

$$T_d = \frac{4k_s t_d}{m_v \gamma_w d_w^2} \tag{2.9}$$

The resulting design charts are shown in Figure 2.9 for N_{EQ}/N_L = 1 – 4 and they take into account the effect of the vertical drainage through the ground in the dissipation of excess pore pressure. Alternatively, when vertical drainage is ignored, the design chart of Figure 2.10 can be used, which is valid for N_{EQ}/N_L = 1, as there is no difference when $N_{EQ}/N_L \geq 2$. The design charts indicate that an increase in the coefficient of well resistance leads to an increase in the required spacing ratio (i.e., smaller spacing) in order to achieve the desired design value of $\bar{r}_{u,max}$.

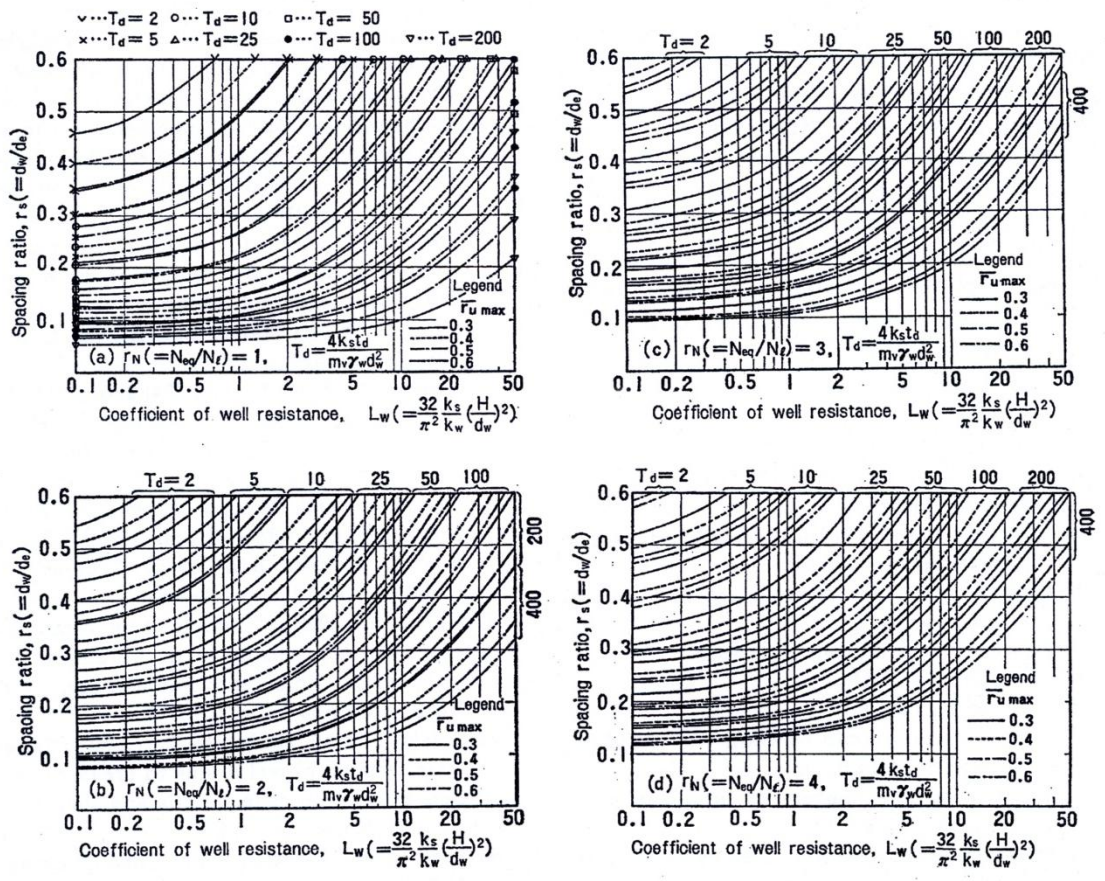

Figure 2.9: Relationship between coefficient of well resistance and spacing ratio for (a) N_{EQ}/N_L=1, (b) N_{EQ}/N_L=2, (c) N_{EQ}/N_L=3, (d) N_{EQ}/N_L=4 (Onoue, 1988)

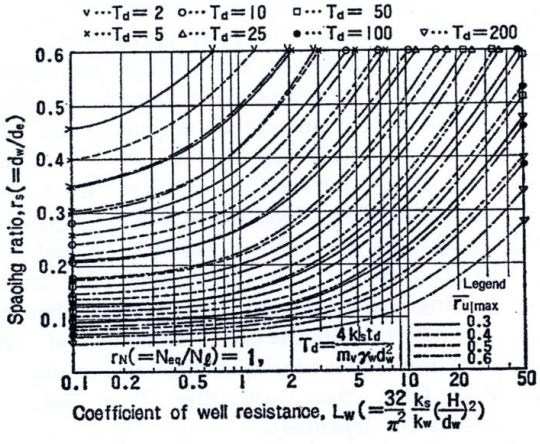

Figure 2.10: Relationship between coefficient of well resistance and spacing ratio for N_{EQ}/N_L=1 when the vertical drainage is ignored (Onoue, 1988)

Some issues arise when trying to apply chart solutions for gravel drains to the design of prefabricated vertical drains (PVD). PVDs consist of a hollow plastic pipe covered by a geotextile filter to prevent clogging (Figure 2.11). The prevention of clogging is an important advantage over gravel drains. The typical diameter of prefabricated vertical drains ranges from 75 mm to 100 mm and they are installed usually in a triangular pattern in a (center-to-center) distance of 1.2 m – 2 m. The simple installation process along with the improved drainage capacity favor the use of PVDs over gravel drains, despite the limited densification of the surrounding soil during the installation. Because of the small diameter of PVDs compared with gravel drains (7.5-10 cm vs. 80 to 120 cm), computed values of Tad and a/b for PVDs can be quite large and outside the range depicted on the design charts of Seed and Booker (1977) or Onoue (1988).

The Japanese Geotechnical Society (1998) proposed new design charts for prefabricated vertical drains based on the approaches of both Seed and Booker (1977) and Onoue (1988). The Japanese Geotechnical Society (JGS) incorporates the effect of well resistance by using a modified time factor T_d. The initial time factor (T_{d0}) is calculated using the same expression previously discussed (e.g., Equation 2.6) and then it is scaled by a correction factor "m" (Equation 2.10). The correction factor "m" is a function of the coefficient of well resistance L (L_w) and the spacing ratio (b/a), as shown graphically in Figure 2.12.

$$T_d = m \cdot T_{d0} \tag{2.10}$$

The new design charts (Figure 2.13) plot the maximum average r_u as a function of the ratio b/a for T_d = 200 – 3000 and for N_{EQ}/N_L 2 – 4. Note that the spacing ratio (a/b) of the previous charts in now inverted (b/a) in order to avoid

very small values of (a/b) for the small values of a for PVDs. According to JGS, it is preferable to select a spacing that keeps the maximum average r_u below 0.3. This threshold of 0.3 is larger than the value of 0.5 – 0.6 specified by previous researchers, and is recommended due to the sudden increase in r_u in the charts at around 0.3.

Figure 2.11: Prefabricated vertical drain covered with geotextile filter (Marinucci, 2010)

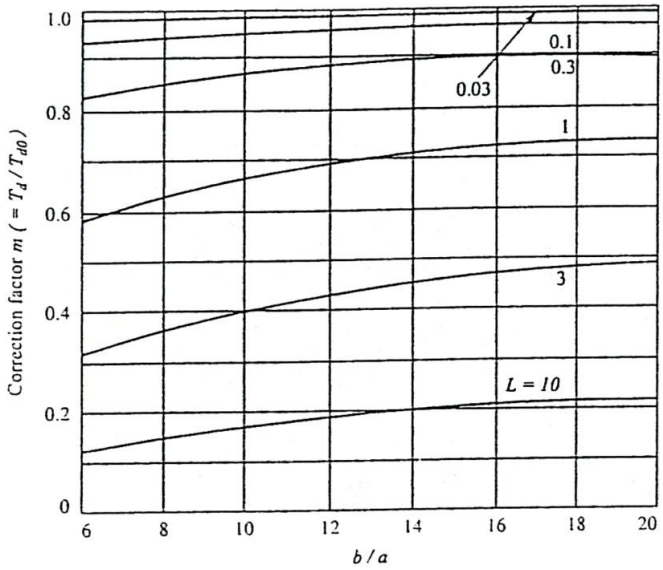

Figure 2.12: Correction factor m as a function of coverage ratio and well resistance (JGS, 1998)

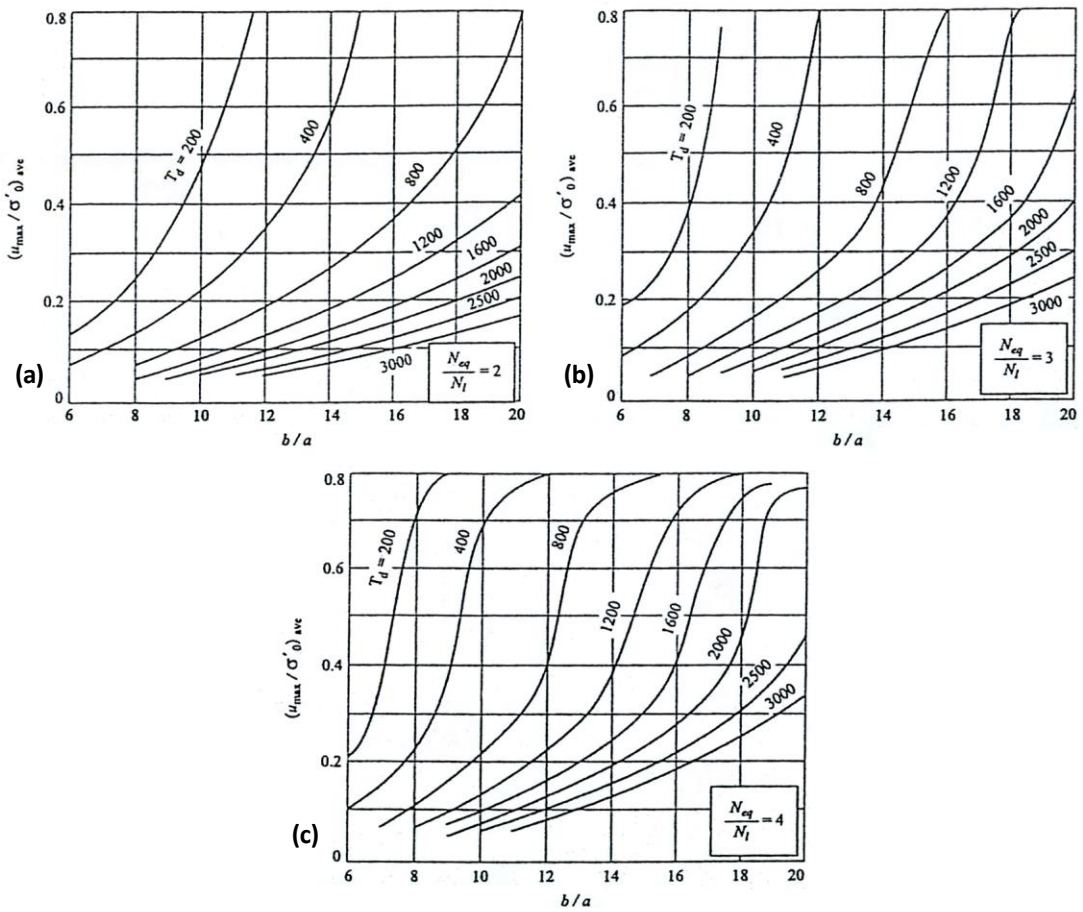

Figure 2.13: Maximum average pore pressure ratio for PVDs versus drain spacing when (a) N_{EQ}/N_L=2, (b) N_{EQ}/N_L=3, (c) N_{EQ}/N_L=4 (JGS, 1998)

2.3 Numerical Codes

Pestana et al. (1997) developed a finite element computer program, FEQDrain, to evaluate the performance of vertical drains for liquefaction mitigation. The program was mainly developed for the design of prefabricated vertical drains but it is capable of modeling four different types of drains:

a) no drains

b) "perfect" drains

c) equivalent granular drains

d) prefabricated vertical drains

Unlike chart solutions, FEQDrain incorporates layered soil profiles with different soil properties, simulates the flow from the ground to the drain and then to the surface in a more sophisticated way and provides the distribution of pore pressure at any point. Additionally, it considers the effect of the rise in the water level inside the drain due to the volume of water that is collected and fills, in most of the cases, the drain. When the groundwater table is not at the ground surface, there is a head inside and outside the drain, which results in the development of additional excess pore pressure.

Figure 2.14 shows a typical configuration along with the boundary conditions for the analysis of a vertical drain system in FEQDrain. The diameter of influence depends on the drain spacing and the shape of the installation mesh (triangular or square), as shown in Figure 2.15. FEQDrain models axisymmetric conditions and uses four–node element mesh. The discretization of the mesh is determined by the user. Typically, axial symmetry is considered for most drainage cases and so only one slice of the model, equal to the radius of influence, is analyzed.

The input parameters for FEQDrain can be classified into three main groups: a) geometric parameters and soil properties, b) earthquake loading conditions and c) drain geometry and drainage properties. The parameters of the first two groups are the same for any type of drain analysis and are presented in Table 2.1. Note that the soil properties must be repeated for each soil layer. Additionally, the user specifies the number of time steps, the total time of analysis, the number of iterations in a given time step, the duration of the time step for the integration scheme and the print resolution. Finally, the user can select either constant or

variable compressibility using the theoretical relationships between m_v and r_u (Seed et al., 1975), as presented in Figure 2.5.

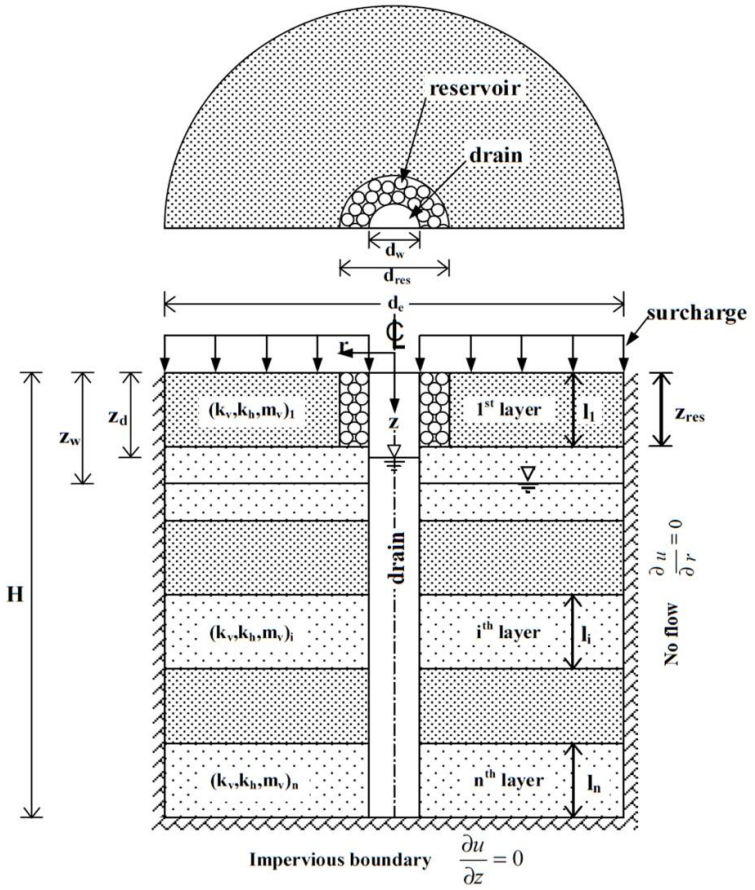

Figure 2.14: Boundary conditions for analysis of drain systems in FEQDrain (Pestana et al., 1997)

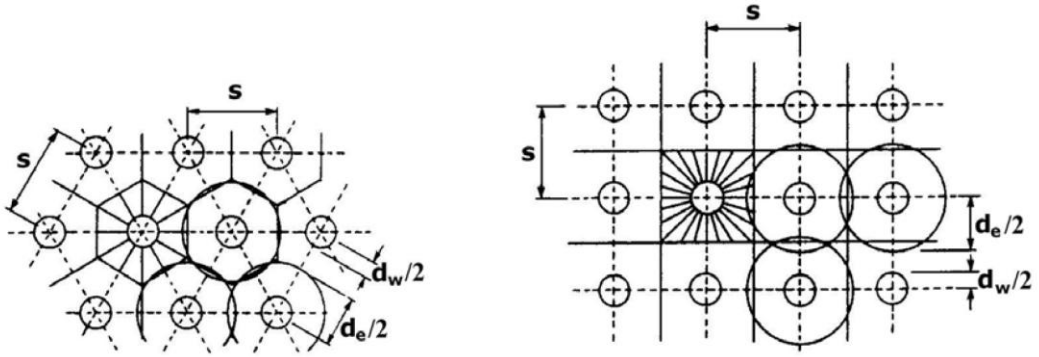

(a) Triangular Installation $d_e = 1.053 \cdot s$

(b) Square Installation $d_e = 1.13 \cdot s$

Figure 2.15: Effective circular area in (a) triangular and (b) square installation (Pestana et al., 1997)

Table 2.1: List of required geometric parameters, soil properties and earthquake loading conditions

Geometric Parameters	
nlayers:	Number of layers in the soil profile
nrinc:	Number of radial increments
gammaw:	Unit weight of water
depwat:	Depth of the static groundwater table
efforb:	Effective overburden stress
Soil Properties	
lay_linc:	Number of vertical increments
lay_thick:	Thickness of soil layer
lay_kx:	Horizontal hydraulic conductivity
lay_ky:	Vertical hydraulic conductivity
lay_mv:	Coefficient of volumetric compressibility
lay_gammat:	Total unit weight of soil layer
lay_nl:	Number of cycles to cause liquefaction
lay_dr:	Relative density
lay_theta:	Coefficient of pore pressure generation
Earthquake Loading Conditions	
nq:	Equivalent number of cycles due to EQ loading
td:	Equivalent time of earthquake shaking

In a drain – treated analysis, the user must specify additional information about the drain and drainage geometry, independently of the type of drain (perfect, granular or PVD) that is considered. The list of the required input parameters is presented in Table 2.2. As for "perfect drain" analysis, no additional input information is required and an analysis similar to the approach of Seed and Booker (1977) is performed. The only difference is that FEQDrain considers the vertical flow in the soil profile and the water rise in the drain. The effect of well resistance for gravel drains is considered in "equivalent granular drain" analysis, in a way similar to the work of Onoue (1988). Consequently, the values of vertical and

horizontal hydraulic conductivity within the drain must be specified, in addition to the previous input parameters (Table 2.2).

The last type of analysis in FEQDrain consists of "prefabricated vertical drains", which are characterized by a nonlinear discharge capacity as a function of hydraulic gradient. To solve this problem, the drain is divided into two elements: an outer and an inner core, in order to represent separately the flow through the geofabric/pipe orifices and the flow in the pipe (Figure 2.16). The ultimate purpose is the calculation of the equivalent hydraulic conductivities representing the head gradient in the vertical and horizontal directions. The flow in the outer core, "dQ_r", is assumed to be radial and the associated head loss is caused by the energy loss due to orifice entrance and the geofabric permeation:

$$\Delta h = \frac{dQ_r}{A_{surf} \cdot \psi} + \frac{c_{orf}}{a_{orf}^2} \cdot \frac{(dQ_r)^2}{2g \cdot A_{surf}^2} \tag{2.11}$$

where A_{surf} is the surface area of the drain element, c_{orf} is a constant for head loss through perforation (typically $c_{orf} = 1$), ψ is the permittivity of the geofabric and a_{orf} is the dimensionless ratio of the area of pipe openings (i.e. orifices) per unit length to the lateral surface area of the pipe. On the other hand, the flow in the inner core, "Q_d", is assumed to be vertical and to follow the modified Manning's equation:

$$\left.\frac{\partial h}{\partial z}\right|_{z,t} = c_1 \left(Q_d\left(z,t\right)\right)^{c_2} \tag{2.13}$$

The constant coefficients c_1 and c_2 describe the discharge capacity of the plastic drain and their values are provided from the manufacturer. The list of all the additional input parameters for this type of analysis is presented in Table 2.2 and

some typical values for PVDs with diameters of 3in., 4in, and 6in. are summarized in Table 2.3

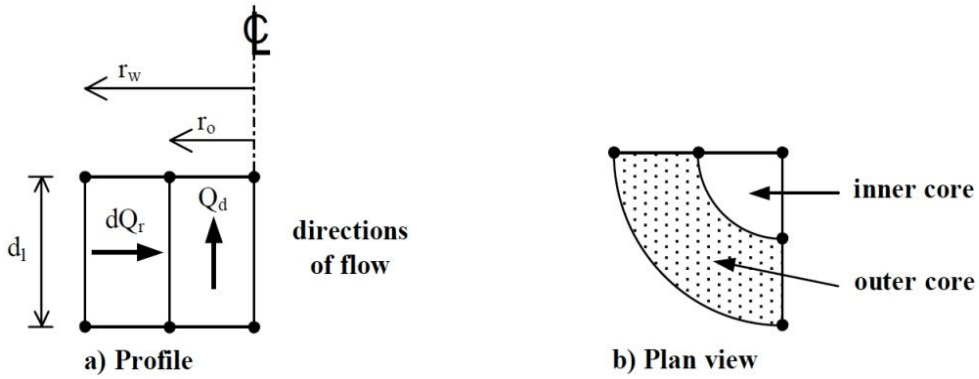

Figure 2.16: Flow within drain elements (Pestana et al., 1997)

Table 2.2: List of required drain geometry and drainage parameters for all types of drains

Drain Geometry and Drainage Parameters for all Drain Types	
rw:	Equivalent outside radius of the drain
rout:	Radius of the tributary area to the drain
aread:	Effective storage area of the drain
arear:	Effective storage area of the reservoir
depres:	Depth below surface to bottom of reservoir
Additional Parameters for Equivalent Granular Drains	
kxd:	Constant horizontal hydraulic conductivity in the drain
kyd:	Constant vertical hydraulic conductivity in the drain
Additional Parameters for Prefabricated Vertical Drains	
c1:	Material constant for vertical reristance in drain
c2:	Material constant for vertical reristance in drain
corf:	Constant for head loss through perforation
orf:	Area of openings per unit length in perforated pipe
permit:	Depth below surface to bottom of reservoir

Table 2.3: Typical parameters of PVDs needed for FEQDrain analysis

D (in)	C_1 (s^2/ft^6)	C_2	corf	orf (ft^2/ft)	ψ (1/sec)
3	1.7049	2	1	0.00990	0.08325
4	0.3676	2	1	0.01319	0.08325
6	0.04229	2	1	0.01979	0.08325

2.4 Summary

The pore pressure response in the case of radial drainage and the design of vertical drains against earthquake induced liquefaction were discussed in this chapter. The first design charts for gravel drains were provided by Seed and Booker (1977), assuming uniform ground properties, solely radial drainage and infinitely permeable drains. In these charts, the maximum drain spacing is determined based on the desired maximum pore pressure ratio, the ground motion characteristics and the soil properties. Onoue (1988) developed revised design charts which take into account the effect of the well resistance and the vertical drainage in the excess pore pressure response. Prefabricated vertical drains (PVD) are a new type of drain that can be installed in lieu of gravel drains as they provide more efficient drainage capacity. To cover the properties range associated with PVDs, the Japanese Geotechnical Society (1998) published new design charts based on the two previously mentioned approaches.

Pestana et al. (1997) developed a finite element program – "FEQDrain" to predict the pore pressure response in a drain – treated ground. FEQDrain is based on the same theoretical background as the chart solutions but it can deal with layered strata and it models the flow through the drain as well as the effect of the water level in the drain in a more sophisticated way.

Chapter 3

Sensitivity Analysis

3.1 Introduction

Before comparing the numerical predictions of pore pressure generation with the experimental results from centrifuge testing, it is very important to understand the behavior of each input parameter that influences the pore pressure predictions. To investigate the effect of these parameters on the drain response, a parametric study is performed using the finite element computer program FEQDrain (Pestana et al. 1997). A baseline model is initially developed and then the effect of soil properties, ground motion characteristics and drain parameters is examined. The sensitivity analysis will not only be focused on the single effect of each parameter, but the response due to different property combinations also will be examined.

3.2 Baseline Model

The first step for the sensitivity analysis is to consider the baseline geometry along with the baseline soil and ground motion characteristics. The model, which is presented in Figure 3.1, consists of 4.6 m of liquefiable medium clean sand with a 1 m thick clay cap. 100 mm (4 in.) diameter prefabricated vertical drains (PVDs), equally spaced every 1.5 m (center-to-center distance), are installed in a triangular pattern for liquefaction mitigation. The liquefiable sand is expected to liquefy in 10

cycles of motion (N_L = 10). The site is subjected to 20 cycles of harmonic motion over 10 sec at a frequency of 2Hz (N_{EQ} = 20, t_d = 10 sec), to generate a ratio of N_{EQ}/N_L = 2. Soil properties, drain and ground motion characteristics are summarized in Tables 3.1 and 3.2 respectively.

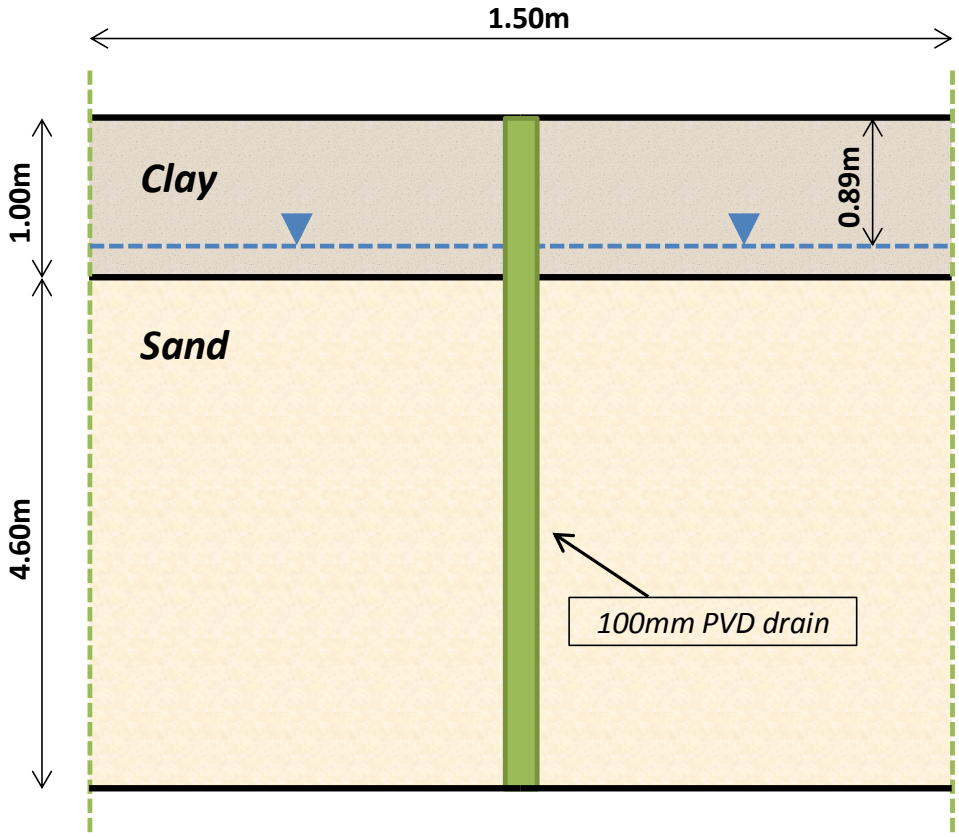

Figure 3.1: Cross-sectional view of the model

Table 3.1: Soil properties of baseline model

Soil Property	Clay Layer	Sand Layer
Layer Thickness - H (m)	1.00	4.6
Horizontal Hydraulic Conductivity - k_x (cm/s)	$2x10^{-5}$	0.02
Vertical Hydraulic Conductivity - k_y (cm/s)	$2x10^{-5}$	0.02
Coefficient of Volumetric Compressibility - m_v (1/kPa)	$4x10^{-6}$	$4x10^{-5}$
Total Unit Weight - γ (kN/m^3)	19.9	19.5
Number of cycles for liquefaction - N_L	10000	10
Relative Density - D_R (%)	90	40
Coefficient of Pore Pressure Generation - A	0.70	0.70

Table 3.2: Ground motion and drain characteristics used in baseline model

Duration of Shaking - t_d (sec)	10
Equivalent Number of Cycles - N_{EQ}	20
Drain Diameter - D_w (m)	0.1016
Center-to-Center Drain Spacing - s (m)	1.50
Material Constant for Vertical Resistance - C_1 (s^2/m^6)	458.76
Material Constant for Vertical Resistance - C_2	2
Area of Openings (per unit length) - Orf (m^2/m)	0.004021
Permittivity of Drain Fabric (1/sec)	0.08325

The effectiveness of the drains is examined by comparing the average excess pore water pressure ratio ($r_{u,avg}$) time-histories for the case of untreated soil ("No drains" case) with the results of treated soil using PVDs. $r_{u,avg}$ represents the average r_u value over the zone of influence. Two different analyses are performed for the treated soil: in the first one the well resistance of the drain is ignored ("Perfect drains" case), whereas in the second one it is taken into account ("PVD drains" case). It must be stated that FEQDrain does not directly compute the $r_{u,avg}$, but only the values of r_u at the nodes of the finite element mesh. Hence, the average values must be separately calculated by the user. To calculate the $r_{u,avg}$, a dense mesh discretization of the sand layer was selected using a trial and error procedure

until the same average values are calculated for two different meshes. For this particular problem, the discretization is 60 horizontal and 10 vertical sublayers.

The $r_{u,avg}$ time-histories for the three cases (No drain, Perfect drain, PVD drain) are plotted in Figure 3.2. Note that the time (t) in Figure 3.2 is normalized to the duration of shaking (t_d). It is observed that the site liquefies in the absence of drains because N_{EQ}/N_L = 2. The presence of drains significantly reduces the $r_{u,avg}$, which in this case reaches a maximum at the end of shaking of approximately 0.50. After shaking ends (t/t_d > 1) the pore pressures in the drain treated cases decrease, but they remain high in the untreated case because of the clay cap. The results for perfect drains and PVDs are almost identical, leading to the conclusion that well resistance is very small for this type of drain and hence it can be ignored. For this reason, only the results of perfect drains will be presented for the next analyses.

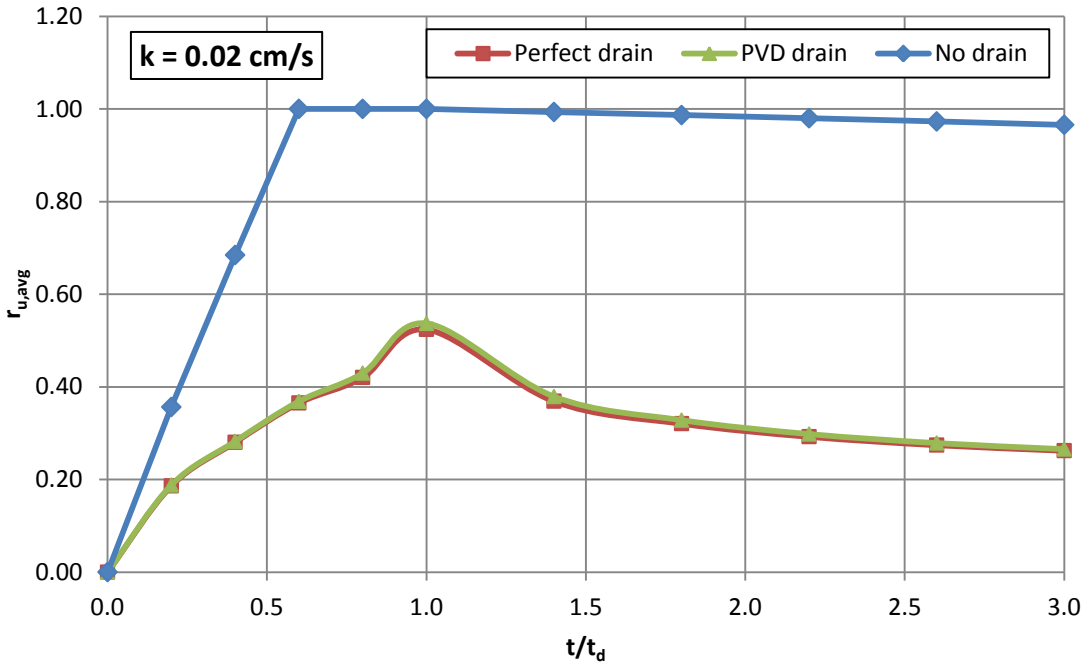

Figure 3.2: Average excess pore water pressure ratio $r_{u,avg}$-time histories for the baseline model

3.3 Sensitivity: Soil Properties

The first set of sensitivity analyses investigates the soil properties that affect the generation of excess pore water pressures. Specifically, the effects are investigated for: a) the hydraulic conductivity - "k", which controls the rate of water flow, b) the coefficient of volumetric compressibility - "m_v", which controls the volumetric strain and hence the volume of water that needs to drain, and c) the exponent "A", which controls the shape of the pore pressure generation curve,. For each parametric study, the analyses of FEQDrain are repeated after changing only the examined parameter.

For the sensitivity analysis of the hydraulic conductivity, the k of the liquefiable layer is taken as 0.2 cm/s, 0.02 cm/s (baseline) and 0.05 cm/s. These values represent the range of k for coarse to silty sand. The $r_{u,avg}$ time-histories are plotted in Figures 3.3 and 3.4 for these k values for the untreated and treated cases. For the untreated case (Figure 3.3), the curves are almost the same during shaking (t/t_d < 1) and then the pore pressure curve that corresponds to the larger k attenuates faster. For the drain – treated case (Figure 3.4), $r_{u,avg}$ is significantly increased (maximum $r_{u,avg}$ > 0.90) for the case of the lowest k, as horizontal drainage becomes more difficult. The more interesting result is in the case of the larger k, where the $r_{u,avg}$ reaches a maximum value of 0.25 at the end of shaking and then it remains approximately constant, indicating the presence of some residual excess pore water pressures. The curve for k = 0.02 cm/s peaks at $r_{u,avg}$ equal to 0.5 and then gradually decreases after shaking to the same value as k = 0.2 cm/s, supporting the idea of the residual r_u .

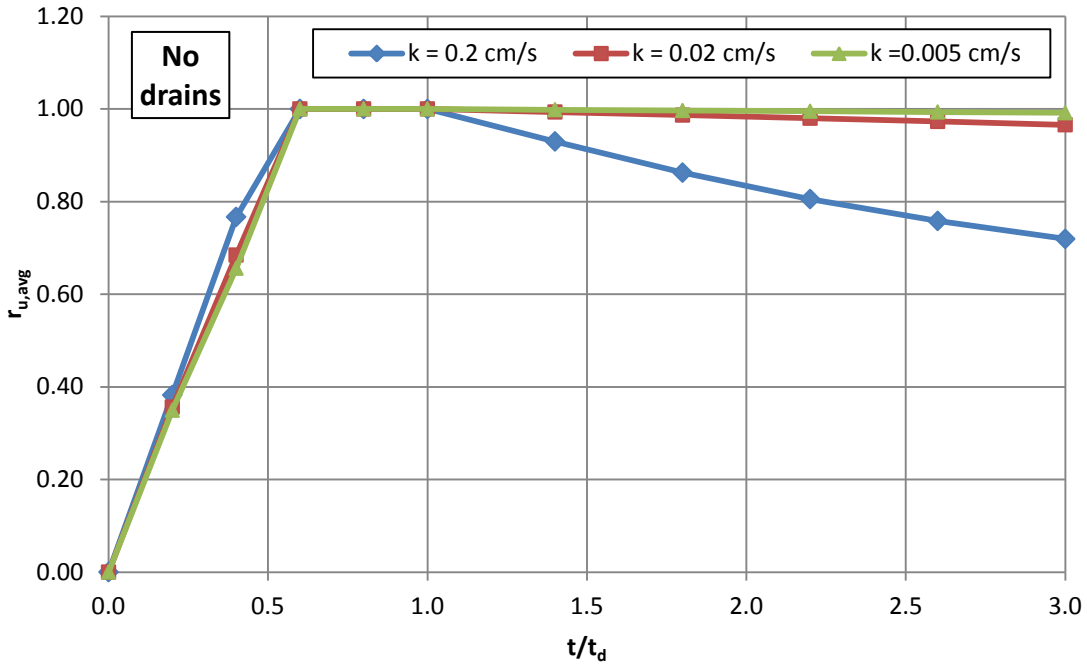

Figure 3.3: Untreated $r_{u,avg}$-time histories for different values of hydraulic conductivity k

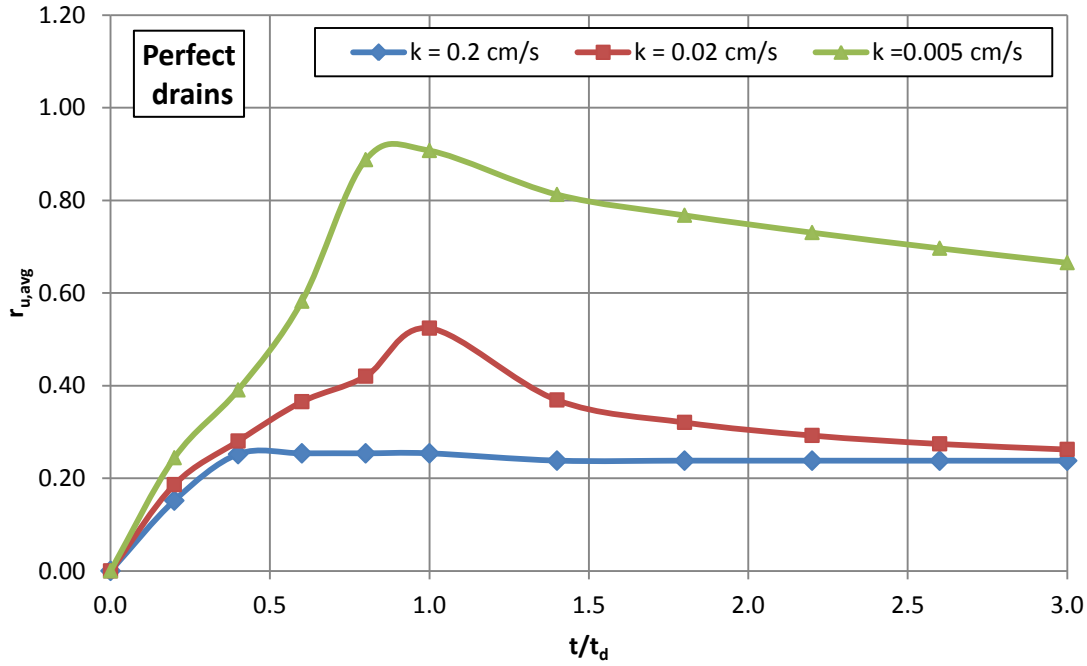

Figure 3.4: Treated $r_{u,avg}$-time histories for different values of hydraulic conductivity k

To explain this effect, the distribution of excess pore pressure with depth at the end of shaking (t/t_d = 1) and at t/t_d = 3 is plotted in Figures 3.5 and 3.6, respectively, for 4 different radial locations (i.e., r/b, where r is the radial location and b the area-of-influence radius). In Figure 3.5, the pore pressure at the edge of the drain (r/b = 0.06) is constant with depth and equal to Δu = 8.73kPa, which corresponds to pressure head of 0.89 m. This distance is equal to the depth of the groundwater table. At t/t_d = 3 (Figure 3.6), when the excess pore pressures have stabilized to a constant value, the pore pressure at any radial location is not zero, but equal to Δu = 8.73kPa. As shown in Figure 3.7, the volume of water that is collected by the drain during shaking fills the drain and brings its water surface, which initially is at the same level as the groundwater table, to the ground surface. Consequently, there is a head difference inside and outside the drain, which leads to a development of residual excess pore pressures.

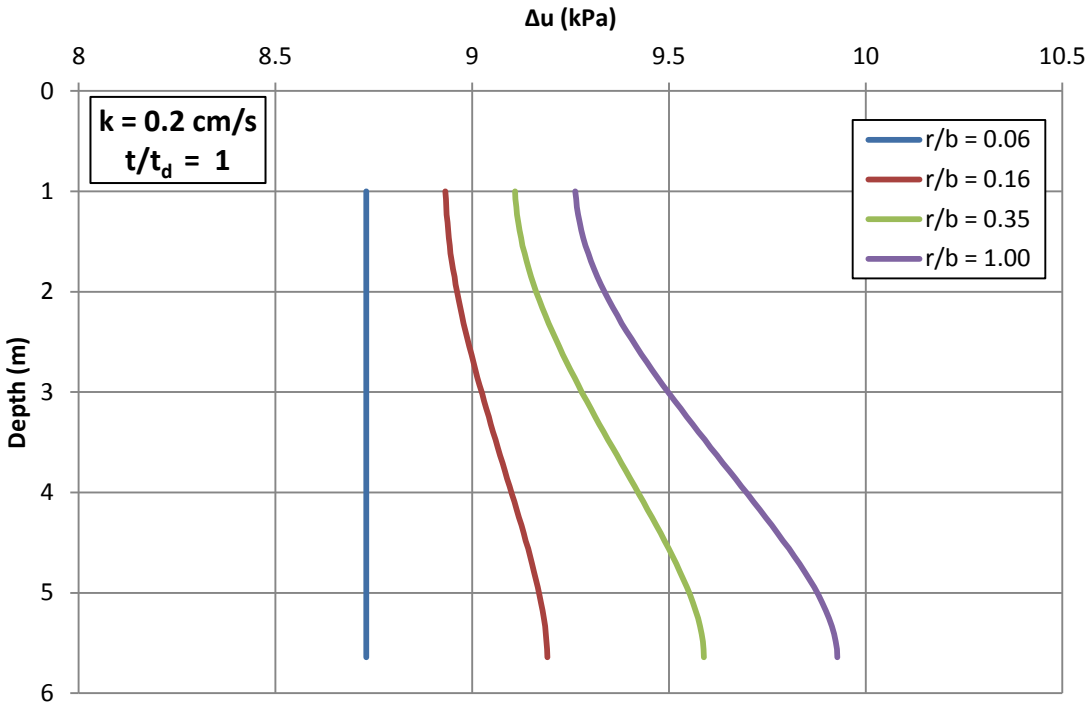

Figure 3.5: Pore water pressure distribution at t/t_d =1 for k = 0.2 cm/s for treated conditions

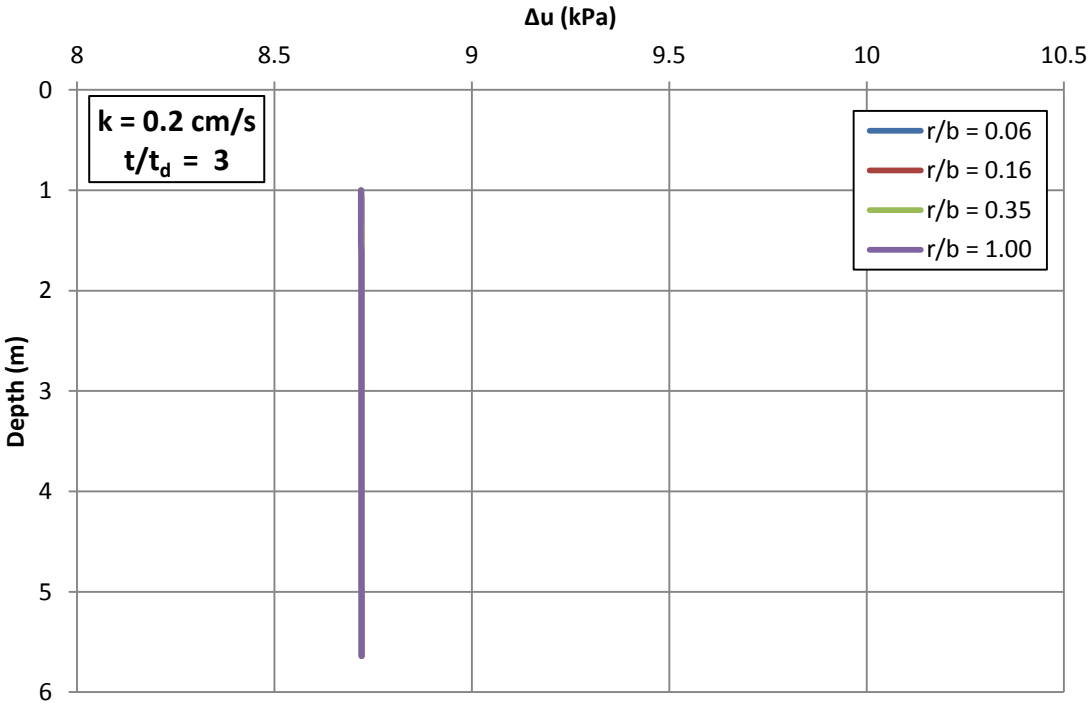

Figure 3.6: Pore water pressure distribution at t/t_d =3 for k = 0.2 cm/s for treated conditions

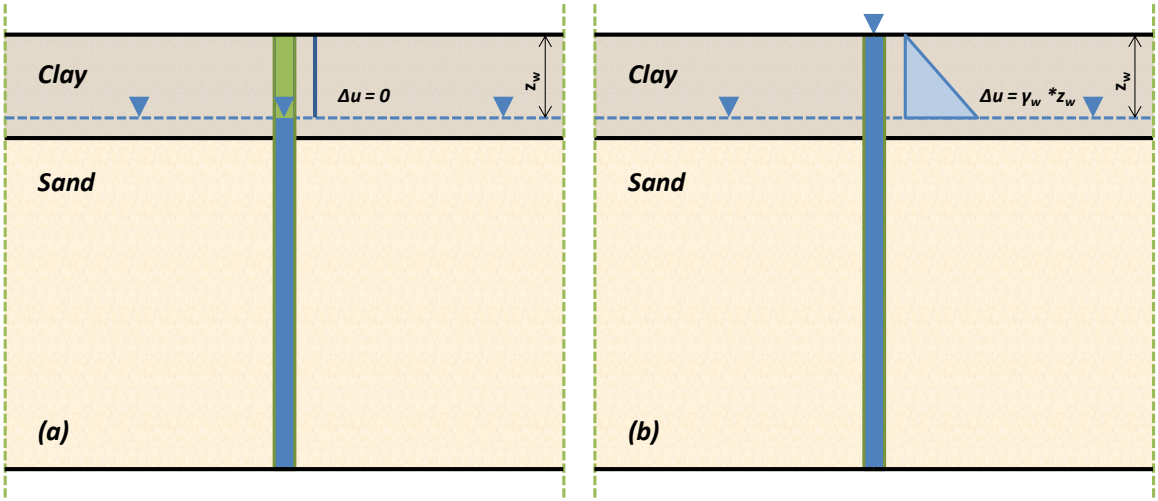

Figure 3.7: Total heads in and out of the drain: (a) before shaking and (b) during shaking

The effect of the coefficient of compressibility m_v is presented in Figures 3.8 and 3.9, where the baseline case (i.e. $k = 0.02\ cm/s$ and $m_v = 4x10^{-5}\ 1/kPa$) is repeated for 3 additional m_v values ($m_v = 2x10^{-5}\ 1/kPa, m_v = 8x10^{-5}\ 1/kPa$, $m_v = 50x10^{-5}\ 1/kPa$), in order to cover the entire range of values for liquefiable sands. The impact of m_v on pore pressure generation is negligible for the untreated case (Figure 3.8), but very important for the treated case (Figure 3.9). An increase in m_v leads to a significant increase in $r_{u,avg}$. Recall that m_v represents the volumetric strain induced for a unit change in effective stress. Larger values of m_v result in more volumetric strain being induced in the soil with an associated larger volume of water that needs to be drained to dissipate the excess pore pressures. Because it will take longer to drain larger volumes of water, larger m_v values lead to larger $r_{u,avg}$. It is must be stated that the input m_v values represent small strain values and FEQDrain increases these values for $r_u > 0.6$. This issue explains the significant increase in $r_{u,avg}$ when the baseline m_v doubles ($m_v = 4\ vs\ 8\ x10^{-5}\ 1/kPa$). In this case, as $r_{u,avg}$ becomes greater than 0.6, m_v increases even further leading to additional excess pore pressures.

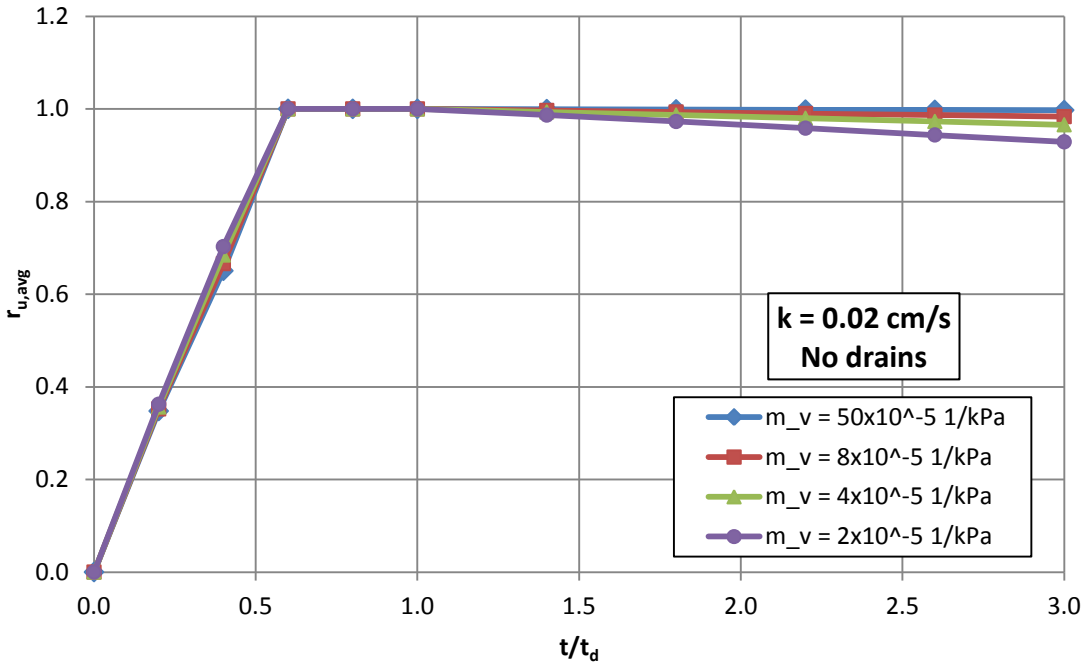

Figure 3.8: Untreated $r_{u,avg}$-time histories for different coefficients of compressibility m_v

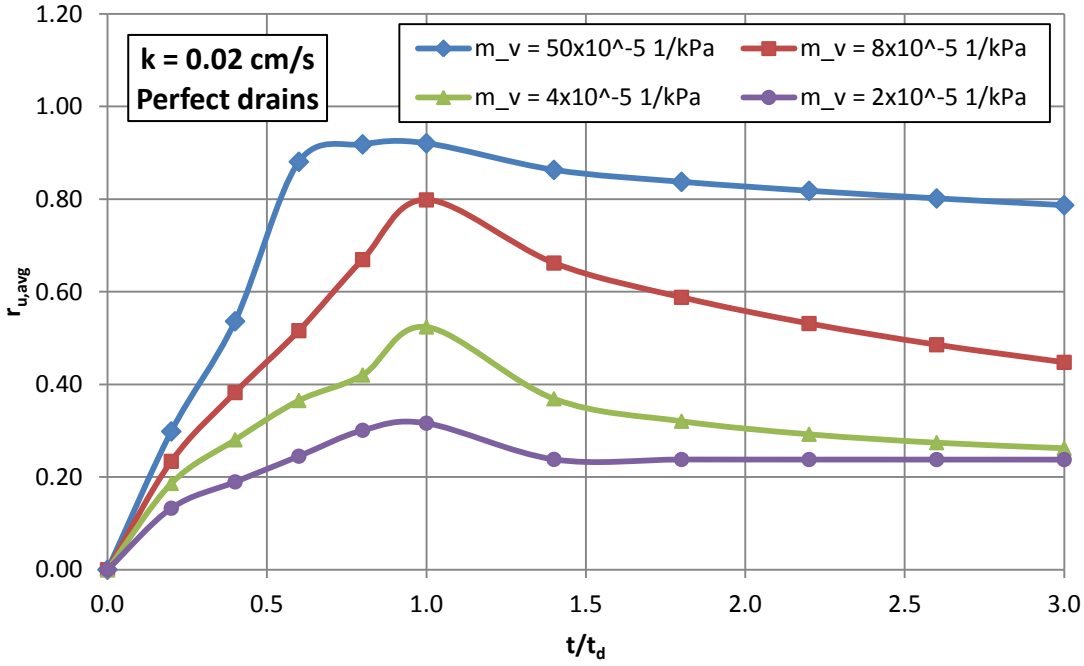

Figure 3.9: Treated $r_{u,avg}$-time histories for different coefficients of compressibility m_v

To examine the effect of m_v in more detail, the same sensitivity analysis is repeated for $k = 0.005\ cm/s$ and $k = 0.2\ cm/s$. Comparing the results for the untreated case (Figures 3.10 and 3.11) and the treated case (Figures 3.12 and 3.13), it is observed that the effect of m_v is different as the hydraulic conductivity of the sand changes. For the untreated case, the variation of m_v has an effect in excess pore water pressures only when $k = 0.2\ cm/s$ and the effect is only present during dissipation (Figure 3.10). For the treated case and $k = 0.2\ cm/s$ (Figure 3.12), the $r_{u,avg}$ curves corresponding to the three smaller m_v values have approximately the same maximum, which is slightly higher than the residual r_u, and only the rate of pore pressure generation is affected by m_v. However, the $r_{u,avg}$ curve is significantly increased when the biggest m_v value is used. A similar response is observed in the case of $k = 0.005\ cm/s$, but the difference is that now the three largest m_v values are those with the same maximum, which is about 0.9, whereas the model with the smallest m_v encounters smaller excess pore pressures.

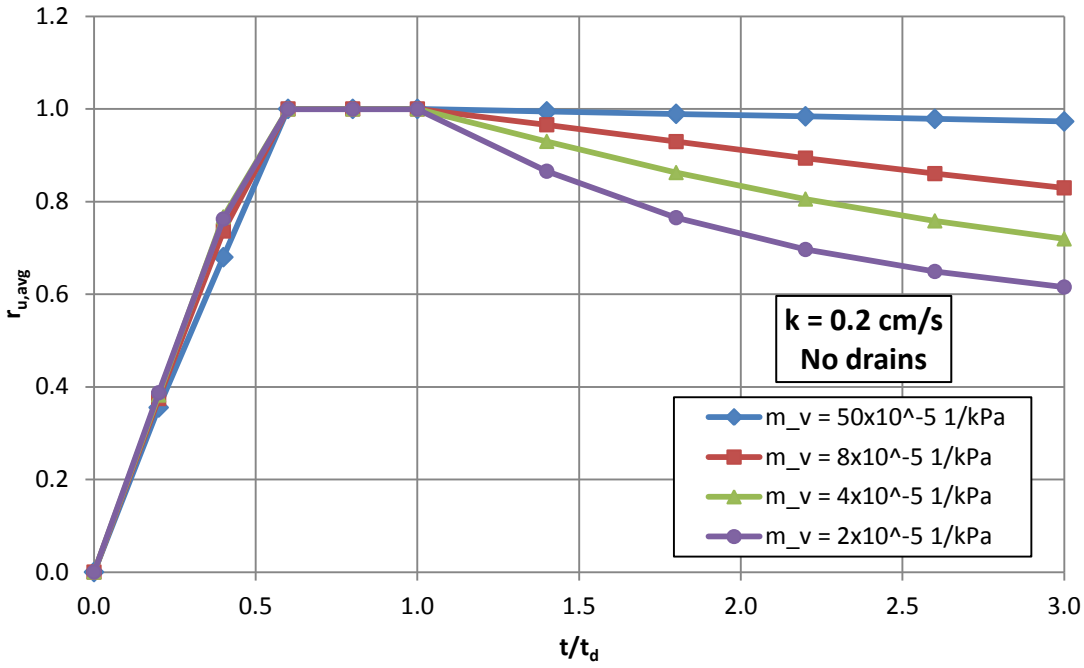

Figure 3.10: Untreated $r_{u,avg}$-time histories for $k = 0.2\ cm/s$ and different values of m_v

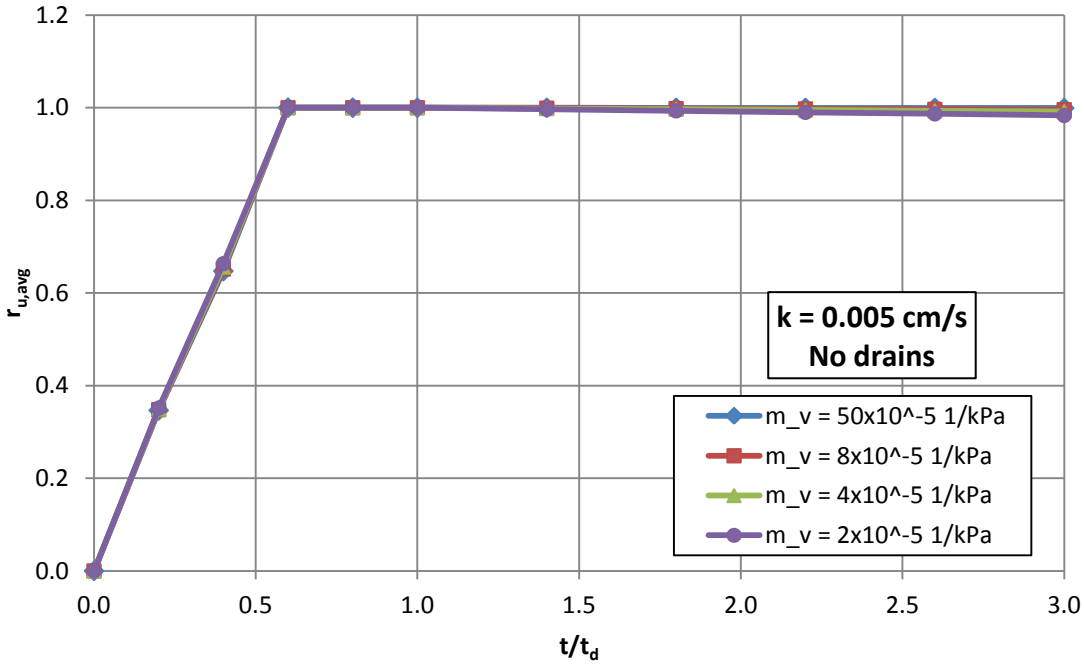

Figure 3.11: Untreated $r_{u,avg}$-time histories for $k = 0.005\ cm/s$ and different values of m_v

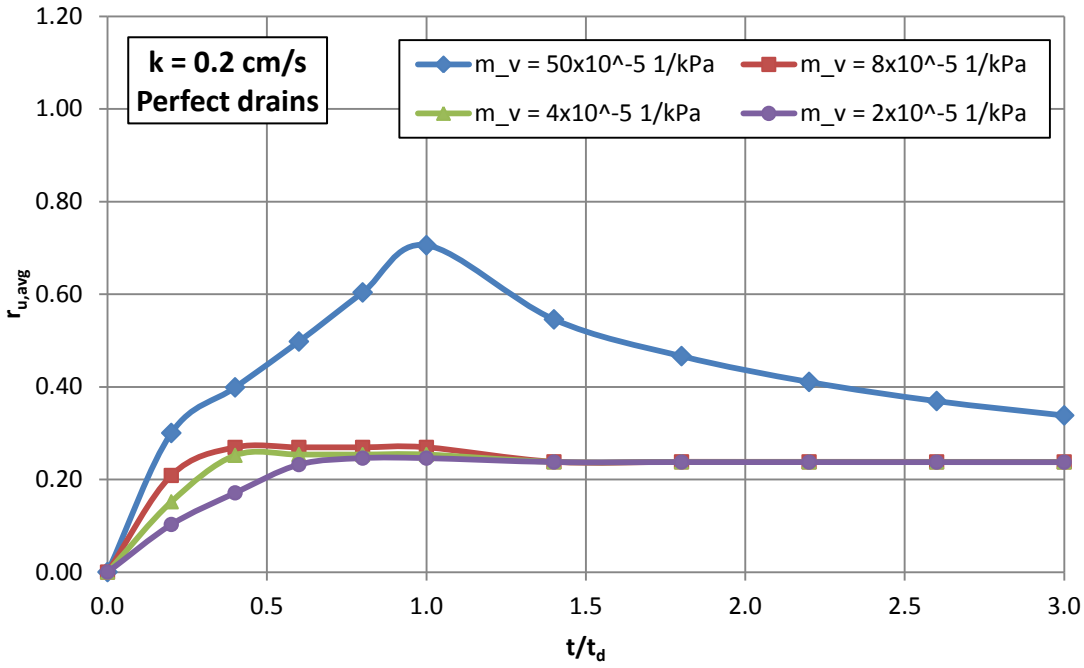

Figure 3.12: Treated $r_{u,avg}$-time histories for $k = 0.2\ cm/s$ and different values of m_v

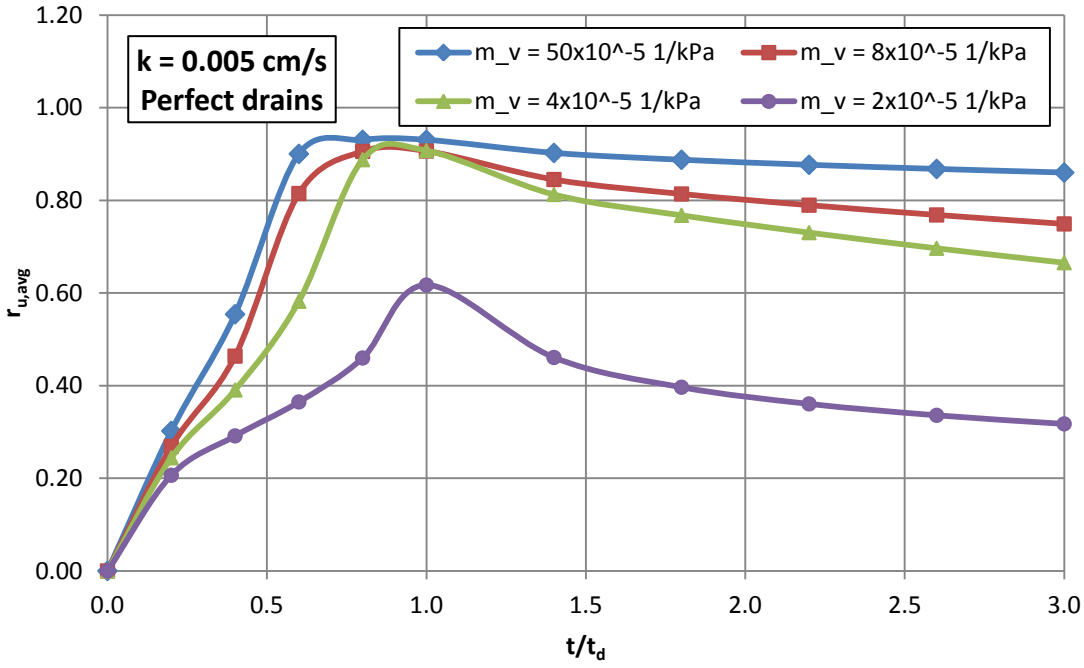

Figure 3.13: Treated $r_{u,avg}$-time histories for $k = 0.005\ cm/s$ and different values of m_v

It can be concluded that the effect of the hydraulic conductivity cannot be separated from the effect of the volumetric compressibility, because in reality their combination is the main soil parameter that affects the generation and dissipation of excess pore water pressure. This combination can be expressed by the coefficient of consolidation, c_v:

$$c_v = \frac{k}{\gamma_w \cdot m_v} \tag{3.1}$$

where γ_w is the unit weight of water. It is noted that the equation of c_v is consistent with the results of the sensitivity analyses, where it was found that k and m_v have opposite effects on the pore pressure generation. Smaller values of k and larger values of m_v lead to less pore pressure dissipation and larger $r_{u,avg}$. The values of c_v for all the analyzed combination of k and m_v are presented in Table 3.3 along with the corresponding maximum $r_{u,avg}$ for each case and the $r_{u,avg}$ time-histories are plotted in Figure 3.14. It is observed that soils with c_v of the same order of magnitude exhibit a similar excess pore pressure response and consequently Figure 3.14 can be divided in three regions according to the range of c_v and the resultant pore pressure ratio. The upper region consists of sands with $c_v = 0.01 - 0.13\ m^2/s$, in which the drain design is completely inadequate as the maximum values of $r_{u,avg}$ are greater than 0.90. The lower region is defined by the soils with $c_v = 1.09 - 10.19\ m^2/s$ and the excess pore pressure ratio is close to the residual r_u curve (excellent performance of drains). In these two regions, the variation of r_u is very small. However, the behavior of the soil is not the same in the middle region (corresponding $c_v = 0.25 - 0.50\ m^2/s$), in which the $r_{u,avg}$ curves vary significantly with changes in c_v. Not only does $r_{u,avg}$ vary more with c_v in this region, but the $r_{u,avg}$ curves do not consistently increase with decreasing c_v. In particular, two

analyses with $c_v = 0.25\, m^2/s$ but different k and m_v (analyses 5 and 6) have different $r_{u,avg}$ responses. However, these analyses correspond to different values of k and m_v, and hence the rate of the increase in water level inside the drain is not the same. To verify this assumption, the depth of the water inside the drain for the middle range of c_v values is plotted in Figure 3.15. It is observed that the water level increases slower in the case of the smaller k and consequently the additional pore pressures induced by the head difference of the drain are smaller compared to the other cases, leading to smaller total excess pore pressures. It must be stated that in the other two regions the either excellent or poor performance of the drains eliminates the differences in the rate of water level increase. This effect explains adequately the inconsistency of the results in the middle region and narrows the area of the exclusive control of excess pore pressure generation from the coefficient of consolidation, when the ground water table is not on ground surface.

Table 3.3: Values of c_v and corresponding maximum $r_{u,avg}$

N$_o$	**k (cm/s)**	**m$_v$ (1/kPa)**	**c$_v$ (m^2/s)**	**maximum r$_{u,avg}$**
1	0.005	50E-05	0.01	0.93
2	0.02	50E-05	0.04	0.92
3	0.005	8.0E-05	0.06	0.91
4	0.005	4.0E-05	0.13	0.91
5	0.02	8.0E-05	0.25	0.80
6	0.005	2.0E-05	0.25	0.62
7	0.2	50E-05	0.41	0.71
8	0.02	4.0E-05	0.51	0.52
9	0.02	2.0E-05	1.02	0.32
10	0.2	8.0E-05	2.55	0.27
11	0.2	4.0E-05	5.10	0.25
12	0.2	2.0E-05	10.19	0.25

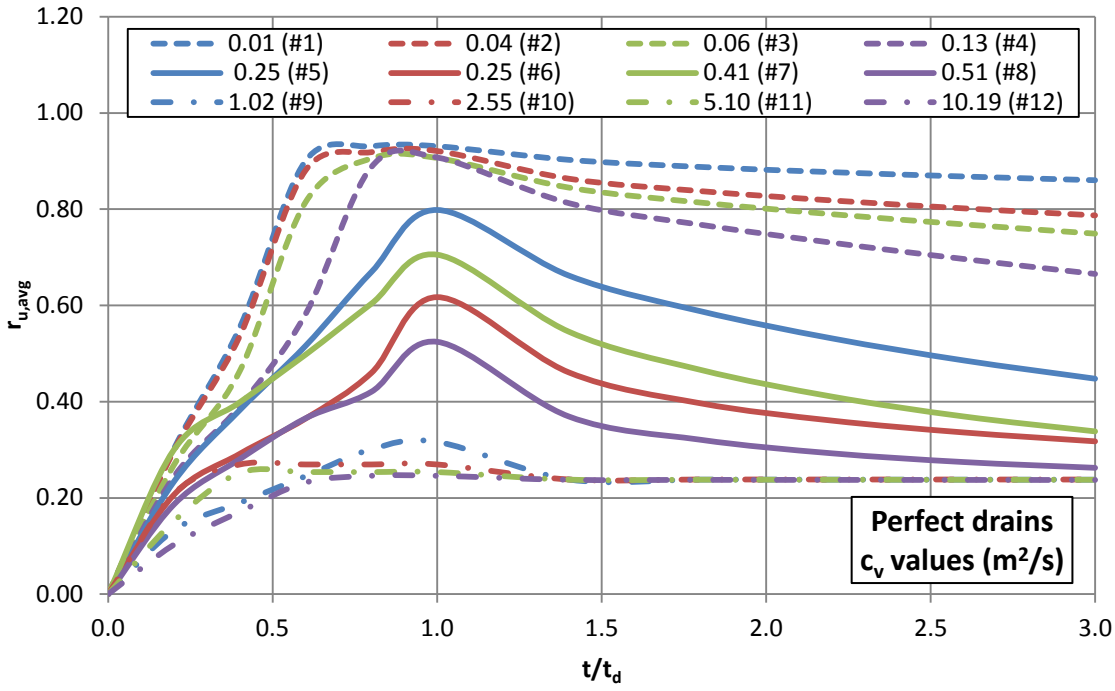

Figure 3.14: Treated $r_{u,avg}$-time histories for the same coefficient of consolidation c_v

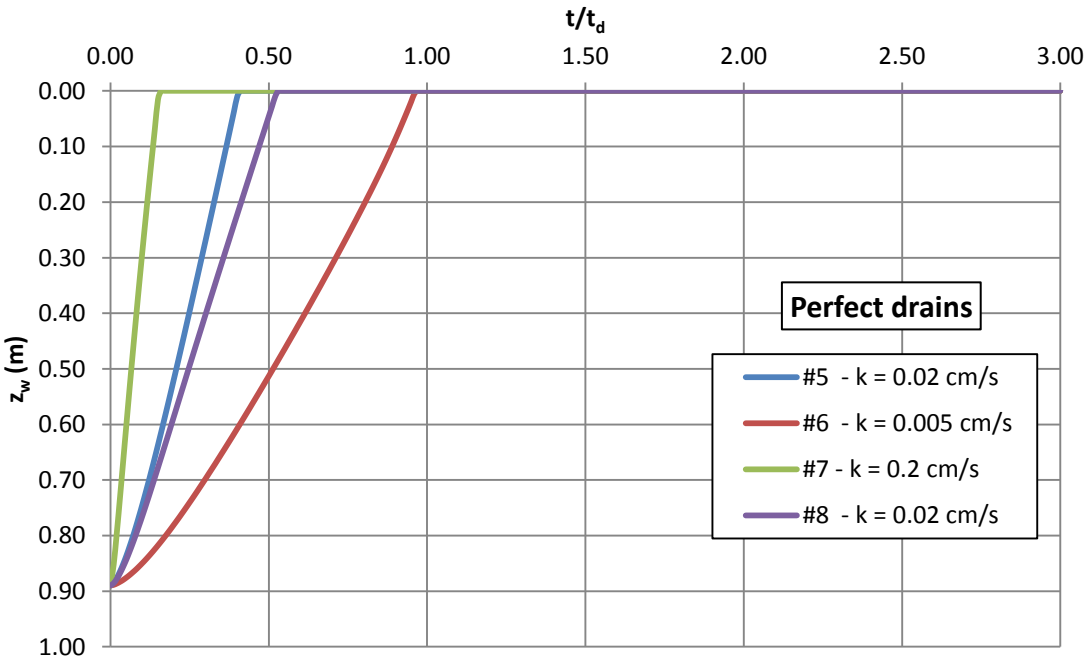

Figure 3.15: Depth of water inside the drain for the analyses of the middle range

The next parameter to be investigated is of the shape of the pore pressure generation function, developed by Seed et al. (1975), which is controlled by the exponent "A":

$$\frac{u_g}{\sigma_0^{'}} = \frac{2}{\pi}\sin^{-1}\left(\frac{N}{N_L}\right)^{1/2A} \tag{3.2}$$

As mentioned in Chapter 2, the exponent A has a typical value of 0.70, but recent studies (Bouckovalas et al., 2011) indicate that larger values of A give more representative results for many soils. The pore pressure response modeled by Equation 3.2 is plotted in Figure 3.16 for A = 0.7, 1.4 and 2.0. As shown in Figure 3.16, the larger the exponent A, the stiffer the pore pressure build-up curve becomes at small values of N/N_L. To examine the effect of A, the baseline case is repeated both for untreated and treated conditions considering $A = 1.4$ and $A = 2.0$ in Figures 3.17 and 3.18. It is observed that as A is increased, the pore pressure curves in both cases become steeper at the beginning and the maximum $r_{u,avg}$ is reduced for the treated case. To cover the lower and upper region, the same sensitivity analysis is repeated for $k = 0.2\,cm/s$ and $k = 0.005\,cm/s$ and baseline m_v in Figures 3.19 and 3.20 respectively for the treated case. For these two cases, the increase in A results only in the faster build-up of $r_{u,avg}$ whereas its maximum value is practically unaffected.

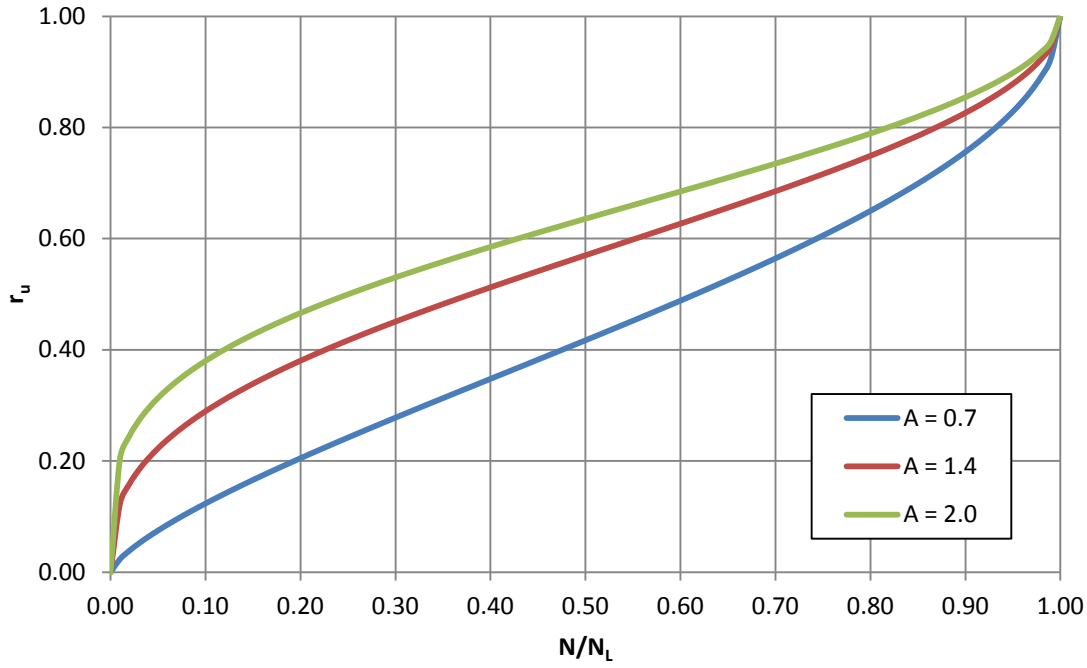

Figure 3.16: Rate of excess pore pressure build-up for different values of exponent A

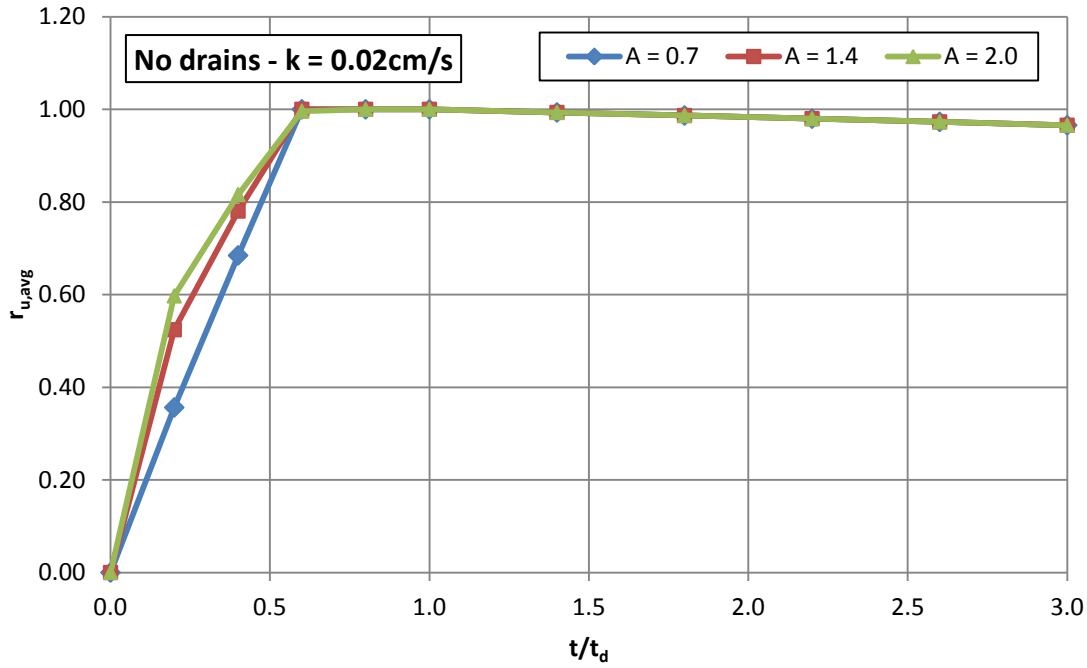

Figure 3.17: Untreated $r_{u,avg}$-time histories for different values of exponent A – $k = 0.02\ cm/s$

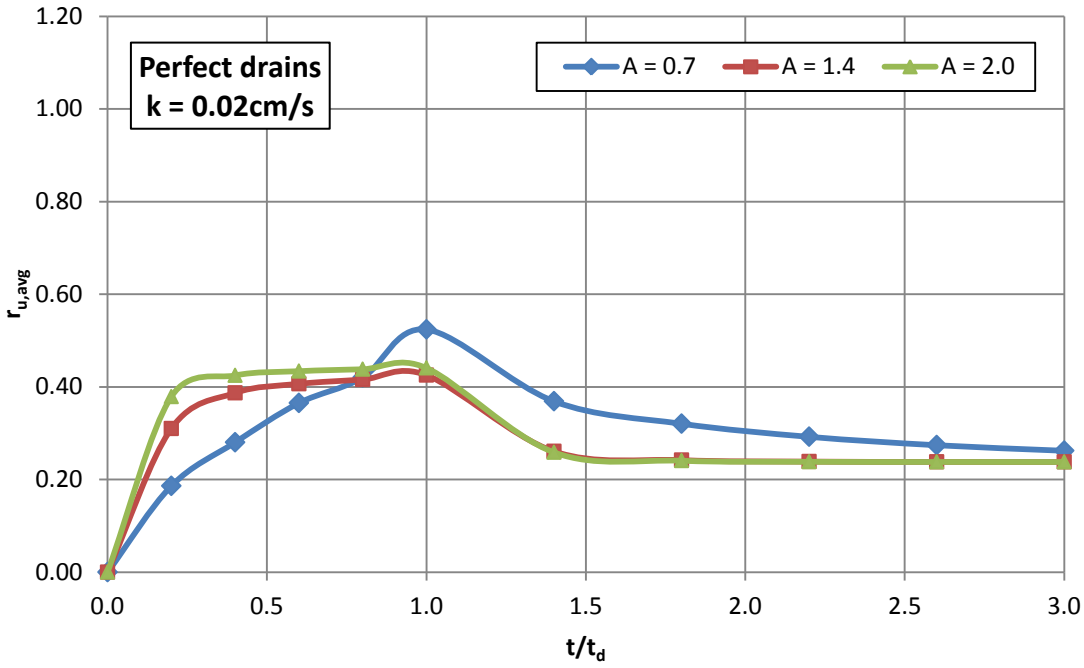

Figure 3.18: Treated $r_{u,avg}$-time histories for different values of exponent A – $k = 0.02\ cm/s$

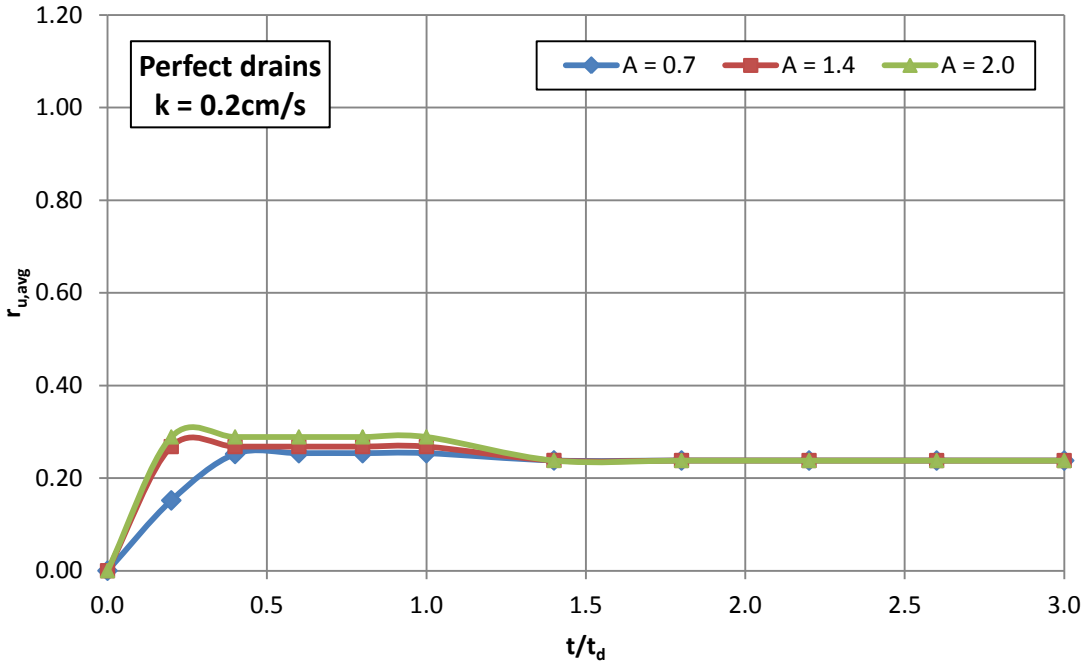

Figure 3.19: Treated $r_{u,avg}$-time histories for different values of exponent A – $k = 0.2\ cm/s$

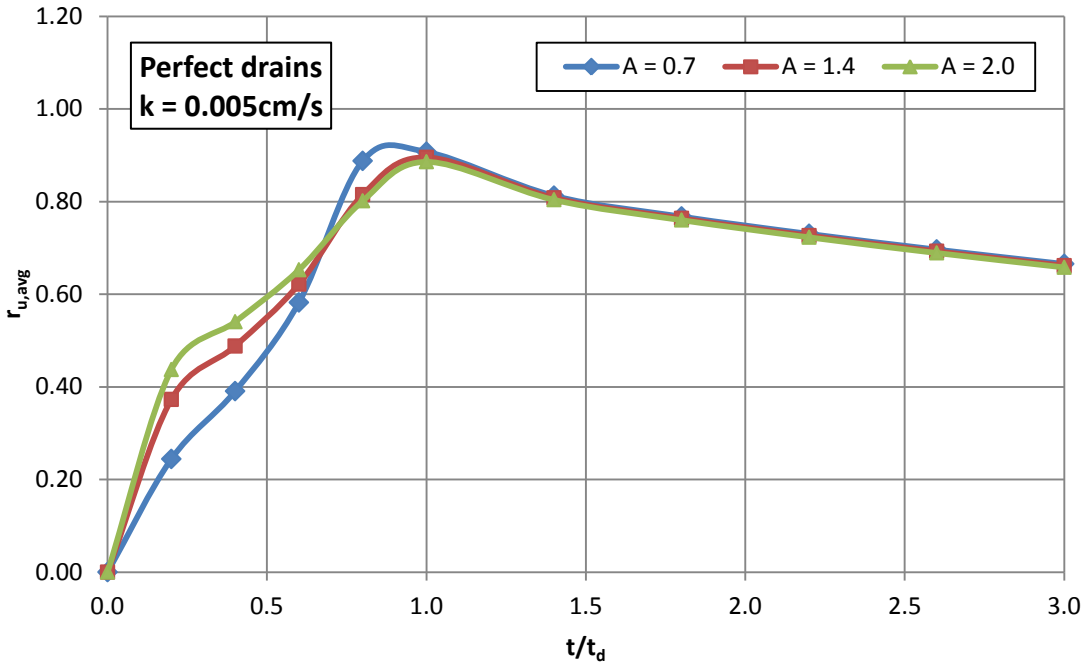

Figure 3.20: Treated $r_{u,avg}$-time histories for different values of exponent A – $k = 0.005\ cm/s$

3.4 Sensitivity: Characteristics of Shaking

The second part of the sensitivity analyses investigates the characteristics of shaking and in particular the duration of shaking and the number of cycles of motion. Starting with the effect of the duration, the baseline model is repeated for the cases of half ($t_d = 5$ sec) and double ($t_d = 20$ sec) the duration. The results for the untreated and treated cases are plotted in Figures 3.21 and 3.22, respectively.

For the untreated case, the response is essentially the same for all values of t_d. For the treated case, the shorter duration of motion results in a larger the $r_{u,avg}$. As the motion is applied over a longer period, the rate of excess pore pressure dissipation is larger. Taking into account the effect of hydraulic conductivity on the rate of pore pressure dissipation, the treated analyses are repeated for the different

values of k (Figures 3.23 and 3.24). It is observed that the effect of the duration is very small when the hydraulic conductivity is either very big (Figure 3.23, $k = 0.2\ cm/s$) or very small (Figure 3.24, $k = 0.005\ cm/s$).

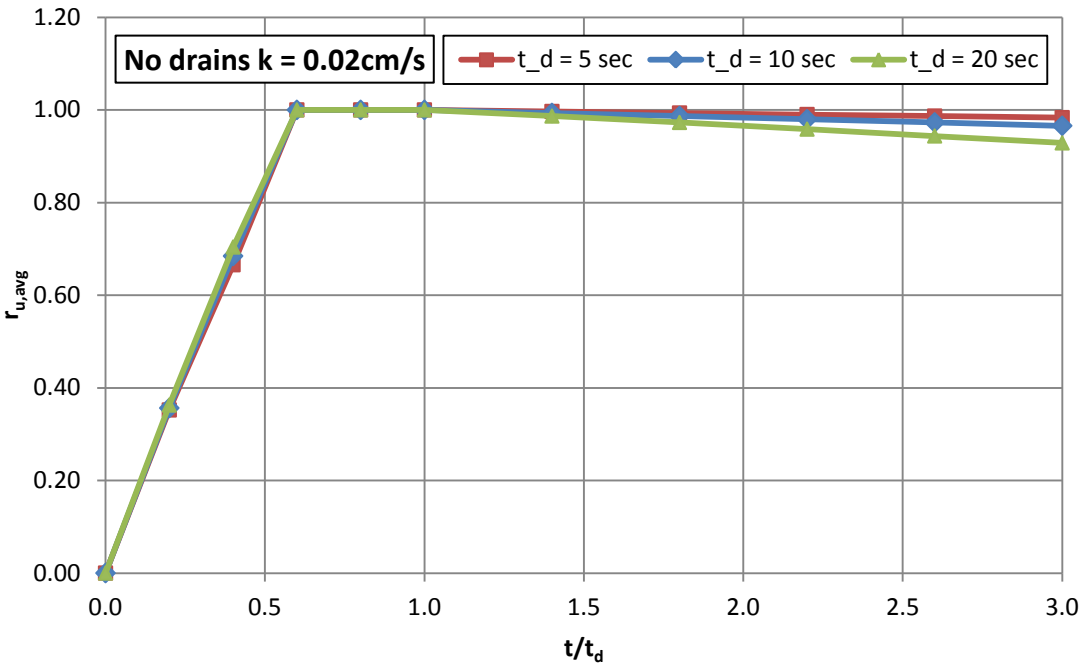

Figure 3.21: Untreated $r_{u,avg}$-time histories for different durations of shaking t_d - $k = 0.02\ cm/s$

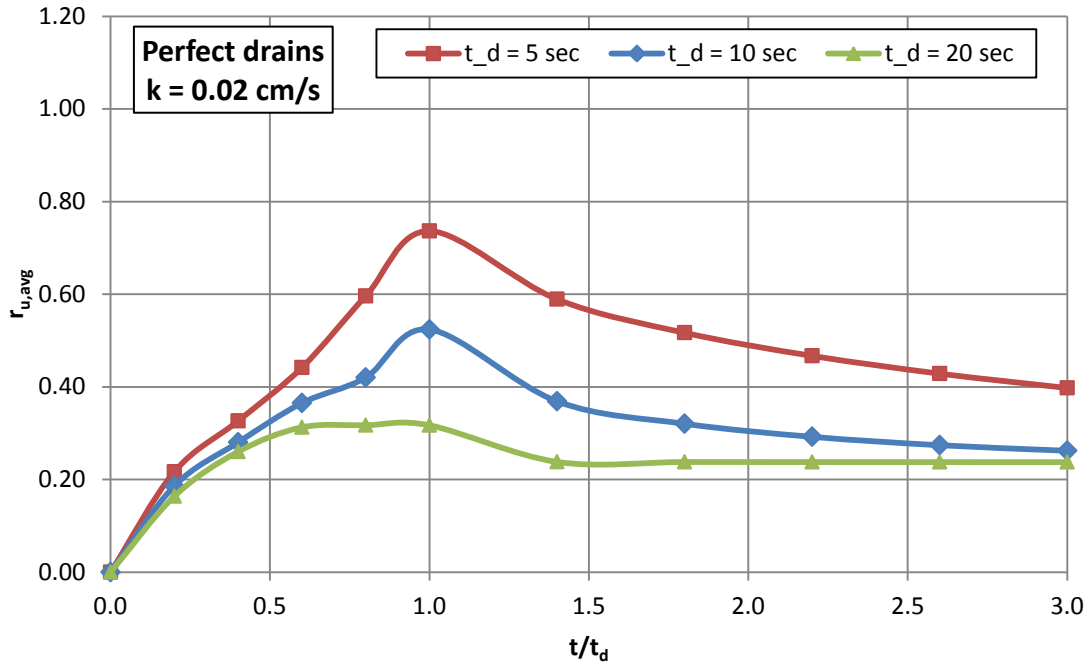

Figure 3.22: Treated $r_{u,avg}$-time histories for different durations of shaking t_d - $k = 0.02\ cm/s$

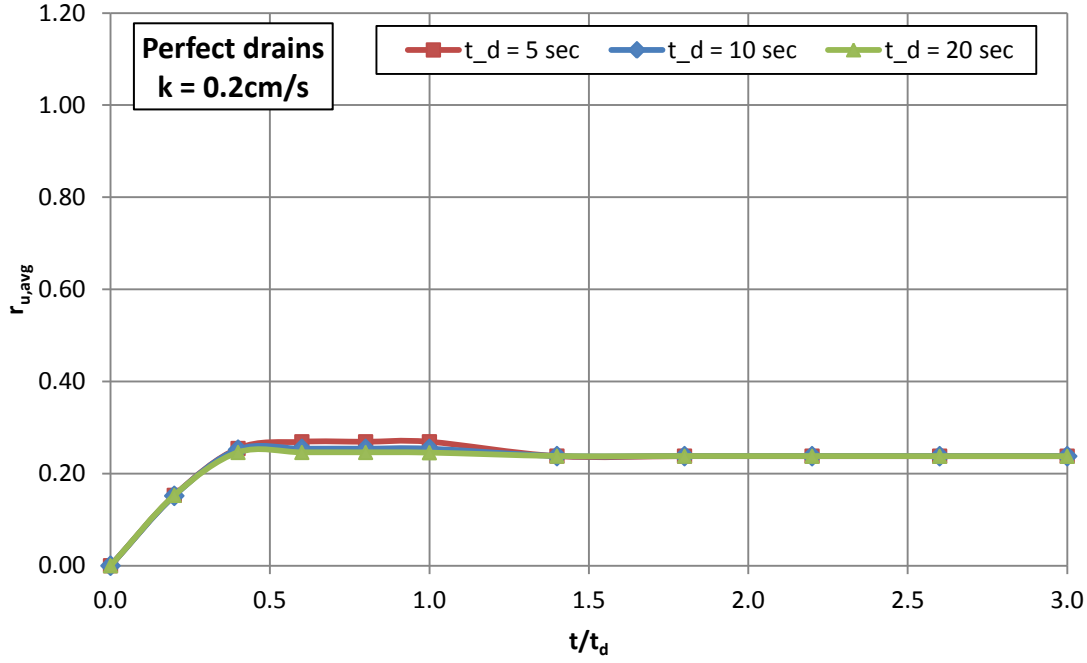

Figure 3.23: Treated $r_{u,avg}$-time histories for different durations of shaking t_d - $k = 0.2\ cm/s$

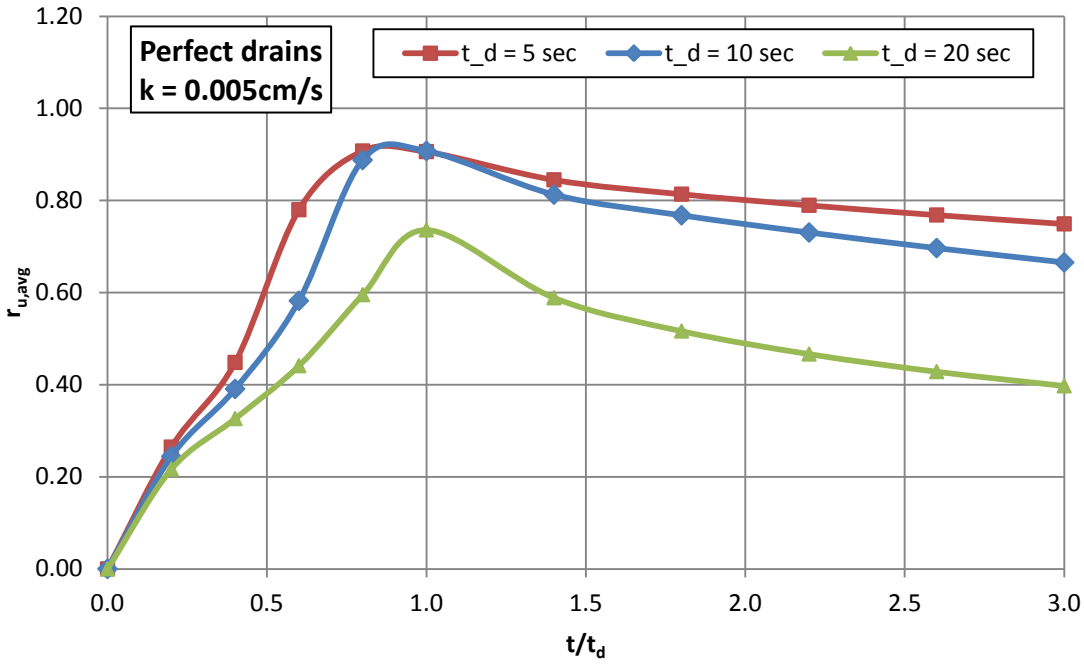

Figure 3.24: Treated $r_{u,avg}$-time histories for different durations of shaking t_d - $k = 0.005\ cm/s$

The effect of the number of cycles of motion is the next parameter that is examined and it is expressed by the equivalent number of cycles N_{EQ}. This increase in loading cycles relative to a constant N_L increases the excess pore water pressures. The baseline model is analyzed for 5 and 10 loading cycles, so that the ratio N_{EQ}/N_L is 0.5 and 1 (Figure 3.25 for untreated and Figure 3.26 for treated case). The results agree with the previously mentioned behavior, a decrease in the ratio N_{EQ}/N_L leads to a decrease in the $r_{u,avg}$.

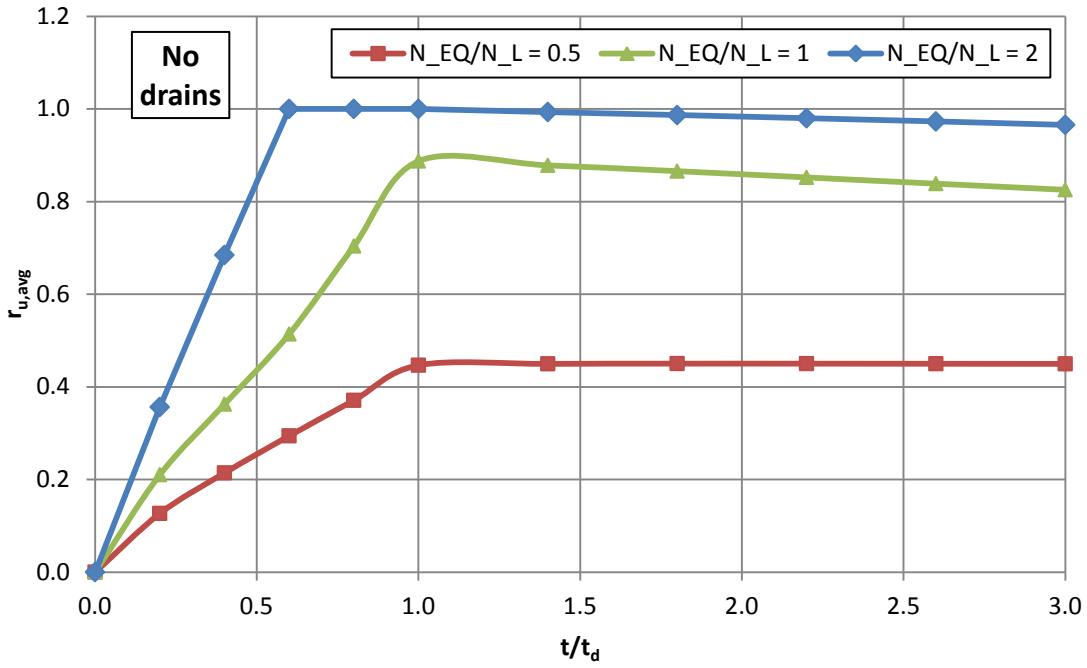

Figure 3.25: Untreated $r_{u,avg}$-time histories for different values of N_{EQ}/N_L

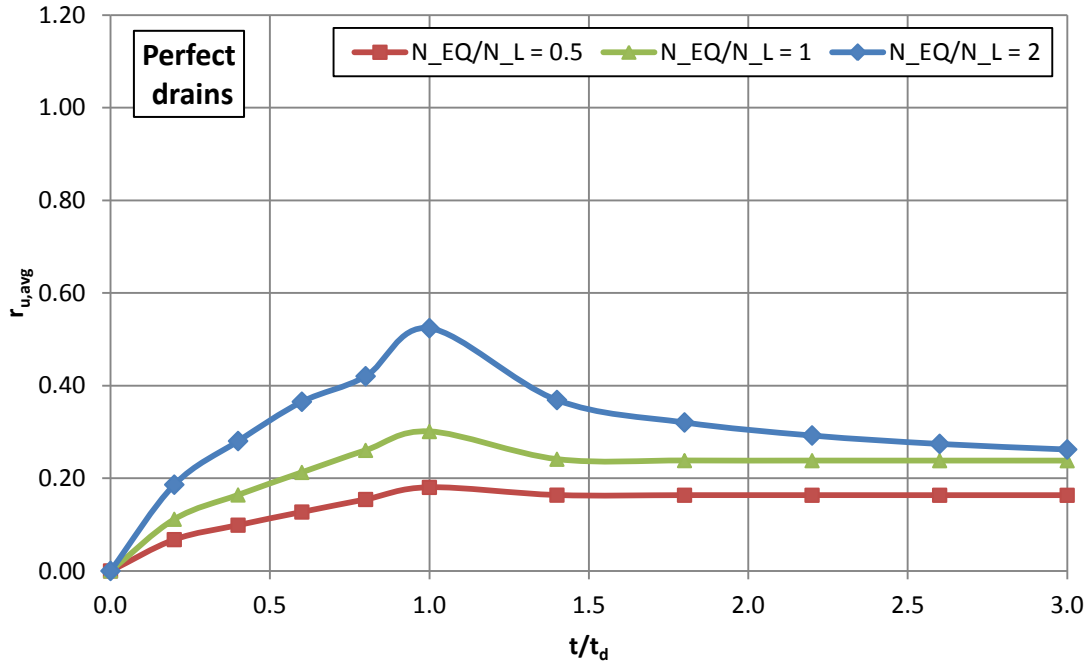

Figure 3.26: Treated $r_{u,avg}$-time histories for different values of N_{EQ}/N_L

3.5 Sensitivity: Groundwater Table and Drain Characteristics

The depth of the groundwater table is a parameter that can affect the development of excess pore pressures. As discussed in Section 3.4, the water inside the drain will rise to the ground surface during shaking and associated pore pressures are induced in the soil due to the difference in hydraulic head inside and outside the drain.

To examine the importance of this parameter, the baseline case ($z_w = 0.89\ m$) is repeated for the groundwater table at the ground surface ($z_w = 0\ m$) so that no additional pore pressures can be developed (the drain will be filled with water before shaking). The results are presented in Figure 3.27. Compared to the baseline case, the $r_{u,avg}$ for the treated site are significantly smaller and drop to zero after the end of shaking when $z_w = 0\ m$. In addition, the slopes of the $r_{u,avg}$ curves for $z_w = 0\ m$ and $z_w = 0.89\ m$ are the same for a short period of time (same rate of excess pore pressure development), but as the water accumulates in the drain for the $z_w = 0.89\ m$ case, the curves separate. Similar results are observed for the case of $k = 0.2\ cm/s$ (Figure 3.28), whereas the effect for $k = 0.005\ cm/s$ is smaller (Figure 3.29) due to the slower increase in the water level in the drain with smaller k (Figure 3.15).

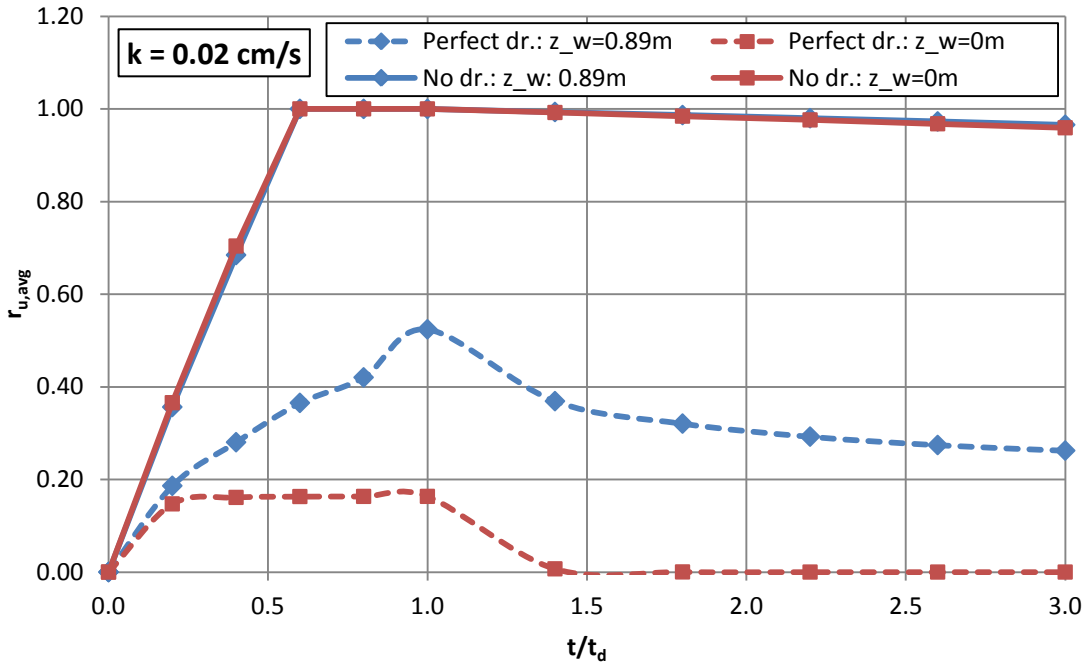

Figure 3.27: Comparison of $r_{u,avg}$-time histories for $k = 0.02\ cm/s$ and different GWT

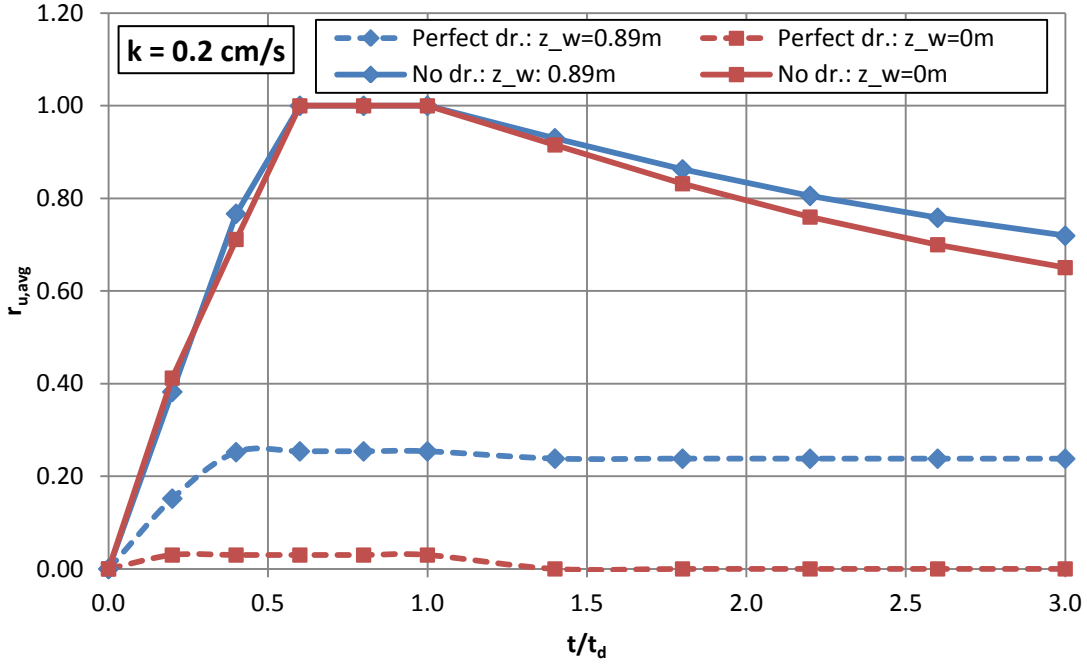

Figure 3.28: Comparison of $r_{u,avg}$-time histories for $k = 0.2\ cm/s$ and different GWT

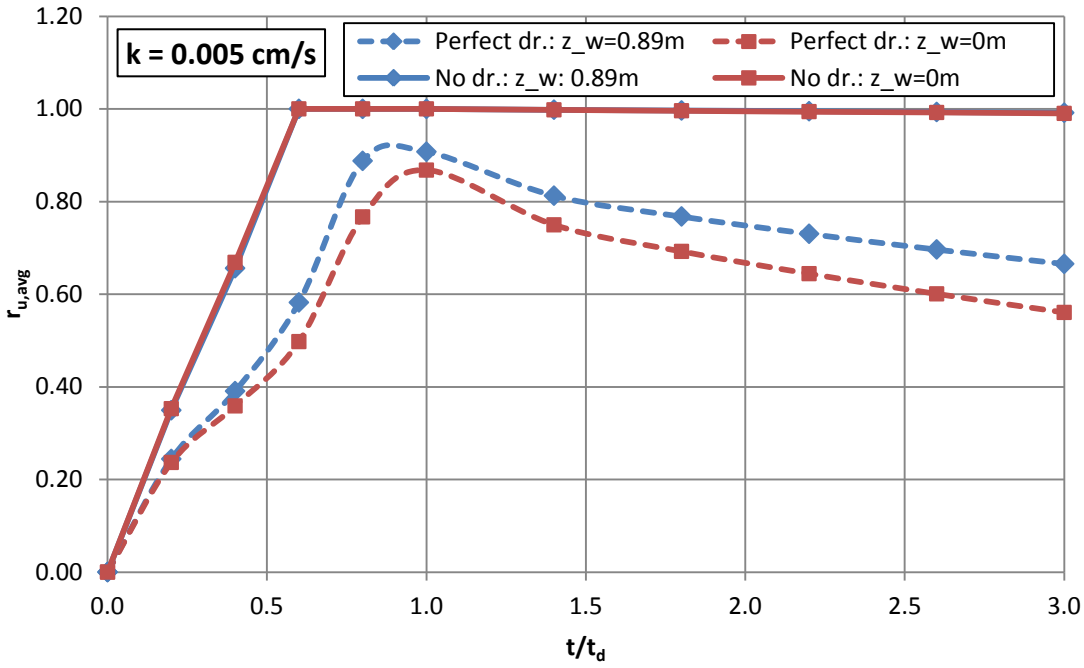

Figure 3.29: Comparison of $r_{u,avg}$-time histories for $k = 0.005\ cm/s$ and different GWT

To better understand the effect of the groundwater table location, the radial distribution of excess pore pressure is compared. Figure 3.30 shows the excess pore water pressure with depth at $r/b = 0.06 - 1.0$ (r = radial distance, b = radius of influence) for the baseline case ($z_w = 0.89\ m$) at the end of shaking. It is observed that further from the drain ($r/b > 0.35$) the upper part of the sand layer is liquefied (i.e. $\Delta u = \sigma'_v$). On the other hand, when $z_w = 0\ m$ (Figure 3.31), the excess pore pressures are significantly lower and far from the liquefaction threshold ($\Delta u = \sigma'_v$). In this case, no excess pore pressures are developed at the drain interface ($r/b = 0.06$), whereas in baseline case the hydraulic head difference induces an excess pore pressure equal to $\gamma_w z_w$ at the drain interface. At $t = 3t_d$ (Figure 3.32) the earthquake induced excess pore pressures for the case of $z_w = 0.89\ m$ have equilibrated to $\gamma_w z_w$, while for the case of $z_w = 0\ m$ they are zero.

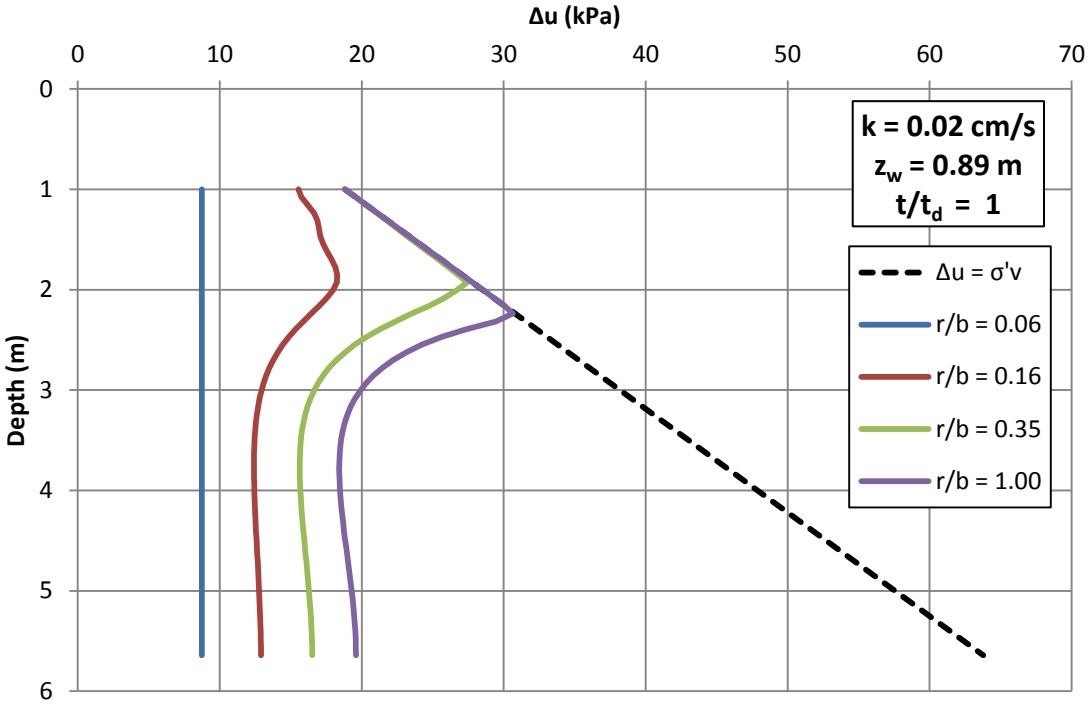

Figure 3.30: Pore water pressure distribution of baseline case at $t/t_d = 1$

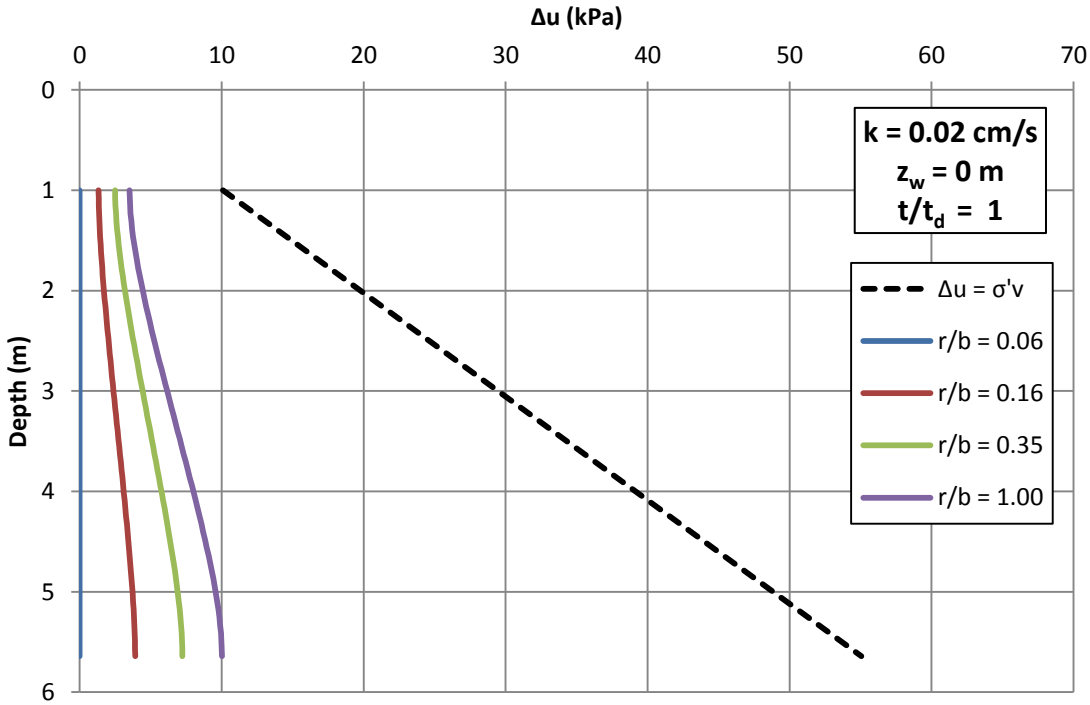

Figure 3.31: Pore water pressure distribution at $t/t_d = 1$ when $z_w = 0\ m$

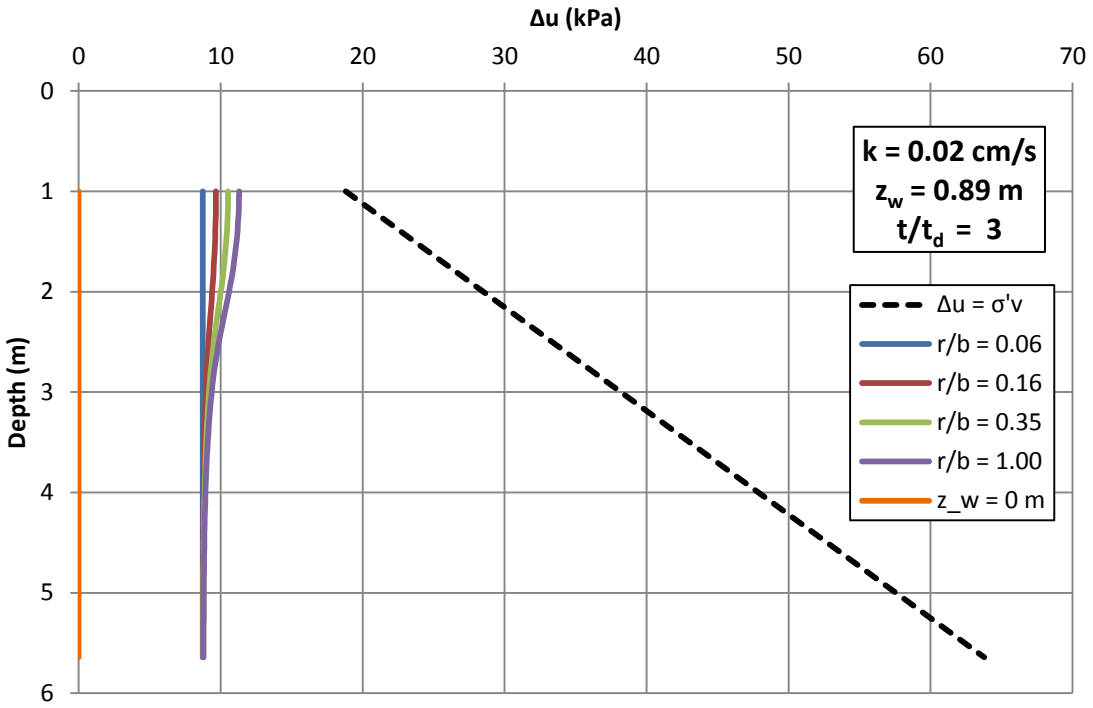

Figure 3.32: Pore water pressure distribution at $t/t_d = 3$ when $z_w = 0.89\ m$

The effect of the coefficient of consolidation (c_v) on excess pore pressure generation is affected by the rate of the water level increase inside the drain, which is mainly a function of the hydraulic conductivity of the sand, as observed in Section 3.3. To examine only the effect of c_v, the sensitivity analysis on c_v is repeated with the water table at the ground surface. The $r_{u,avg}$ time-histories are plotted in Figure 3.33 and it is observed that the range of the middle region has been narrowed and most importantly that the curve with the inconsistent response in the previous analysis (#12 – $c_v = 0.25\ m^2/s$) is now identical with the other curve of the same c_v value. To study the effect of the water table location for different c_v values, the maximum $r_{u,avg}$ are compared in Table 3.4. The performance of sands with $c_v > 0.25\ m^2/s$ (lower and middle region of Figure 3.33) is enormously improved,

namely the pore pressure ratio is smaller, when the water table is at the ground surface. On the other hand, the upper region ($c_v = 0.01 - 0.15\, m^2/s$) is almost unaffected by this change.

The analytical predictions of r_u from the JGS charts for $N_{EQ}/N_L = 2$ are also presented in Table 3.4. The predictions from the JGS charts match well with the results for $z_w = 0\, m$. Therefore, an important conclusion that can be made is that the use of design charts may be unconservative when the groundwater table is deeper than the ground surface because the design chart ignore the additional pore pressures that are developed from the accumulation of the water in the drain.

Table 3.4: Comparison of maximum $r_{u,avg}$

N_o	k (cm/s)	m_v (1/kPa)	c_v (m^2/s)	maximum $r_{u,avg}$		
				z_w = 0.89 m	z_w = 0 m	JGS charts
1	0.005	50E-05	0.01	0.93	0.91	> 0.80
2	0.02	50E-05	0.04	0.92	0.88	> 0.80
3	0.005	8.0E-05	0.06	0.91	0.88	> 0.80
4	0.005	4.0E-05	0.13	0.91	0.87	> 0.80
5	0.02	8.0E-05	0.25	0.80	0.33	0.30
6	0.005	2.0E-05	0.25	0.62	0.32	0.30
7	0.2	50E-05	0.41	0.71	0.20	0.18
8	0.02	4.0E-05	0.51	0.52	0.16	0.15
9	0.02	2.0E-05	1.02	0.32	0.10	< 0.10
10	0.2	8.0E-05	2.55	0.27	0.05	< 0.10
11	0.2	4.0E-05	5.10	0.25	0.03	< 0.10
12	0.2	2.0E-05	10.19	0.25	0.02	< 0.10

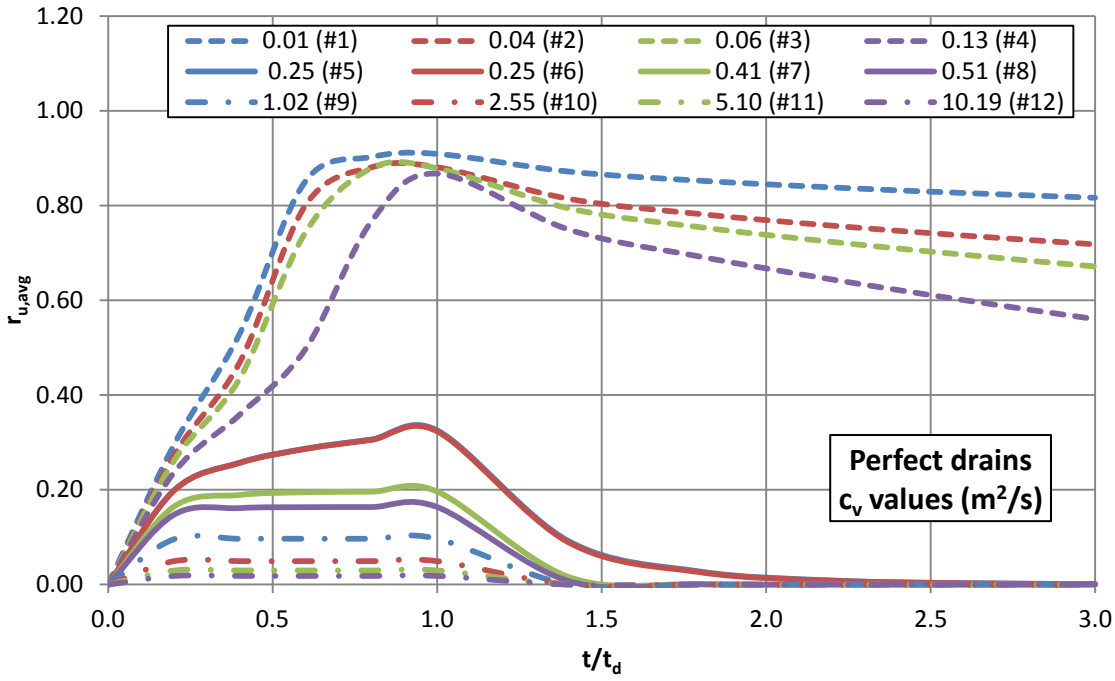

Figure 3.33: Treated $r_{u,avg}$-time histories for the same coefficient of consolidation c_v when $z_w = 0\ m$

The last parameter to be examined in this sensitivity analysis is the drain diameter. The parametric studies on the effect of the hydraulic conductivity and the depth of the water table are now repeated for a drain diameter of 76 mm (3 in.), (Figures 3.34 – 3.35). In most of the cases, the decrease in drain diameter has only a small effect on the development of excess pore pressures. The $r_{u,avg}$ of the baseline case is the only one that is noticeably increased (about 20%) when the drain diameter is 76 mm. The excess pore pressure distributions for this case are compared in Figures 3.36 and 3.37. The depth of the sand layer that has been liquefied at the end of shaking and the amount of existing pore pressure at $t = 3t_d$ are both increased when D = 76 mm because it takes a smaller volume of water to increase the water height in a 76 mm drain.

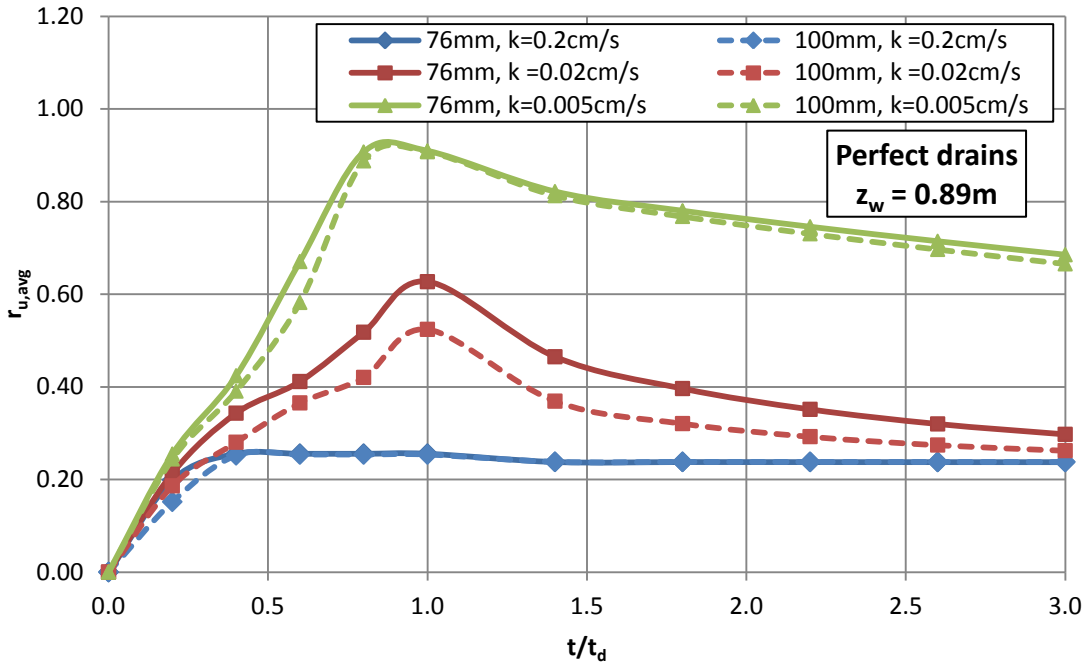

Figure 3.34: Comparison of treated $r_{u,avg}$-time histories for different D and $z_w = 0.89\ m$

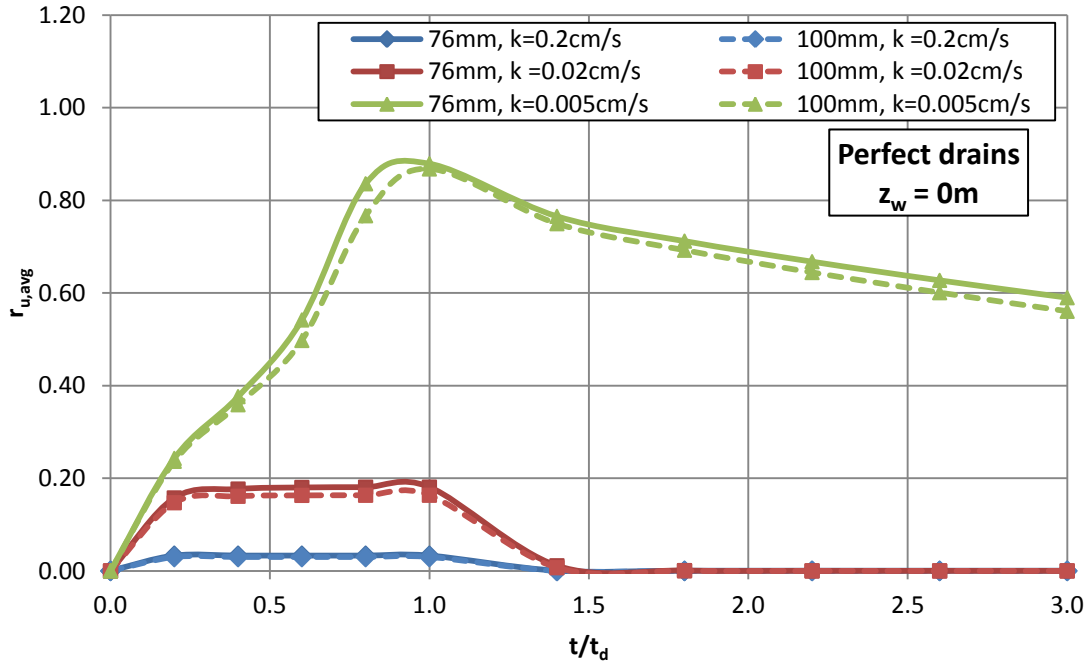

Figure 3.35: Comparison of treated $r_{u,avg}$-time histories for different D and $z_w = 0\ m$

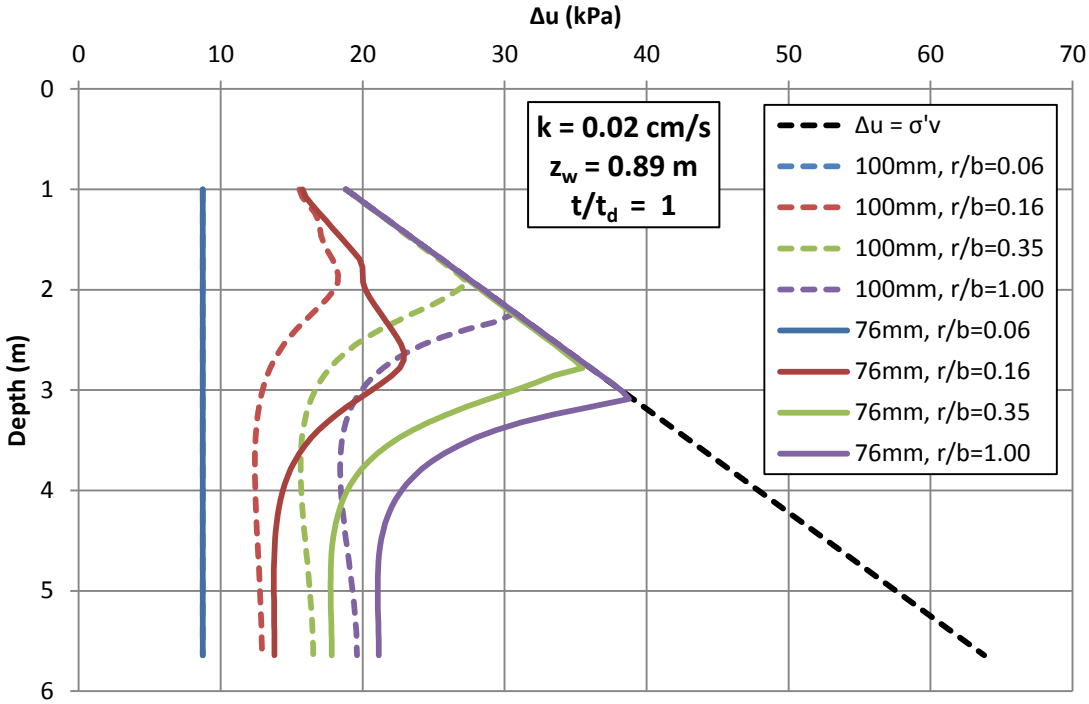

Figure 3.36: Comparison of pore water pressure distribution at $t/t_d = 1$

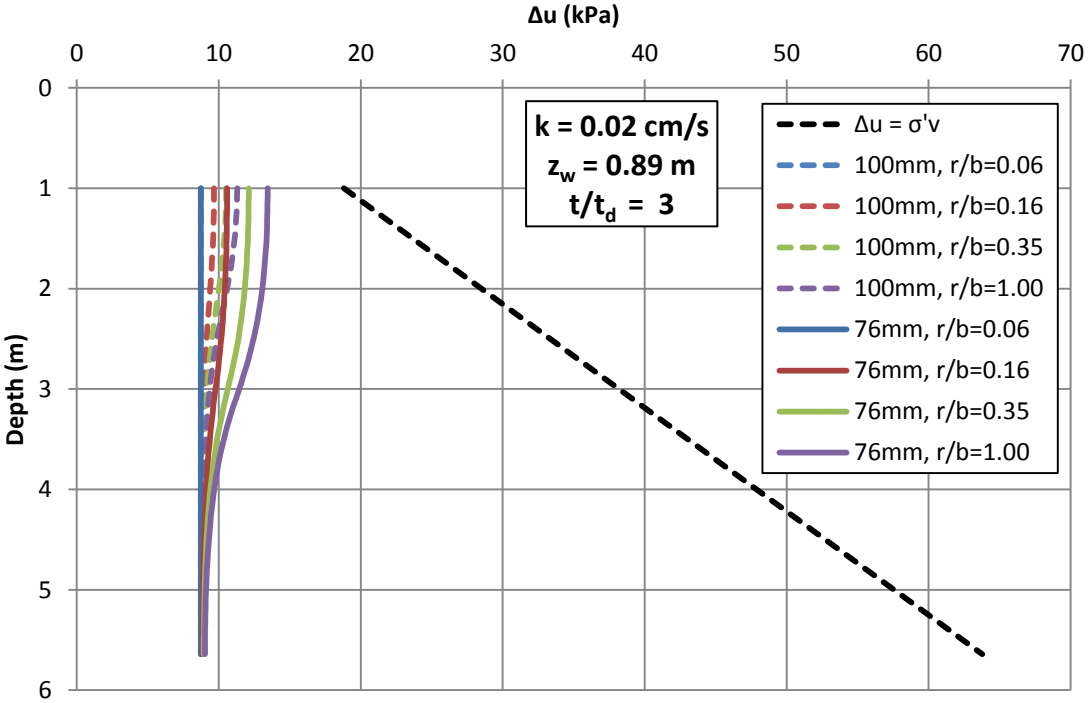

Figure 3.37: Comparison of pore water pressure distribution at $t/t_d = 3$

3.6 Summary

In this chapter, FEQDrain analyses were performed and the influence of model parameters was investigated for treated and untreated sites. The depth of groundwater table plays a significant role in soil response as additional pore pressures are induced due to the head build up in the drain. This detail is not taken into account in the design charts (Seed & Booker and JGS), which are commonly used in practice, leading to prediction of lower maximum pore pressures and hence an unconservative drain design. In addition, the effect of hydraulic conductivity is directly related to the coefficient of compressibility of the examined soil (and vice versa) and consequently these parameters should always been examined together. It was observed that the main soil parameter that drives the response is the coefficient of consolidation, which takes into account both k and m_v, as soils with c_v of the same order of magnitude exhibit similar development of excess pore pressure. The duration of motion and the equivalent number of cycles are the ground motion parameters with the most important effect on drain design and therefore they must be determined or assumed very carefully.

Chapter 4

Theoretical and Measured Excess Pore Pressures Under Harmonic Loading

4.1 Introduction

Centrifuge testing is an experimental method that can be used to study the performance of geotechnical systems under dynamic loading. Dynamic centrifuge testing involves the construction of small-scale models of geotechnical systems and the measurement of the system response under dynamic loading. The main advantage of centrifuge testing is the one –to – one scaling of stresses, which is achieved by applying an increased "gravitational" acceleration to the model in order to produce identical stresses as in the large-scale (i.e., prototype) model.

Recently, the effectiveness of prefabricated vertical drains to mitigate liquefaction was evaluated from centrifuge tests (Marinucci et al. 2008). These tests involved the measurement of pore pressures and deformations of untreated and drain-treated sites. The purpose of this chapter is to compare the experimental results with the numerical predictions of FEQDrain in terms of the excess pore pressure response.

4.2 Centrifuge model

Marinucci et al. (2008) conducted a small – scale centrifuge test (SSK01) on an untreated soil deposit and on a soil deposit treated with prefabricated vertical drains. The tests were performed in the NEES Equipment Site at the University of

California at Davis, using a flexible shear beam model container. The model consists of 2 slopes, standing at an inclination of approximately 3^{o}, and a central channel between them (Figures 4.1 and 4.2). A centrifugal acceleration (N) of approximately 15 g was applied, which results in the model representing a prototype soil deposit 15 times larger than constructed. The dimensions of the model are commonly represented in prototype units (i.e., multiplied by the centrifugal acceleration, N), and measured quantities are scaled to represent the prototype system using scaling laws. Three soil layers are found in the model: (1) a 0.75 m thick (prototype) bottom layer of dense Nevada sand overlain by (2) a 4.8 m thick liquefiable layer of loose Nevada sand overlain by (3) 1 m thick crust of compacted Yolo Loam. The material properties of each layer are presented in Table 4.1 (Marinucci, 2010). One of the sloping sides is treated with 58, 7-mm inner diameter, perforated, nylon tubes that are covered with thin fabric. These tubes represent prototype prefabricated vertical drains with 100 mm inner diameter. The vertical drains are placed in a triangular pattern at a center – to – center distance of 1.5 m (prototype scale). The instrumentation included 13 displacement transducers, 57 pore pressure transducers (PPTs), and 58 accelerometers. The PPTs are appropriately placed in order to form one vertical, one radial and two horizontal arrays in each side.

Table 4.1: Soil properties of the centrifuge model (prototype scale) Marinucci (2010)

Soil Property	**Clay Crust**	**Loose Sand**	**Dense Sand**
Layer Thickness - H (m)	1.00	4.2 - 4.8	0.75
Hydraulic Conductivity - k (cm/s)	$2x10^{-5}$	0.03	0.03
Volumetric Compressibility - m_v (1/kPa)	$4x10^{-6}$	$4x10^{-5}$	$4x10^{-5}$
Total Unit Weight - γ (kN/m^3)	19.9	19.5	20.3
Relative Density - D_R (%)	-	40	85

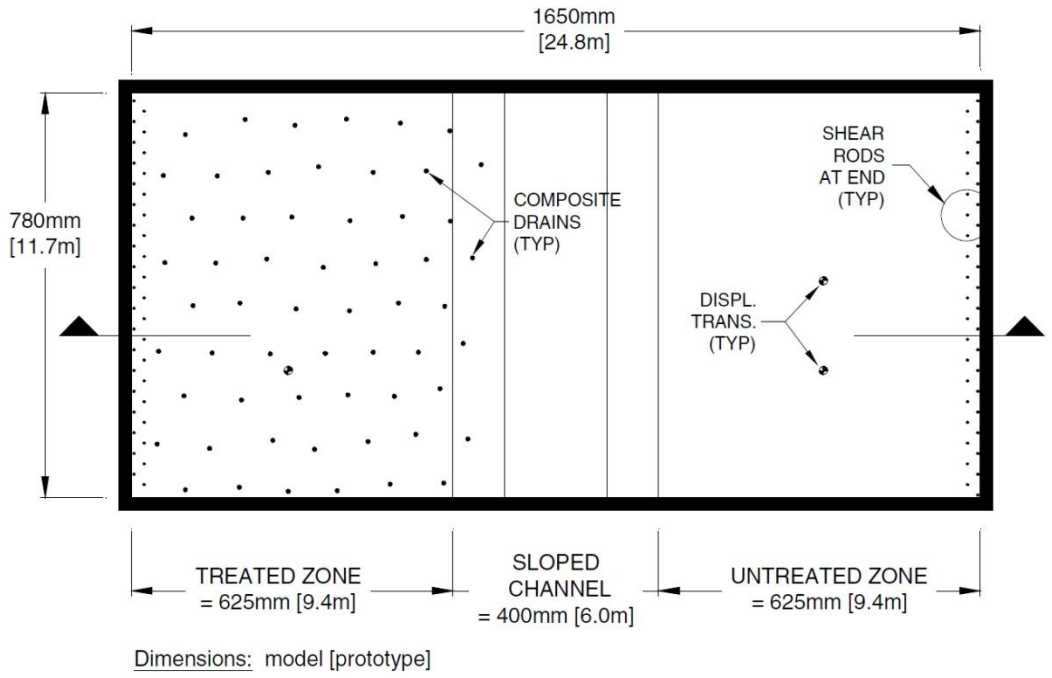

Figure 4.1: Plan view of the model geometry (Marinucci et al., 2008)

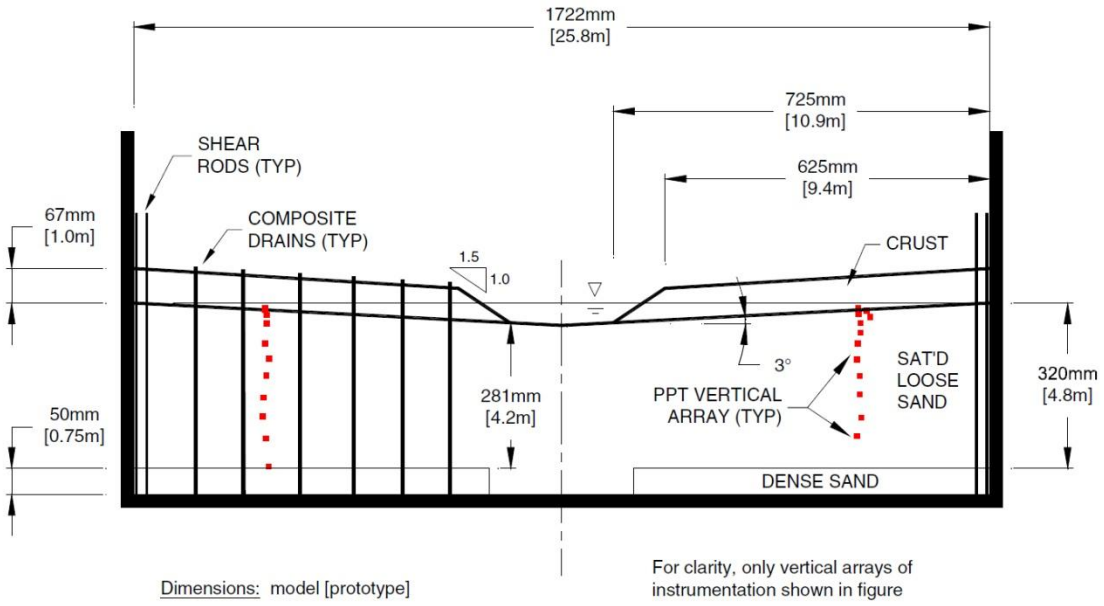

Figure 4.2: Cross-sectional view of the model geometry (Marinucci et al., 2008)

The centrifuge model was subjected to 12 shaking events, each consisting of 20 cycles of sinusoidal motion at a (prototype) frequency of 2 Hz (duration of shaking: $t_d = 10\ sec$). Shaking was applied in the horizontal direction parallel to the slopes shown in Figure 4.2. The drain performance was evaluated only by the last five shaking events (Shakes 8 – 12), as the earlier events were of very small amplitude and were used for the verification of the equipment.

The input peak ground acceleration at the base of the model (PGA_{base}) and the maximum r_u measured in the treated and untreated vertical pore pressure arrays are listed in Table 4.2. PGA_{base} ranged from 0.01 to 0.35 g for the five shaking events. Very small excess pore pressure ($r_u < 0.2$) are developed in the soil deposit under shaking events 8 and 9, even in the untreated side, because of the small amplitude of the base peak ground acceleration. The excess pore pressure ratio-time histories and the recorded base acceleration time – histories of the vertical arrays both on the treated and untreated sides are plotted in Figures 4.3, 4.4, and 4.5 for Shakes 10, 11 and 12, respectively. The soil deposit on the untreated side liquefies under all three of these shaking events, while the presence of vertical drains reduces significantly the developed excess pore pressure ratio, and hence liquefaction is mitigating. As a result, the effectiveness of PVDs is successfully demonstrated.

Table 4.2: Recorded base PGA and maximum r_u at the vertical arrays (prototype scale)

Shake No.	**PGA_{base} (g)**	**maximum r_u**	
		Untreated	**Treated**
8	0.01	0.04	0.01
9	0.04	0.09	0.17
10	0.09	0.8	0.91
11	0.13	0.88	0.92
12	0.35	1.00	0.96

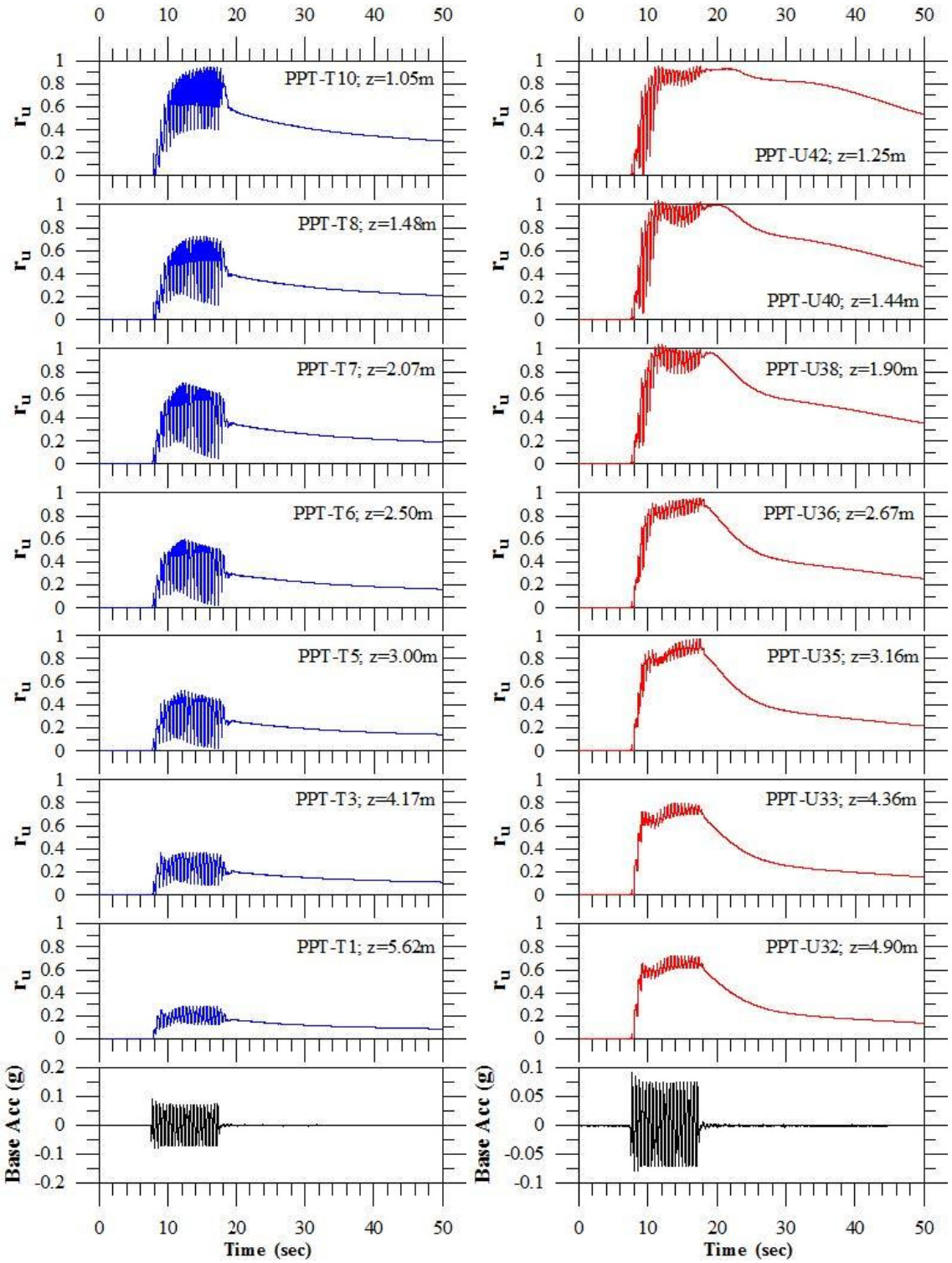

Figure 4.3: Base acceleration and r_u-time histories for the vertical arrays in the (a) treated and untreated sides of the centrifuge model for Shake 10 (Marinucci, 2010)

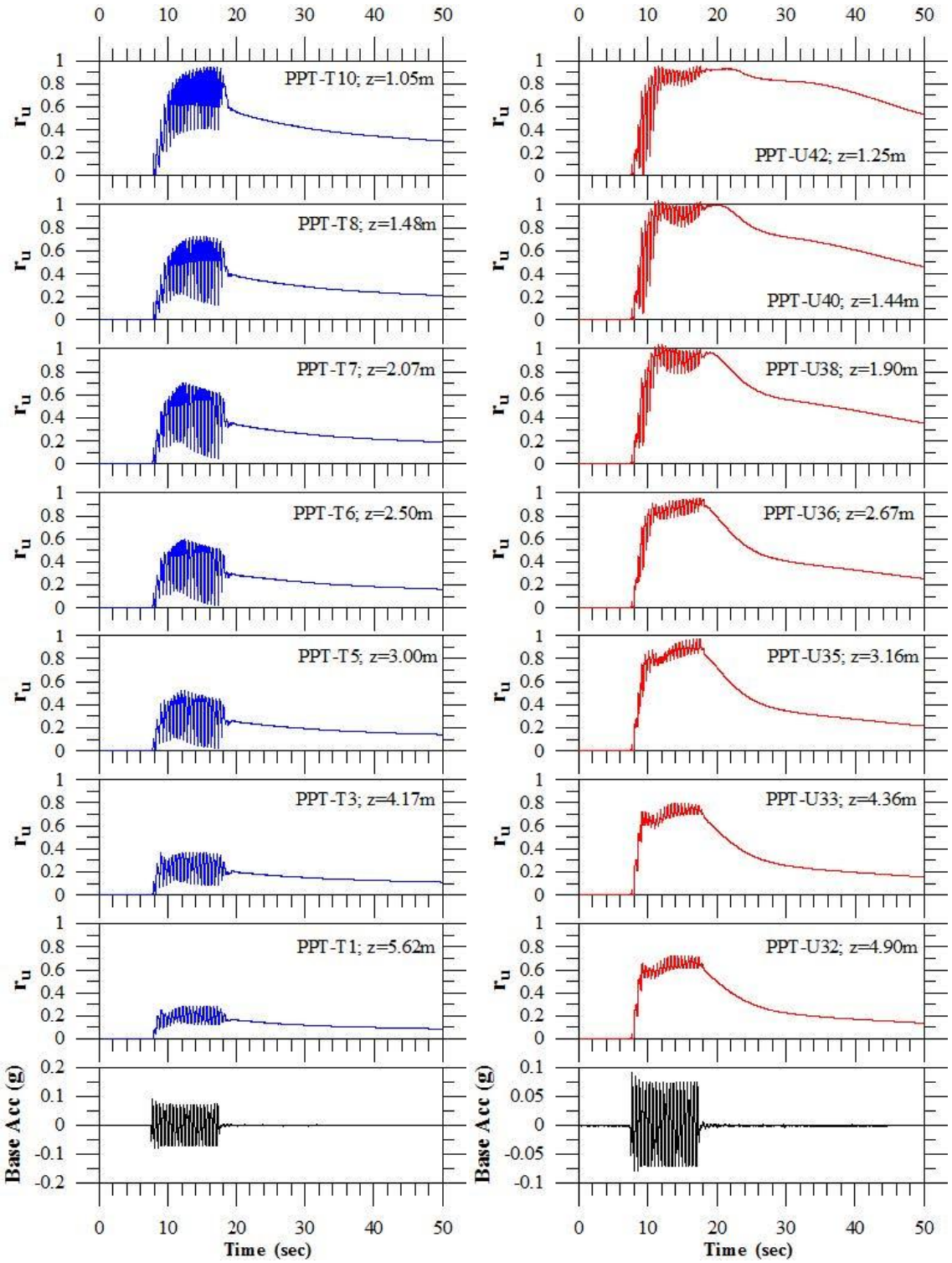

Figure 4.4: Base acceleration and r_u-time histories for the vertical arrays in the (a) treated and untreated sides of the centrifuge model for Shake 11 (Marinucci, 2010)

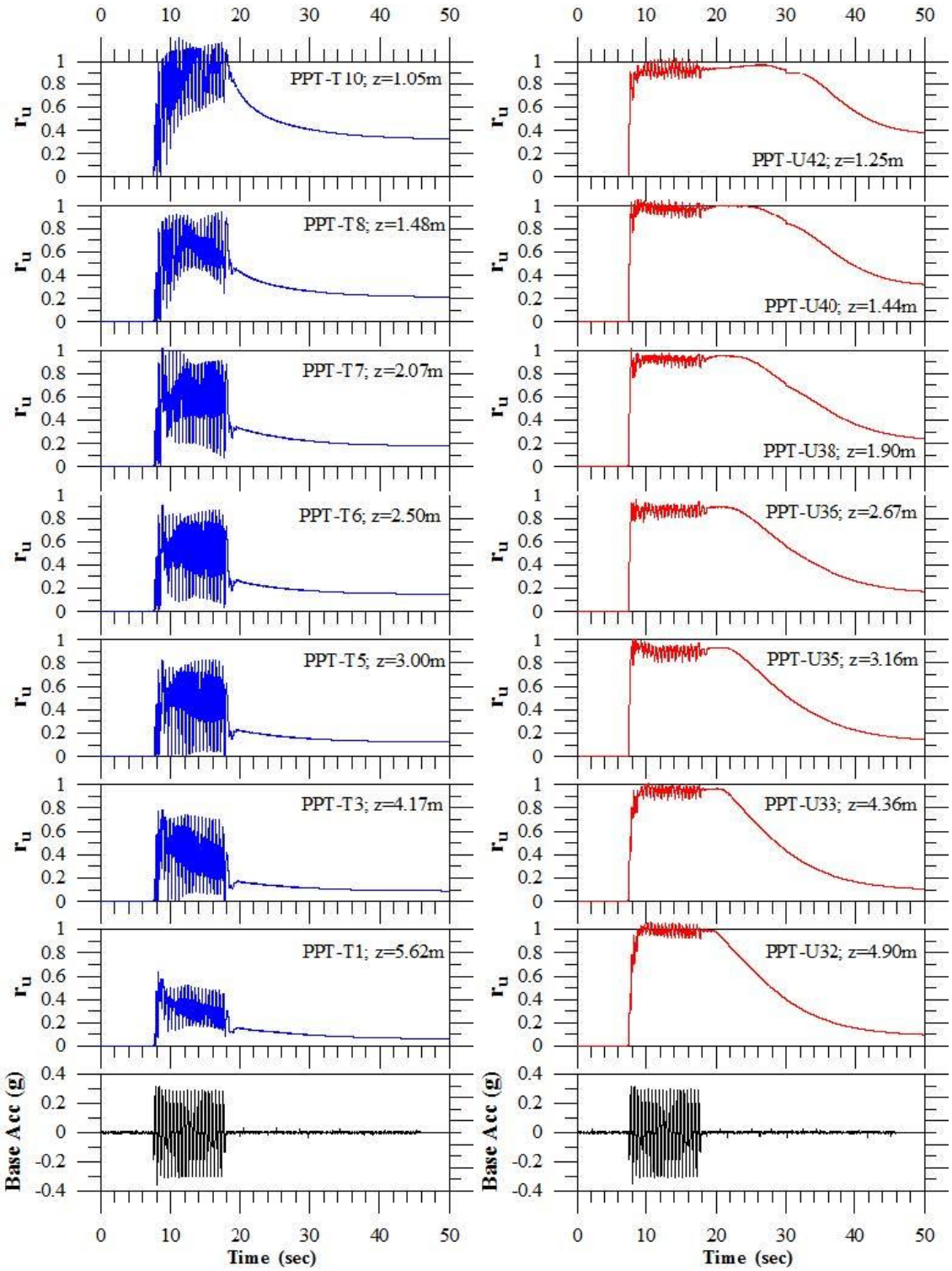

Figure 4.5: Base acceleration and r_u-time histories for the vertical arrays in the (a) treated and untreated sides of the centrifuge model for Shake 12 (Marinucci, 2010)

4.3 Comparison with numerical predictions

To compare numerical predictions of pore pressure generation with the measured pore pressure responses in the centrifuge tests a model in FEQDrain is considered. The comparison between the numerical predictions and the experimental results will focus on the average excess pore pressure ratio ($r_{u,avg}$) that was developed in the location of the vertical array during Shakes 10, 11 and 12. The measured values of $r_{u,avg}$ are derived from the vertical pore pressure arrays. This calculation involves normalizing the measured Δu at each sensor by the estimated vertical effective stress to calculate r_u at each sensor, and then averaging the calculated $r_{u,avg}$ over depth using a weighting scheme based on the spacing between sensors (Howell et al. 2012). This approach assumes that there is no radial variation in Δu, and this assumption was confirmed by Marinucci (2010) using the radial array data measured in the experiments. The resulting measured $r_{u,avg}$ – time histories are plotted in Figure 4.6 for the treated and untreated sides of the model.

The model geometry that was used for the sensitivity analysis in Chapter 3 (Figure 3.1) was developed to model the experiments and consequently it will be used for the numerical evaluation here. In particular, the model consists of 4.6 m thick loose sand layer with a 1 m thick clay cap, while the depth of water table is 0.89m. It must be stated that the bottom layer of dense sand is not included in the numerical model because it cannot liquefy and therefore the drain performance is not affected by its presence. The soil properties of Table 4.1 are used in the numerical analyses, whereas the drain and the ground motion characteristics used in the analyses are presented in Table 4.3. It must be noted that FEQDrain can only represent level ground conditions and hence the inclination of the soil surface in the centrifuge test cannot be taken into account in the numerical analyses. However, it is

estimated that the effect of this limitation will be minor on the pore pressure response due to the small inclination of the sloping ground (3°).

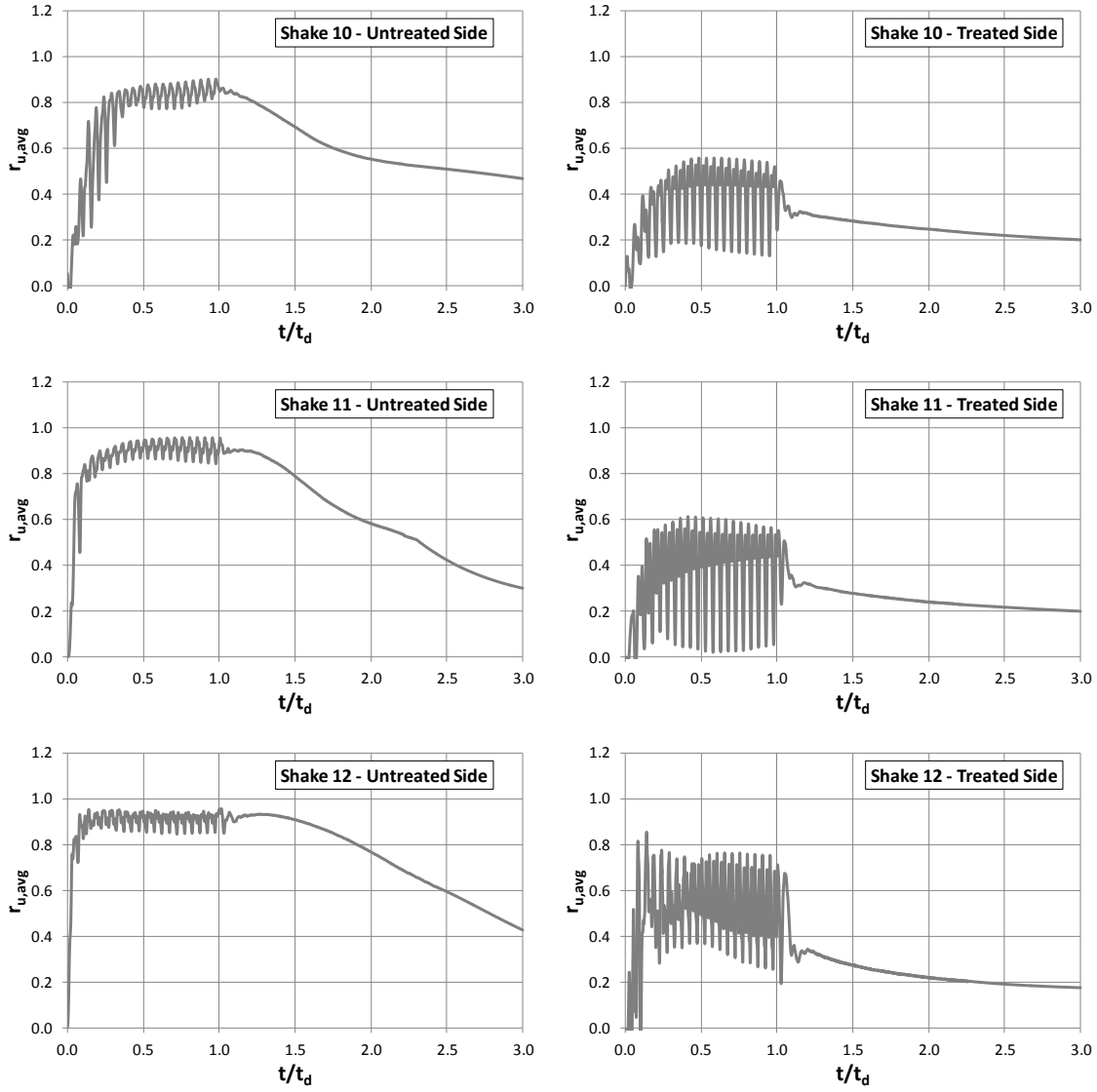

Figure 4.6: Average excess pore pressure ratio ($r_{u,avg}$) time histories for the vertical arrays in the (a) untreated and (b) treated sides of the centrifuge model for Shakes 10, 11 and 12

Table 4.3: Drain and ground motion characteristics used in the numerical model

Drain Diameter - D_w (m)	0.1016
Center-to-Center Drain Spacing - s (m)	1.50
Material Constant for Vertical Resistance - C_1 (s^2/m^6)	458.76
Material Constant for Vertical Resistance - C_2	2
Area of Openings (per unit length) - Orf (m^2/m)	0.004021
Permittivity of Drain Fabric (1/sec)	0.08325
Duration of Shaking - t_d (sec)	10
Equivalent Number of Cycles - N_{EQ}	20

The only input soil parameter that remains unknown is the number of cycles required to cause liquefaction (N_L). However, as the ground motion is sinusoidal with constant frequency (2Hz), the number of cycles is directly related to the recorded time (product of time and frequency). To calculate N_L, the time when $r_{u,avg}$ initially reaches the liquefaction threshold on the untreated side is graphically determined (Figure 4.7). Due to the sloping ground surface, the liquefaction threshold is considered to be slightly lower than $r_u = 1.0$ and take as approximately equal to $r_u = 0.92$. This number represents the mean $r_{u,avg}$ in Shakes 11 and 12 after a constant value is reached. As shown in Figure 4.7, $N_L = 10$ for Shake 10 ($N_{EQ}/N_L = 2$), $N_L = 6$ for Shake 11 ($N_{EQ}/N_L = 3.3$) and $N_L = 2.5$ for Shake 12 ($N_{EQ}/N_L = 8$).

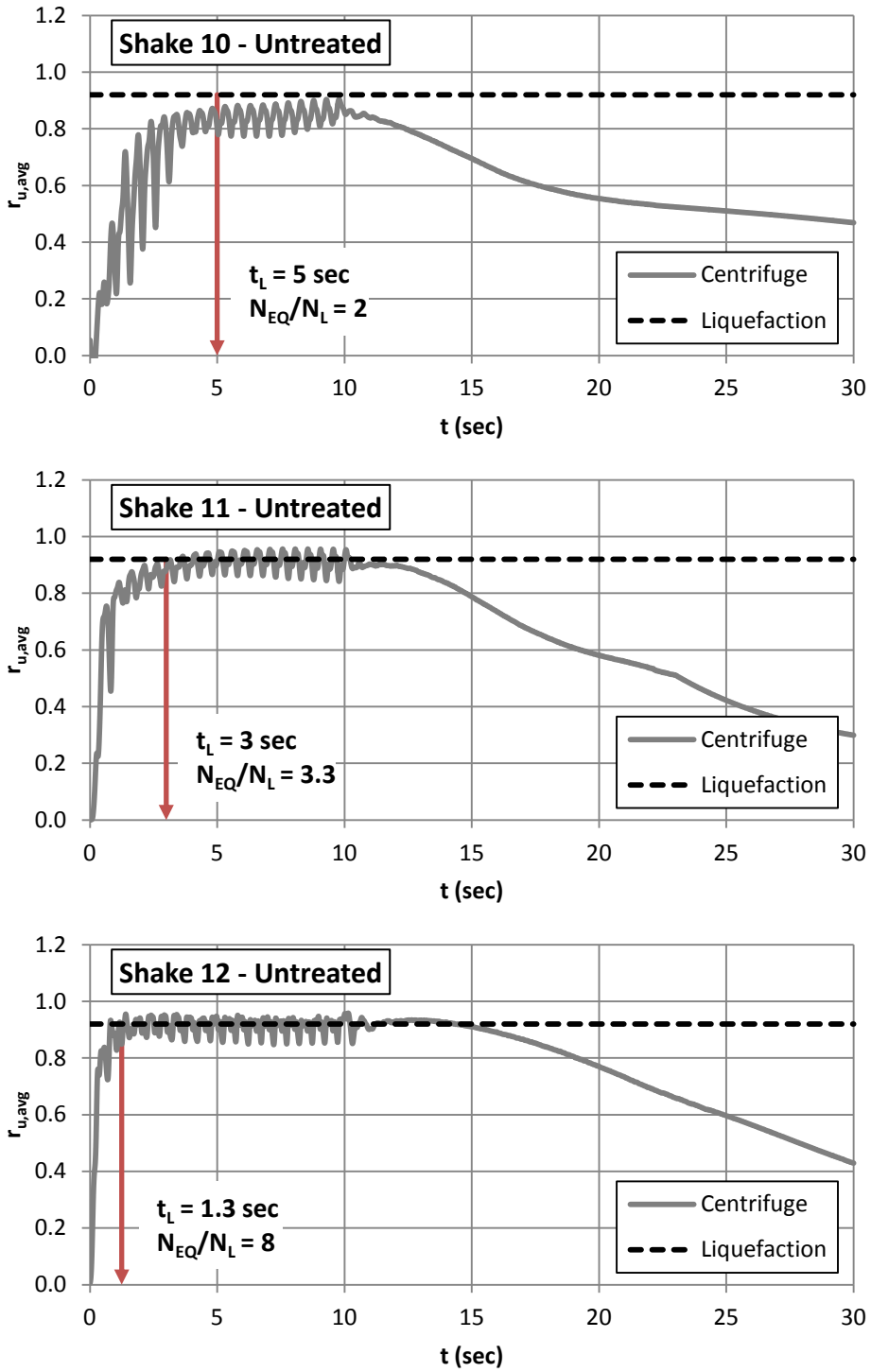

Figure 4.7: Determination of liquefaction time for (a) Shake 10, (b) Shake 11 and (c) Shake 12 from the untreated $r_{u,avg}$-time histories

Knowing the number of cycles, the exponent "A", which controls the shape of the pore pressure generation function of Seed et al. (1975), can be estimated. The $r_{u,avg}$ on the untreated side for each shaking event is plotted in Figure 4.8 as a function of the number of cycles, normalized by N_L, and it is compared with the shape of the pore pressure generation function for different values of A. As shown in Figure 4.8, the typical value of $A = 0.7$ is unrepresentative for these shaking events as the soil deposit exhibits a sudden increase in pore pressure from the first ground motion cycles. To match the experimental results, the value of $A = 7.0$ must be used, which is much larger than values that have been recommended in the past. For this reason, the value of $A = 2.0$ is adopted for all the FEQDrain analyses, because it represents the upper bound of the A values that has been recommended in the literature.

Knowing all the input parameters, the FEQDrain analyses are performed assuming the ground motion characteristics of Shakes 10 – 12 and considering both untreated and drain – treated conditions. The numerical predictions of the $r_{u,avg}$ time – histories are compared with the experimental results for the untreated and the treated sides in Figure 4.9 and 4.10, respectively.

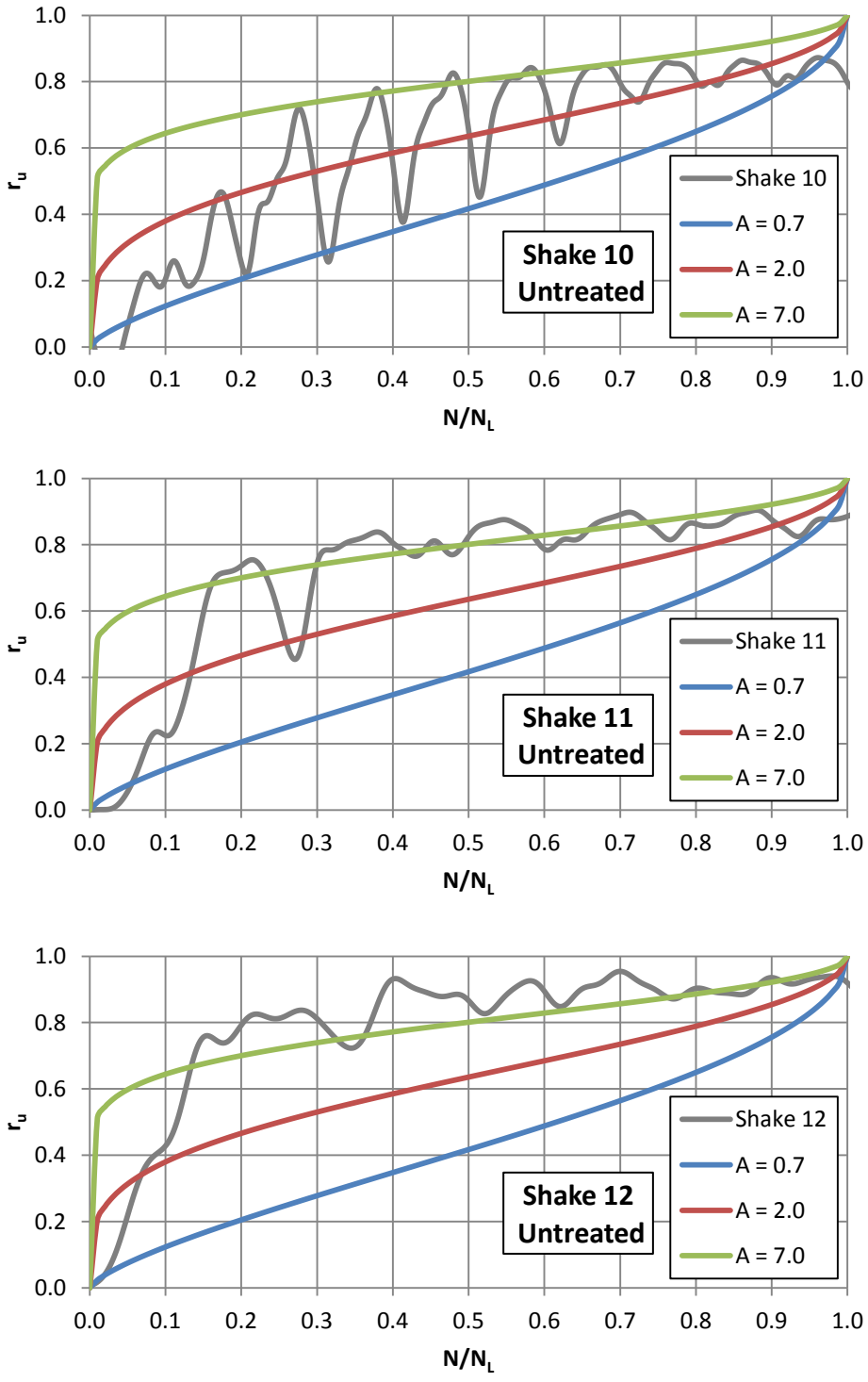

Figure 4.8: Determination of exponent A for (a) Shake 10, (b) Shake 11 and (c) Shake 12 from the untreated $r_{u,avg}$ versus N/N_L

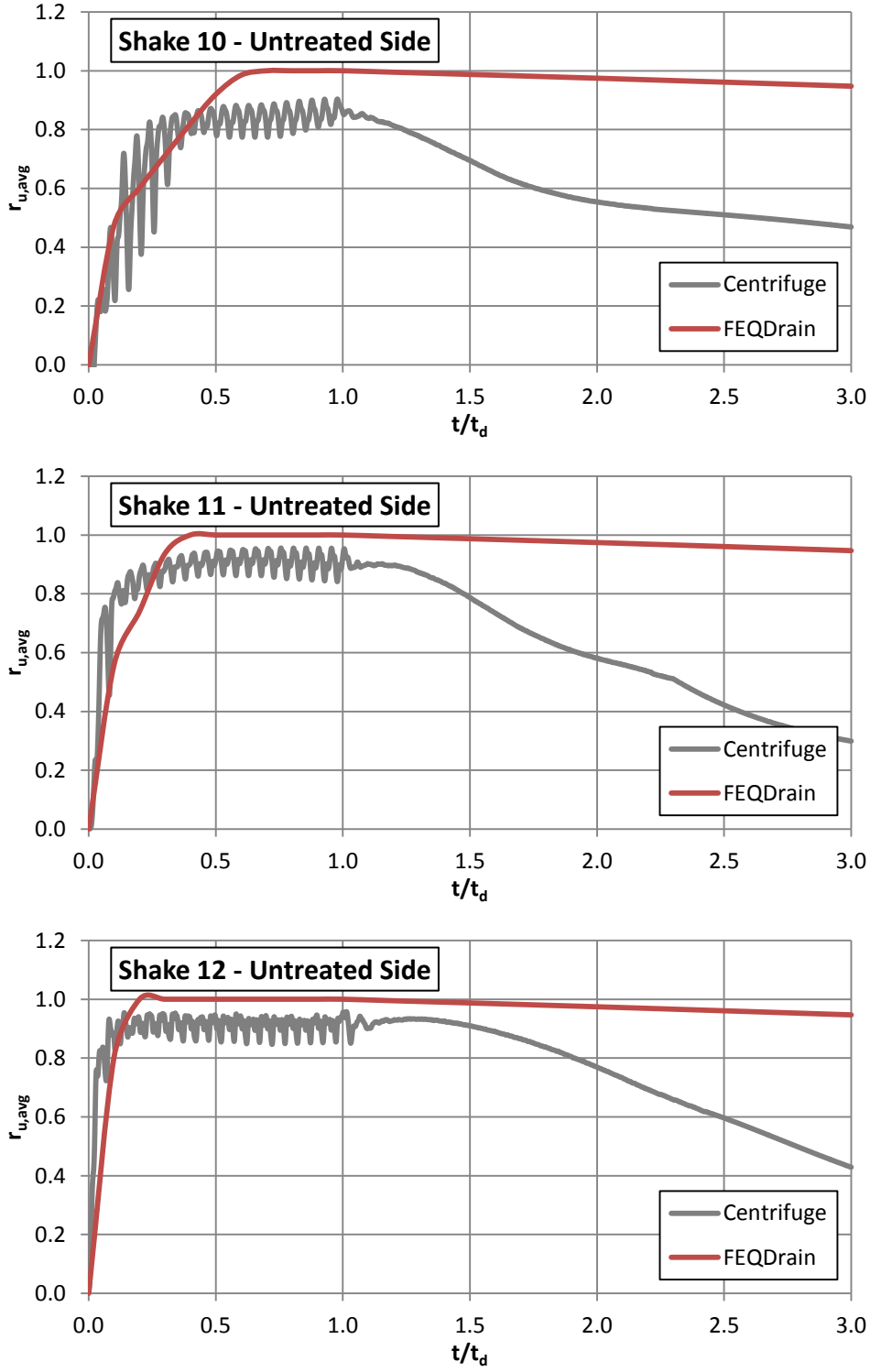

Figure 4.9: Comparison of experimental and numerical untreated $r_{u,avg}$-time histories for (a) Shake 10, (b) Shake 11 and (c) Shake 12

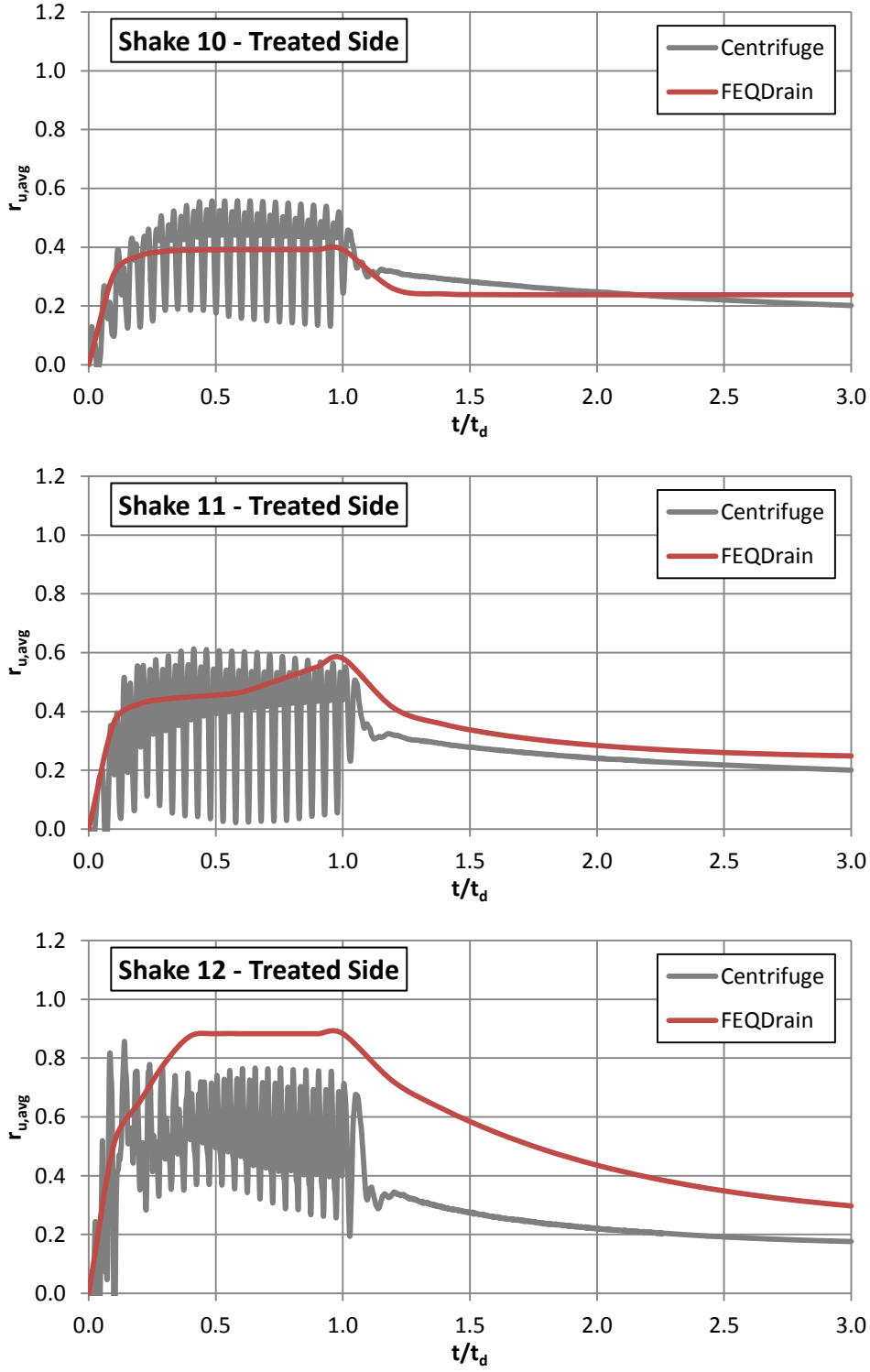

Figure 4.10: Comparison of experimental and numerical treated $r_{u,avg}$-time histories for (a) Shake 10, (b) Shake 11 and (c) Shake 12

The comparisons between the $r_{u,avg}$ – time histories on the untreated side (Figure 4.9) indicate that the build – up in the pore pressure ratio in the FEQDrain results is in good agreement with the experimental results for all shaking events. This is not surprising because the value of N_{EQ}/N_L for each shaking event was selected based on the observed occurrence of liquefaction. Unlike the experimental results, the maximum $r_{u,avg}$ of the numerical analyses reaches 1.0 in all shaking events. The reason is the fact that FEQDrain cannot take into account the existence of static shear stresses in sloping ground, the presence of which limits the maximum possible decrease in effective stress. After the end of shaking ($t/t_d > 1$), the excess pore pressures are dissipating significantly faster in the centrifuge tests compared to the FEQDrain predictions. For example, at $t/t_d = 3$ the experimental $r_{u,avg}$ has been decreased approximately 30 – 50% from its maximum value (depending on the shaking event), whereas the decrease in the numerical predictions is only 5 %. This inconsistency in the response is due to the fact that in the centrifuge model the excess water was draining not only vertically, as it is assumed in the numerical analyses, but also horizontally through the central channel and through any cracks in the clay cap caused by the laterally spreading ground.

Comparing the $r_{u,avg}$ – time histories for the treated side (Figure 4.10), a generally good correlation is observed between the numerical predictions and the experimental results. In particular, the curves are almost identical at the beginning of shaking ($t/t_d < 0.2$). After this time period, the FEQDrain curve for Shake 10 reaches its maximum value ($r_{u,avg} \cong 0.40$) and it remains constant until the end of shaking. However, the maximum $r_{u,avg}$ is somewhat smaller than the experimental one ($r_{u,avg} \cong 0.55$). For $t/t_d > 1$ both curves attenuate in a similar way, indicating that the rate of dissipation of excess pore pressure to the drain is almost the same in

both models. The best fit of the results occurs for Shake 11, in which the maximum $r_{u,avg}$ is essentially matched. The only noticeable difference is on the shape of the $r_{u,avg}$ curves. More specific, the numerical $r_{u,avg}$ plateaus at around 0.45 and then starts to increase more rapidly near the end of shaking, whereas in the centrifuge test the maximum value is been reached earlier ($t/t_d < 0.5$) and no increase is observed near the end of shaking. The FEQDrain curve for Shake 12 peaks at the same $r_{u,avg}$ value with the centrifuge test and the shape of the experimental curve is, in overall, matched. The excess pore pressure ratio increases in two stages with constant rate (linear curves) until $t/t_d \cong 0.4$, when the maximum value is reached ($r_{u,avg} \cong 0.9$). The numerical curve remains constant at this value until the end of shaking and then the dissipation of excess pore pressures is significantly slower compared to the experimental curve.

The comparison of the "treated" r_u – time histories at the top and at the bottom of the liquefiable sand layer (Figure 4.11) indicates generally similar behavior with the $r_{u,avg}$ curves. The only significant difference is found for Shake 12, in which the FEQDrain curve at the bottom of the layer fits initially the experimental results, but at $t/t_d \cong 0.4$ it increases suddenly to $r_u = 0.8$, whereas the recorded r_u is about 0.5, and then it remains constant at this value until the end of shaking.

The comparison of the $r_{u,avg}$ – time histories indicated that the numerical predictions are in good agreement with the experimental results. However, the question that is raised in any comparison with experimental data is the estimation of soil properties for use in the analyses. The biggest uncertainty lies on the values of the hydraulic conductivity and the coefficient of volumetric compressibility, namely the parameters that, as shown in Chapter 3, affect significantly the generation of excess pore water pressures. To cover any possible range of soil

properties, a sensitivity analysis of both k and m_v is performed in FEQDrain. It must be noted that only the results for the treated side will be presented in this set of sensitivity analysis due to the limited effect on the response of the untreated side.

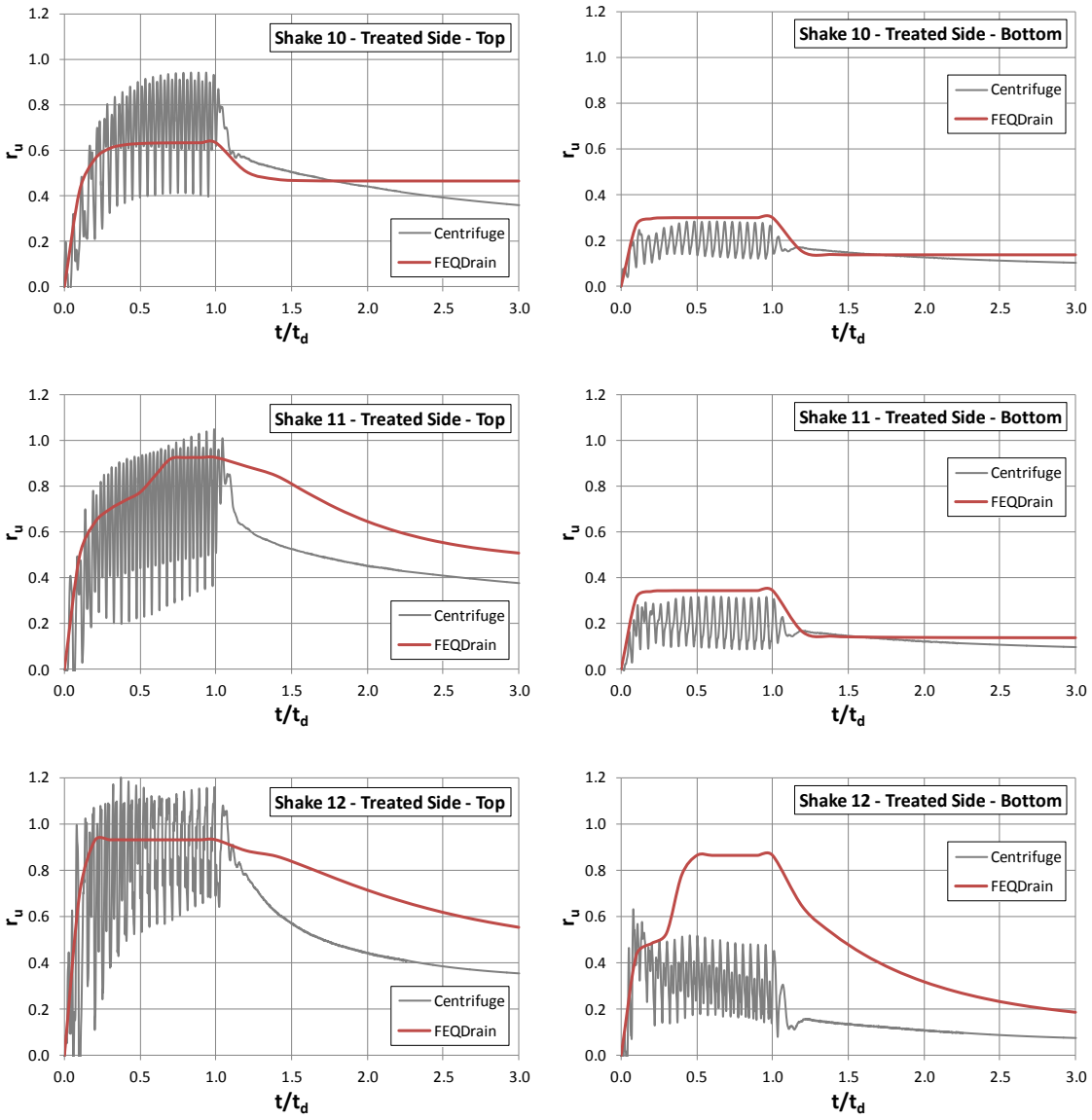

Figure 4.11: Comparison of experimental and numerical treated r_u-time histories at different depths for (a) Shake 10, (b) Shake 11 and (c) Shake 12

For the sensitivity analysis of the hydraulic conductivity, the k of sand layer is taken as 0.02 cm/s, 0.03 cm/s (baseline) and 0.04 cm/s. Namely, the baseline k value is altered by only 0.01 cm/s, which represents a very narrow range of k. The numerical $r_{u,avg}$ – time histories for these k values are compared with the experimental results for Shakes 10 – 12 in Figure 4.12.

For Shake 10, only a small variation in $r_{u,avg}$ is observed when the hydraulic conductivity is altered. More specific, as the k value is decreased, the curves are slightly raised to higher $r_{u,avg}$ levels without any differences to the curve shape. Practically, the response for Shake 10 is considered to be insensitive to these small changes in hydraulic conductivity.

The most interesting sensitivity results concern Shake 11, in which the baseline numerical predictions are in a very good agreement with the experimental data. In this case, the $r_{u,avg}$ curves are significantly affected both in shape and magnitude by even a small variation in k, leading to increasingly different pore pressure responses relative to the centrifuge results. More specific, the new curves are identical to the initial one up to $r_{u,avg} \cong 0.4$ and then the curve with $k = 0.04\ cm/s$ remains constant to this value, whereas the curve for $k = 0.02\ cm/s$ increases to a maximum value of $r_{u,avg} \cong 0.7$ at the end of shaking.

Comparing the numerical results for Shake 12, it is concluded that the pore pressure response is practically unaffected by the variation of k. In particular, the maximum $r_{u,avg}$ remains the same as in the baseline case, but it is reached earlier as k decreases, and then it remains constant at this value until the end of shaking. This fact probably indicates a limitation of FEQDrain in terms of the maximum pore pressure ratio that can be developed for a drain – treated soil deposit.

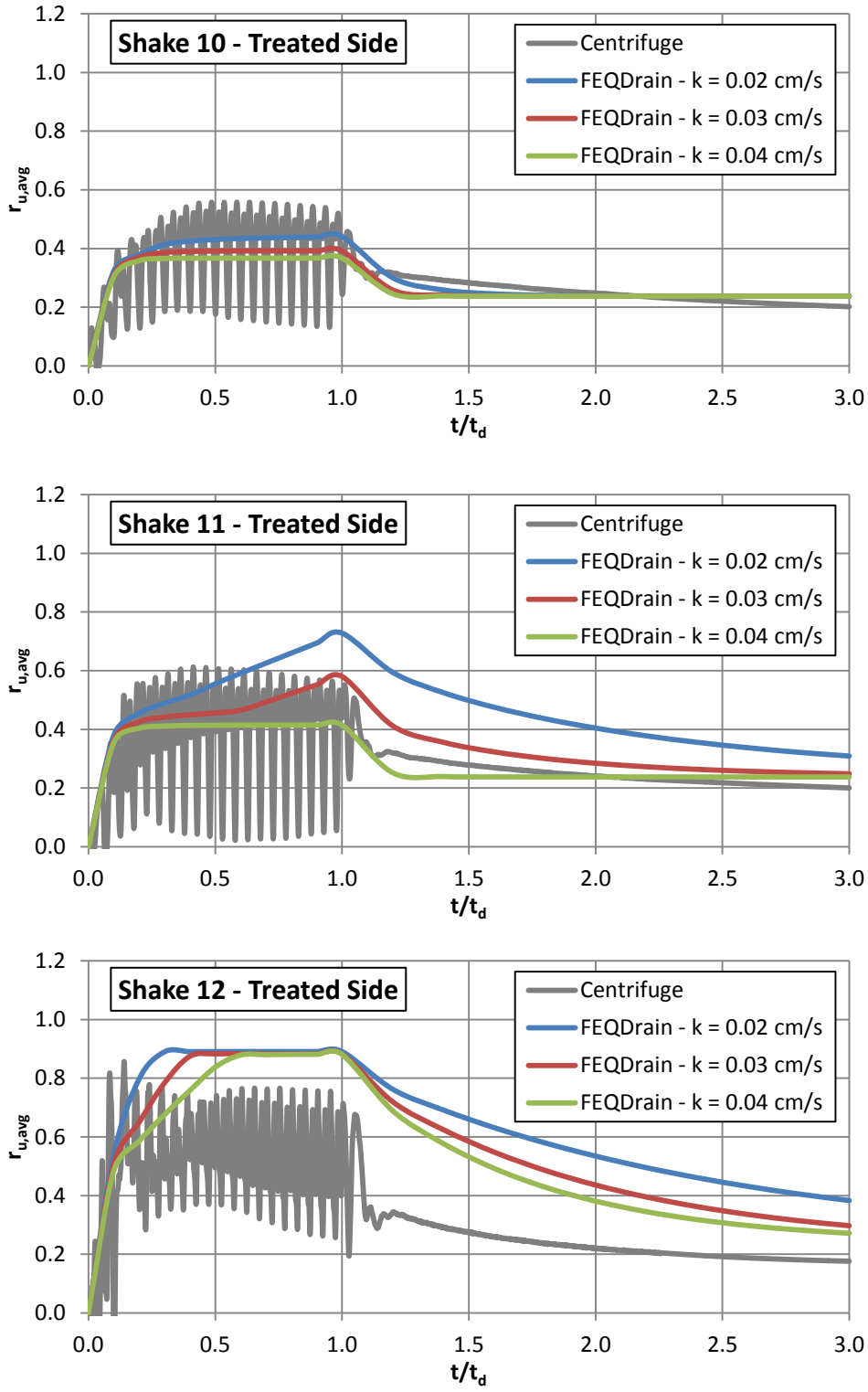

Figure 4.12: Comparison of experimental and numerical treated $r_{u,avg}$-time histories of (a) Shake 10, (b) Shake 11 and (c) Shake 12 for different values of hydraulic conductivity k

The next sensitivity analysis involves the variation in the coefficient of volumetric compressibility, which is the soil property that is the most difficult to determine. The baseline value of m_v used in the previous analyses was $4x10^{-5}$ $1/kPa$. Unlike the sensitivity analysis of k, in which the k values were selected in advance, the m_v values are intentionally selected in order to provide the best match between the experimental and the numerical $r_{u,avg}$ time – histories for each shaking event (mainly Shake 11). This procedure is repeated for each of the hydraulic conductivity values that was previously used (k = 0.02, 0.03 and 0.04 cm/s). The $r_{u,avg}$ time – histories for each combination of k and m_v are compared in Figures 4.13 – 4.15 and the maximum $r_{u,avg}$ values are summarized in Table 4.4.

Table 4.4: Computed maximum $r_{u,avg}$ for different values of k and m_v for the treated condition

k (cm/s)	**m_v (1/kPa)**	**maximum $r_{u,avg}$**		
		Shake 10	***Shake 11***	***Shake 12***
0.02	2.0E-05	0.37	0.41	0.88
0.02	2.5E-05	0.39	0.50	0.88
0.02	3.0E-05	0.40	0.63	0.89
0.03	*3.0E-05*	0.37	0.41	0.88
0.03	*4.0E-05*	0.39	0.58	0.88
0.03	*5.0E-05*	0.41	0.68	0.89
0.04	*4.0E-05*	0.37	0.41	0.88
0.04	*5.0E-05*	0.39	0.53	0.88
0.04	*6.0E-05*	0.40	0.65	0.89
Centrifuge Results		0.56	0.61	0.86

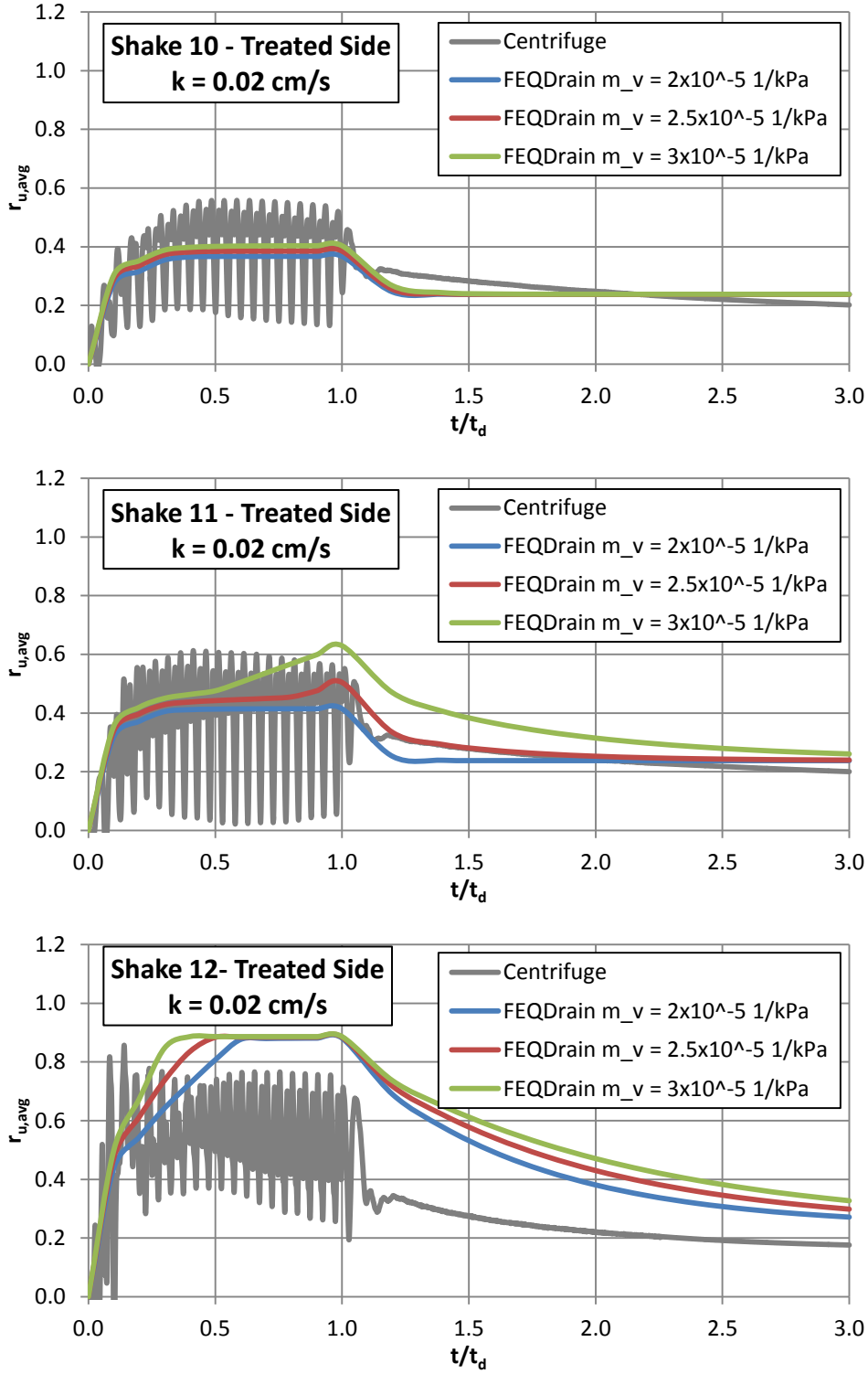

Figure 4.13: Comparison of experimental and numerical treated $r_{u,avg}$-time histories of (a) Shake 10, (b) Shake 11, (c) Shake 12 for $k = 0.02\ cm/s$ and different values of m_v

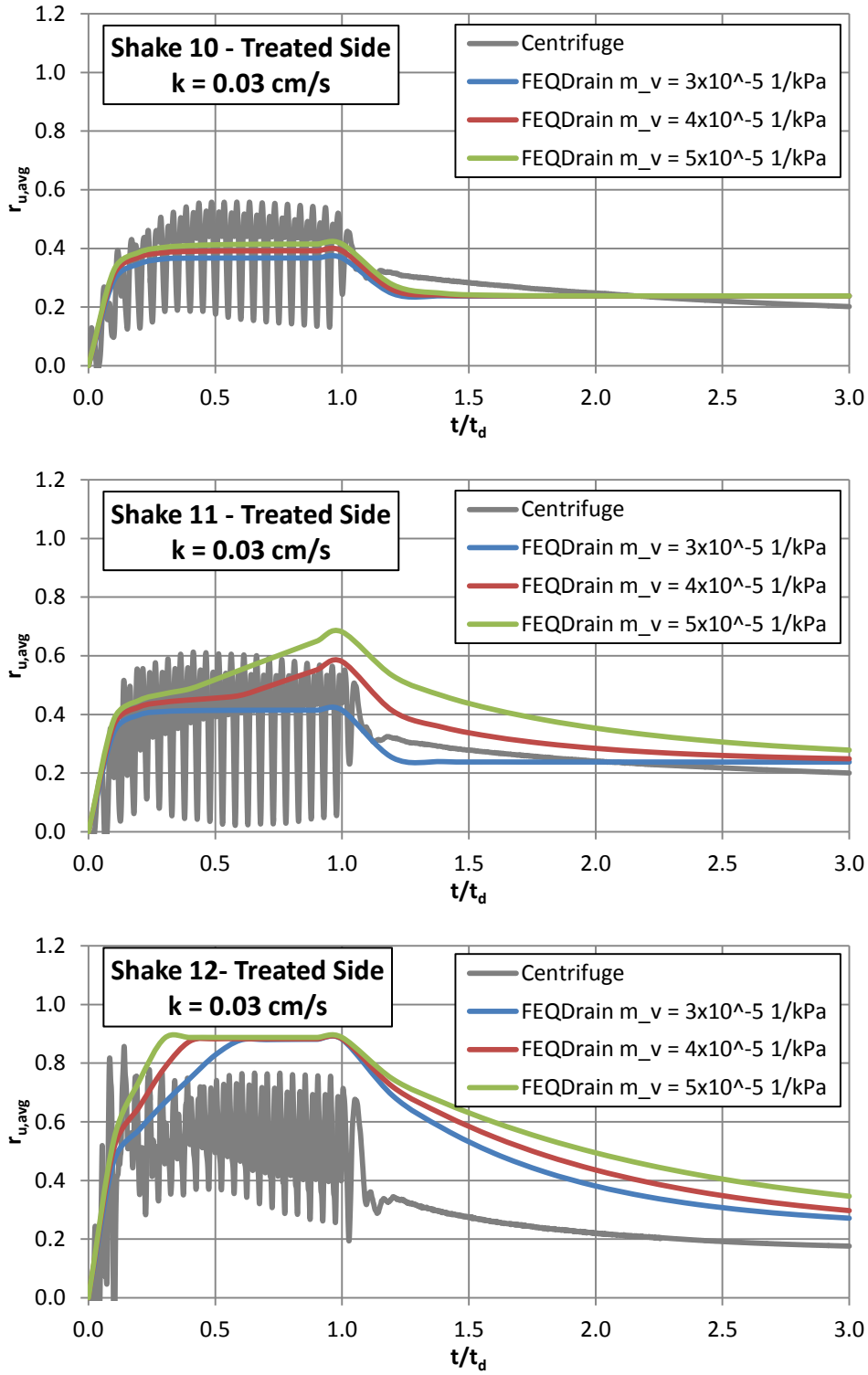

Figure 4.14: Comparison of experimental and numerical treated $r_{u,avg}$-time histories of (a) Shake 10, (b) Shake 11, (c) Shake 12 for $k = 0.03\ cm/s$ and different values of m_v

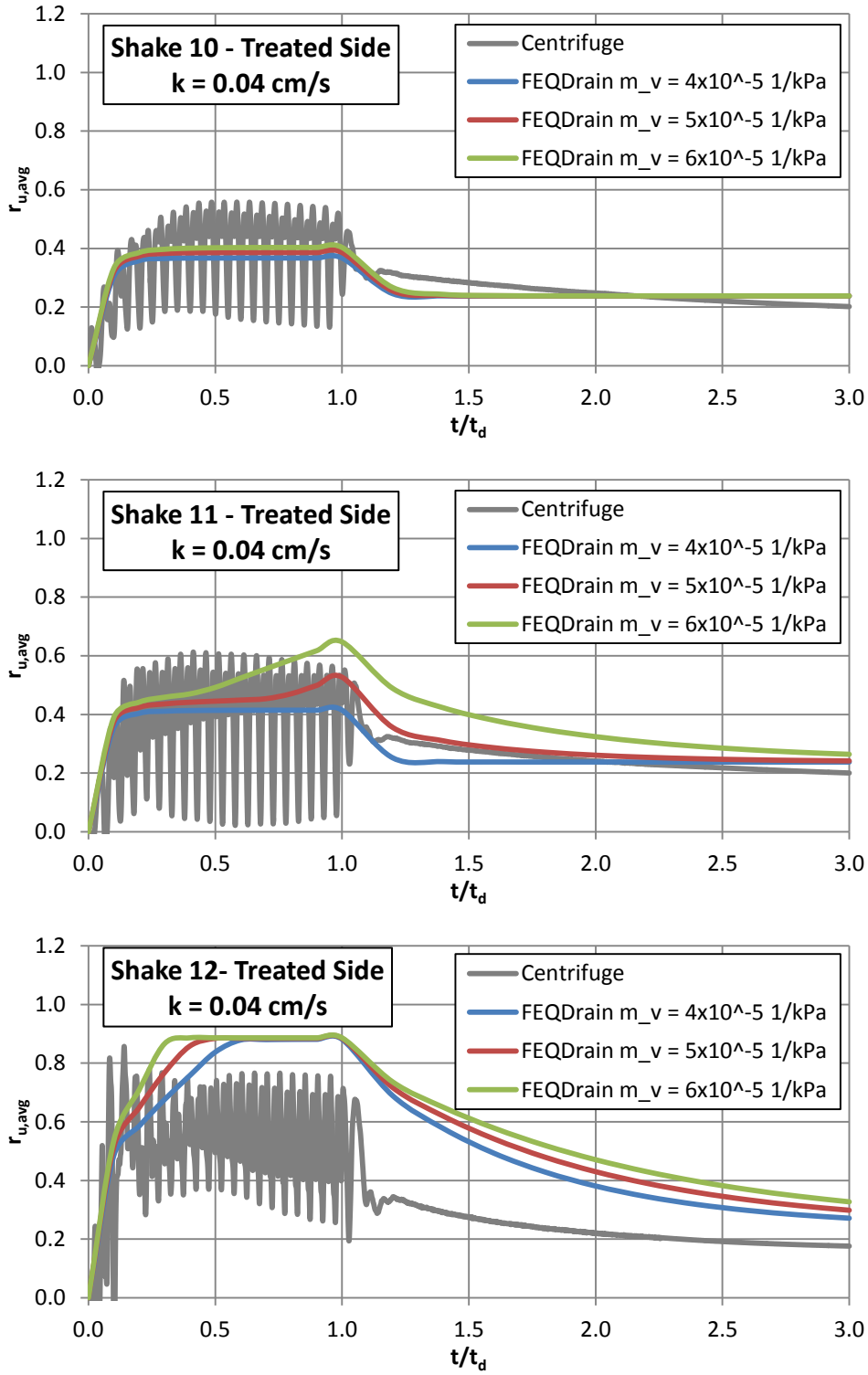

Figure 4.15: Comparison of experimental and numerical treated $r_{u,avg}$-time histories of (a) Shake 10, (b) Shake 11, (c) Shake 12 for $k = 0.04\ cm/s$ and different values of m_v

When $k = 0.02\ cm/s$ is considered (Figure 4.13), the m_v values that were selected for the sensitivity analysis are: $m_v = 2x10^{-5}\ 1/kPa$, $m_v = 2.5x10^{-5}\ 1/kPa$ and $m_v = 3x10^{-5}\ 1/kPa$. The last two values provide the best fit with the results of Shakes 11 and 12 respectively. These values of m_v represent values slightly smaller than the baseline value. On the other hand, the m_v values that are combined with the baseline k value ($k = 0.03\ cm/s$) are: $m_v = 3x10^{-5}\ 1/kPa$, $m_v = 4x10^{-5}\ 1/kPa$ (baseline) and $m_v = 5x10^{-5}\ 1/kPa$ (Figure 4.14). As it was previously mentioned, the FEQDrain analyses of the baseline model match with the recorded values for Shakes 11 and 12. Finally, in the case that $k = 0.04\ cm/s$, the sensitivity analysis is conducted considering in each case: $m_v = 4x10^{-5}\ 1/kPa$ (baseline), $m_v = 5x10^{-5}\ 1/kPa$ and $m_v = 6x10^{-5}\ 1/kPa$ (Figure 4.15). To fit the recorded curves of Shake 11, the larger m_v must be adopted in this case.

The comparison of the $r_{u,avg}$ time – histories leads to the same conclusions for the three sets of sensitivity analysis. In particular, the centrifuge results for Shake 10 are adequately fit by all of the FEQDrain analyses, as the excess pore pressure response is practically unaffected by any change in k or m_v value. On the other hand, the results for Shake 11 are influenced by m_v, in which the maximum $r_{u,avg}$ can increase by as much as 50% when m_v increases by 50% and k decreases by 50%. Consequently, it is shown that differences in either the k or m_v values of the centrifuge model, which are somewhat difficult to estimate precisely, influence the predicted pore pressure responses for Shake 11. For Shake 12, the $r_{u,avg}$ time – histories peak at the same maximum value for any combination of k or m_v. This value is the same as in the baseline case, which, as it was previously mentioned, fits adequately the experimental results. Any change in either k or m_v, changes only the time that the maximum value is reached.

The results shown here are consistent with those shown in Chapter 3. The sensitivity of the computed pore pressure response to the input soil properties (i.e., k and m_v) is most significant when the predicted pore pressures are in the range of $r_{u,avg}$ equal to 0.5 to 0.8. When the predicted $r_{u,avg}$ is less than about 0.5 or greater than 0.8 the results are less sensitive to the specified k and m_v. This observation supports the use of a smaller pore pressure threshold for drain design, somewhere close to $r_{u,avg}$ equal to 0.4.

4.4 Summary

In this chapter, the experimental evaluation of prefabricated vertical drains was compared to the numerical predictions of FEQDrain. The centrifuge model described by Marinucci et al. (2008) consists of an untreated and a drain – treated side and is subjected to sinusoidal ground motions. The most significant conclusion is that the numerical $r_{u,avg}$ time – histories are generally in good agreement with the recorded values. On the treated side, the FEQDrain model managed, in most of the cases, to predict the same maximum $r_{u,avg}$, which is the parameter that is used in drain design. The inability of FEQDrain to incorporate sloped soil profiles affects mainly the results on the untreated side and specifically it over – predicts $r_{u,avg}$ close to liquefaction. The additional drainage that occurred through the main channel of the centrifuge model explains the inconsistency that is observed in the rate of dissipation of excess pore pressures.

Finally, a sensitivity analysis was conducted in FEQDrain for the most uncertain soil properties that affect the excess pore pressure response, namely the hydraulic conductivity and the coefficient of volumetric compressibility of the sand. The numerical analyses indicate that the $r_{u,avg}$ time – histories of Shake 11 are most

sensitive to small changes in the combination of k and m_v. For Shake 10, in which the predicted $r_{u,avg}$ is lower than 0.5, the results are practically unaffected by any change in either k or m_v of the liquefiable layer. For this reason, it is recommended to use drain design value of $r_{u,avg}$ smaller than 0.4, in order to cover any uncertainty on the soil properties.

Chapter 5

Theoretical and Measured Excess Pore Pressures Under Earthquake Loading

5.1 Introduction

The methods that predict the pore pressure response of a liquefiable soil deposit treated with vertical drains, both analytical and numerical, assume that the liquefiable soil deposit is subjected to harmonic motions with a constant frequency. The benefit from this assumption is that it is relatively easy to determine the equivalent number of uniform stress cycles of shaking "N_{EQ}" and the number of cycles required to cause liquefaction "N_L", which are input parameters in these methods. However, earthquake motions do not consist of either uniform amplitude cycles or constant frequency cycles of motion. Therefore, the predictions of pore pressure response from these methods may not be accurate for earthquake motions.

Howell (2008) performed a centrifuge test to study the performance of prefabricated vertical drains in mitigating liquefaction from soil deposits subjected to real earthquake motions. The purpose of this chapter is to simulate this test in FEQDrain and to compare the results with the numerical predictions of FEQDrain.

5.2 Centrifuge Model

Howell (2008) performed a small –scale centrifuge test (RLH01) that was similar to SSK01 (Marinucci et al., 2008). The test was conducted at the NEES Equipment Site at the University of California at Davis, and with a centrifugal

acceleration of 15g. However, there are two major differences between the two tests: the use of real earthquake motions as input motions and a change in model geometry. In particular, the sloping ground stands at an inclination of 10^{o} and is oriented across the shorter dimension of the contained and perpendicular to the direction of shaking (Figure 5.1 and 5.2). The soil layers were similar to the previous test (Table 4.1): (1) a 0.75 m thick (prototype) bottom layer of dense Nevada sand, (2) a 5.55 m thick liquefiable layer of loose Nevada sand and (3) 1.5 m thick layer of compacted Yolo Loam on top.

As shown in Figure 5.2, the model is separated into three different zones in the longitudinal direction: one drain –treated and two untreated. The first zone is treated with 40, 6.4 – mm diameter perforated, flexible tubes covered with a woven geotextile. At a centrifuge acceleration of 15 g, these tubes correspond to PVDs with an inner diameter of 95 mm. and they were installed in a triangular pattern at a center – to – center distance of 1.5 m (prototype scale). The second zone is untreated with no PVDs. To examine the effect of the tube stiffness on the soil stiffness, non – draining tubes are installed in the third zone. The centrifuge model contained 32 accelerometers, 21 displacement transducers and 48 pore pressure transducers (PPT). There are two vertical arrays of PPTs in each soil zone: a primary array with 8 PPTs and a secondary array with 4 PPTs (Figure 5.1).

The centrifuge model was subjected longitudinally, namely orthogonally to the slope, to 9 shaking events. Two earthquake acceleration-time histories were used as the principal input motions: PAC175 – a short duration motion from the 1994 Northridge earthquake and PSL180 – a long duration motion from the San Fernando earthquake (Figure 5.3). The input motion of the first 8 shaking events consists of scaled PAC175 and PSL180 input motions, ranging in PGA from 0.11 to

0.95 g. For the last shaking event, a sine wave with 20 cycles of motion at a frequency of 2 Hz and a PGA of 0.6 g was used.

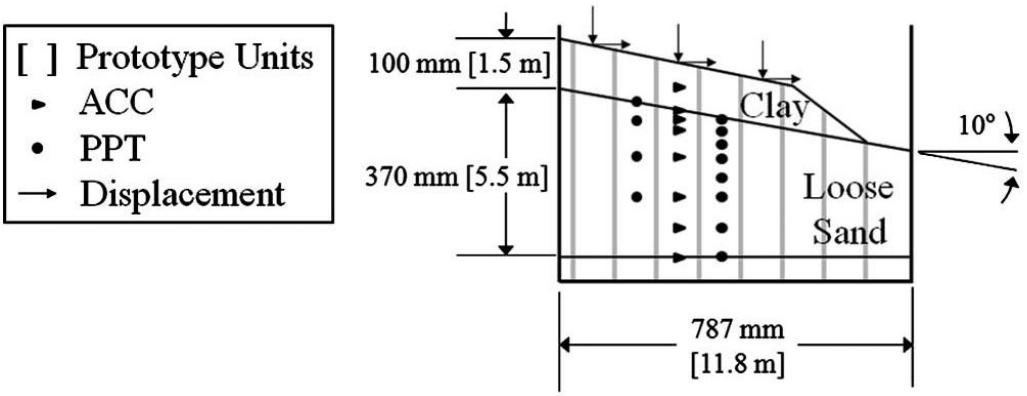

Figure 5.1: Cross-sectional view of the model geometry (Howell et al., 2012)

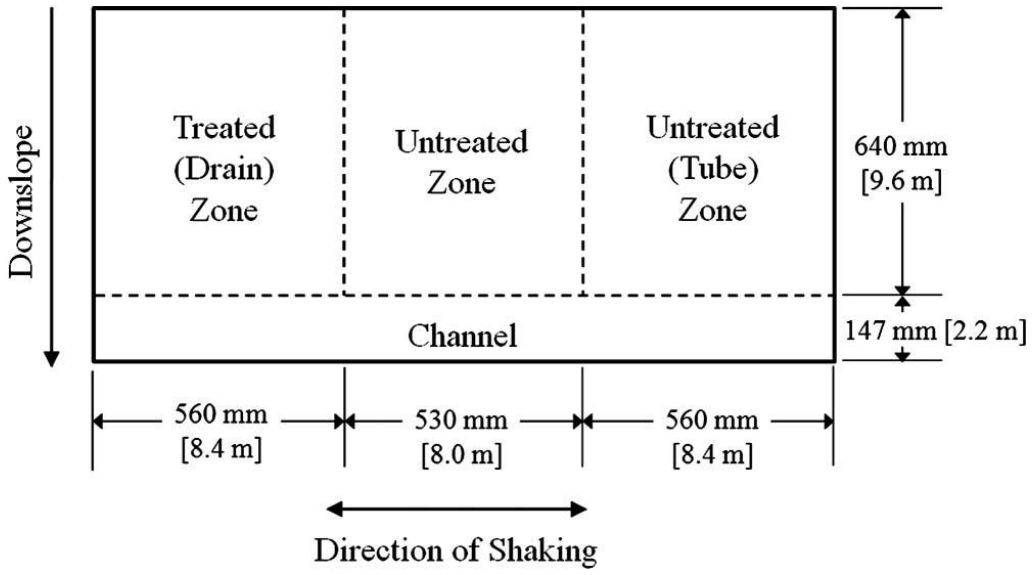

Figure 5.2: Plan view of the model geometry (Howell et al., 2012)

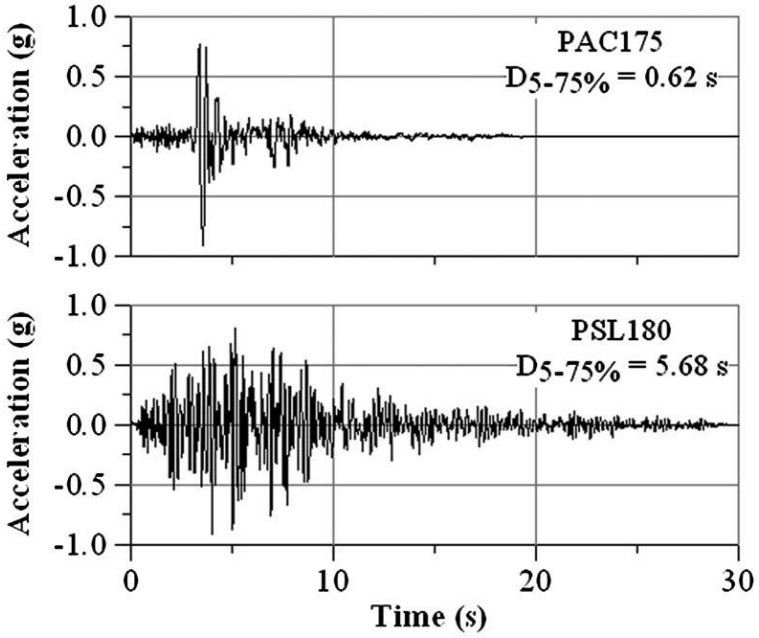

Figure 5.3: (a) PAC175 and (b) PSL180 input motions (Howell et al., 2012)

The maximum r_u values within the treated and the untreated zones along with the peak ground acceleration of the five highest intensity shaking events (PAC03, PSL03, PAC04, PSL04 and SIN01) are presented in Table 5.1. The induced pore pressures were much smaller for the less intense events, and therefore they are not discussed. The maximum r_u values in the treated zone similar to those measured in the untreated zone, or even higher in some cases. However, the comparison between the r_u – time histories at various depths for the 5 shaking events (Figures 5.4 – 5.8) indicates that excess pore pressures dissipate faster in the treated zone. In the PSL events (Figure 5.5, 5.7), the drains are more efficient in dissipating excess pore pressures, due to longer duration of motion, which allows more time for drainage during shaking. The short duration PAC events do not allow for drainage. Additionally, the sine event produces larger r_u than the more intense earthquake motions (PAC04 or PSL04) despite the significantly lower PGA value (0.60 g versus 0.90 – 0.95 g), due to the repetitive cycles of the same intensity.

Finally, similar pore pressure responses were observed in the two untreated zones, indicating that the stiffness of the soil deposit is unaffected by the tubes.

As mentioned in Chapter 4, the maximum r_u is affected by the static shear stress that is developed in the soil due to the inclination of the ground surface. In this case, the effect is expected to be bigger because the inclination is increased to 10^o compared to 3^o of SSK01. Howell (2008) performed an infinite slope analysis and estimated that the maximum r_u is limited to about 0.72 for the 10^o slope angle. This value agrees with the maximum r_u on the untreated side during PAC03 and PSL03. However, as the model was subjected to more intense shaking events, the slope flattened, the static shear stress decreased and the threshold on maximumr_u was increased, explaining the larger recorded values of r_u for PAC04, PSL04 and SIN01.

Table 5.1: Recorded base PGA and maximum r_u at the vertical arrays (prototype scale)

Event Name	**PGA_{base} (g)**	**maximum r_u**	
		Untreated	**Treated**
PAC03	0.38	0.57	0.57
PSL03	0.46	0.71	0.58
PAC04	0.95	0.91	1.07
PSL04	0.90	0.93	0.84
SIN01	0.50	0.98	1.07

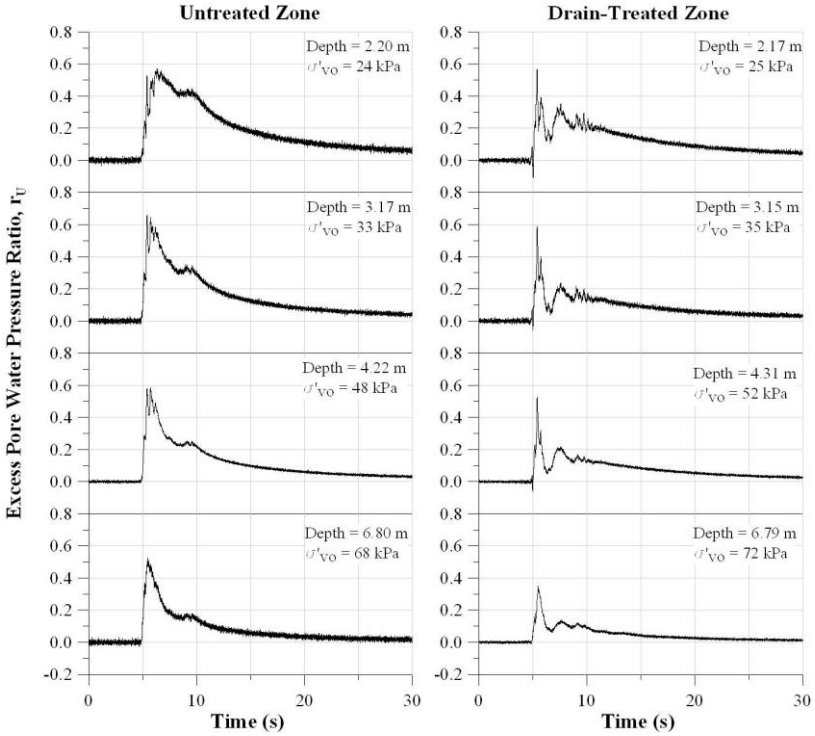

Figure 5.4: PAC03 (PGA = 0.38 g): Untreated and treated zone r_u - time histories (Howell, 2008)

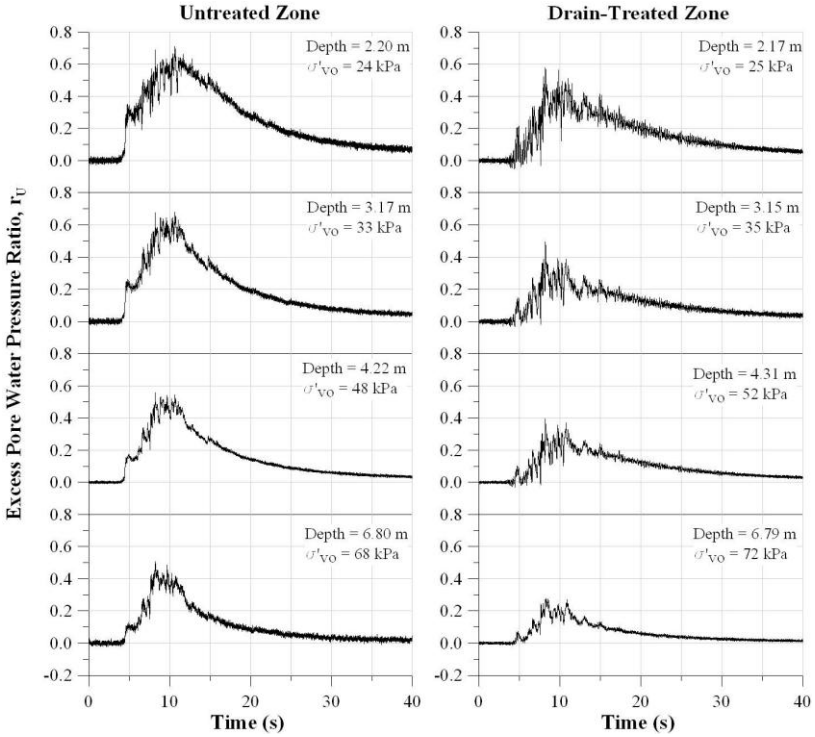

Figure 5.5: PSL03 (PGA = 0.46 g): Untreated and treated zone r_u - time histories (Howell, 2008)

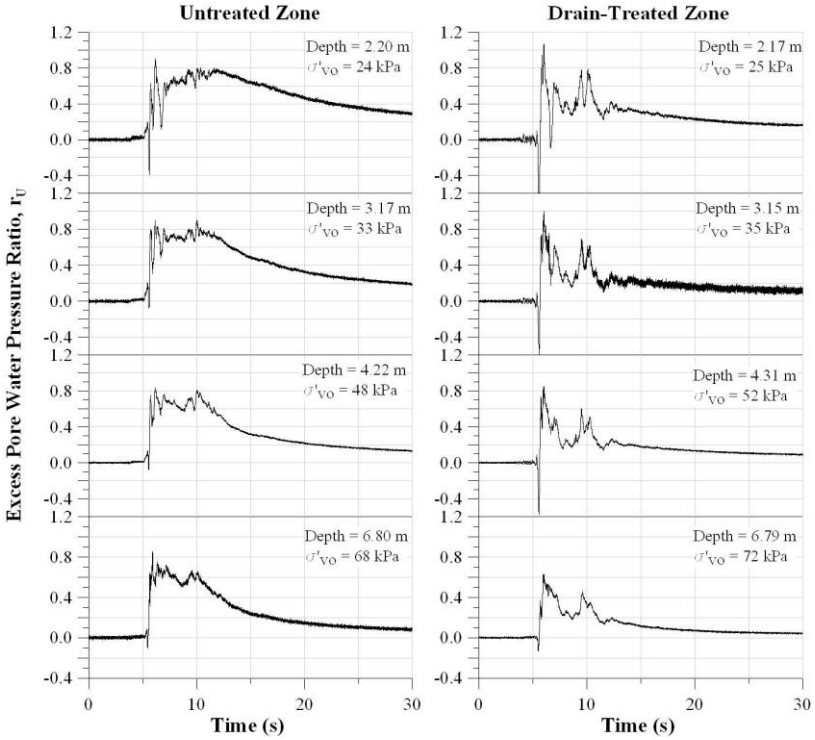

Figure 5.6: PAC04 (PGA = 0.95 g): Untreated and treated zone r_u - time histories (Howell, 2008)

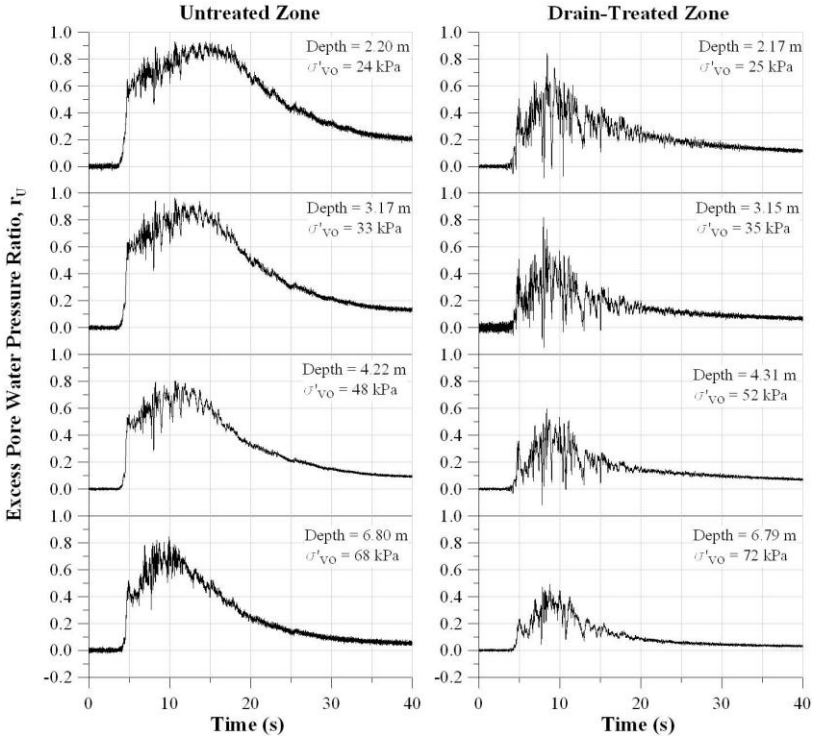

Figure 5.7: PSL04 (PGA = 0.90 g): Untreated and treated zone r_u - time histories (Howell, 2008)

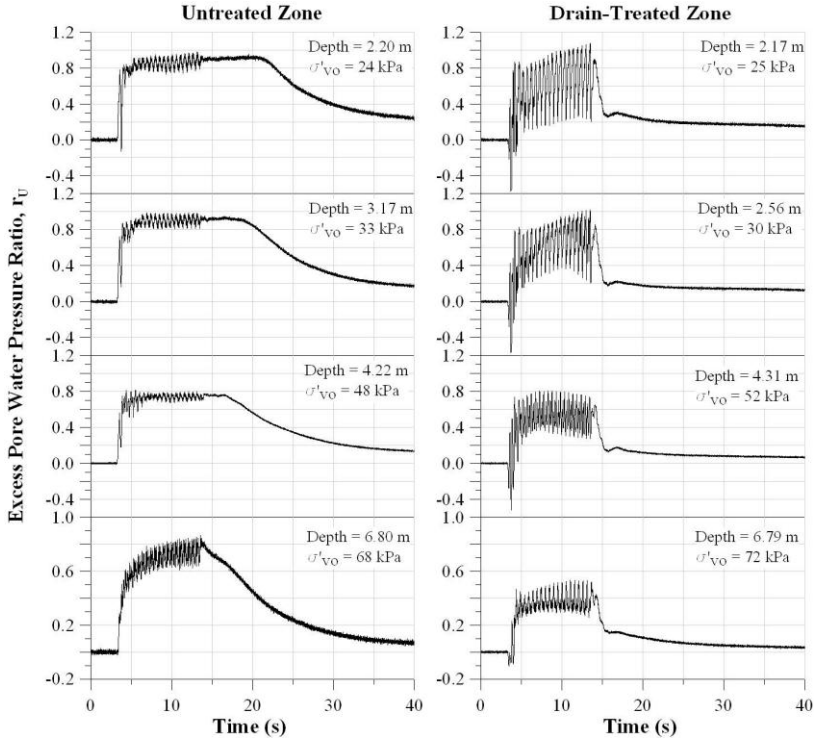

Figure 5.8: SIN01 (PGA = 0.60 g): Untreated and treated zone r_u - time histories (Howell, 2008)

5.3 Comparison with Numerical Predictions

The geometry of the FEQDrain model that was used for the comparison with SSK01 (Section 4.3) is adjusted for RLH01 to model the layer dimensions of the primary vertical array and the smaller inner diameter of drains (95 mm versus 100 mm). In this case, the sand layer is 4.67 m thick, overlain by 1.37 m thick clay crust, while the water table is 0.33 m below the ground surface (Figure 5.9). The basic soil properties, namely the hydraulic conductivity, the coefficient of volumetric compressibility and the relative density, remain the same as in SSK01 (Table 4.1). The comparison between the numerical predictions and the experimental results will be based on the developed $r_{u,avg}$ in the vertical array during PAC03, PSL03, PAC04, PSL04 and SIN01 (Figure 5.10). The values of $r_{u,avg}$ have been weighted to account for the sensor spacing, as explained in Chapter 4 (Howell et al. 2012).

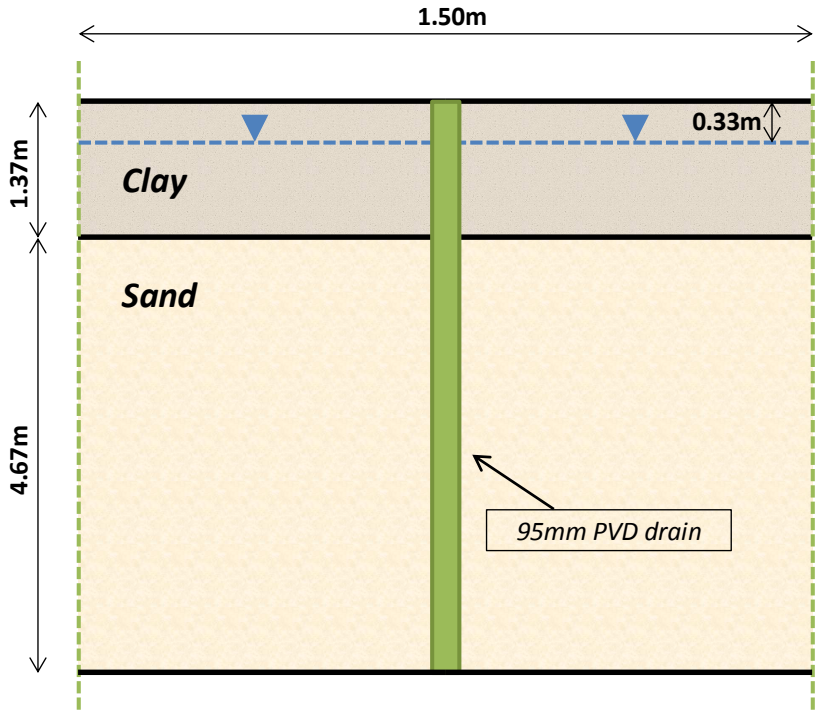

Figure 5.9: Cross-sectional view of the FEQDrain model

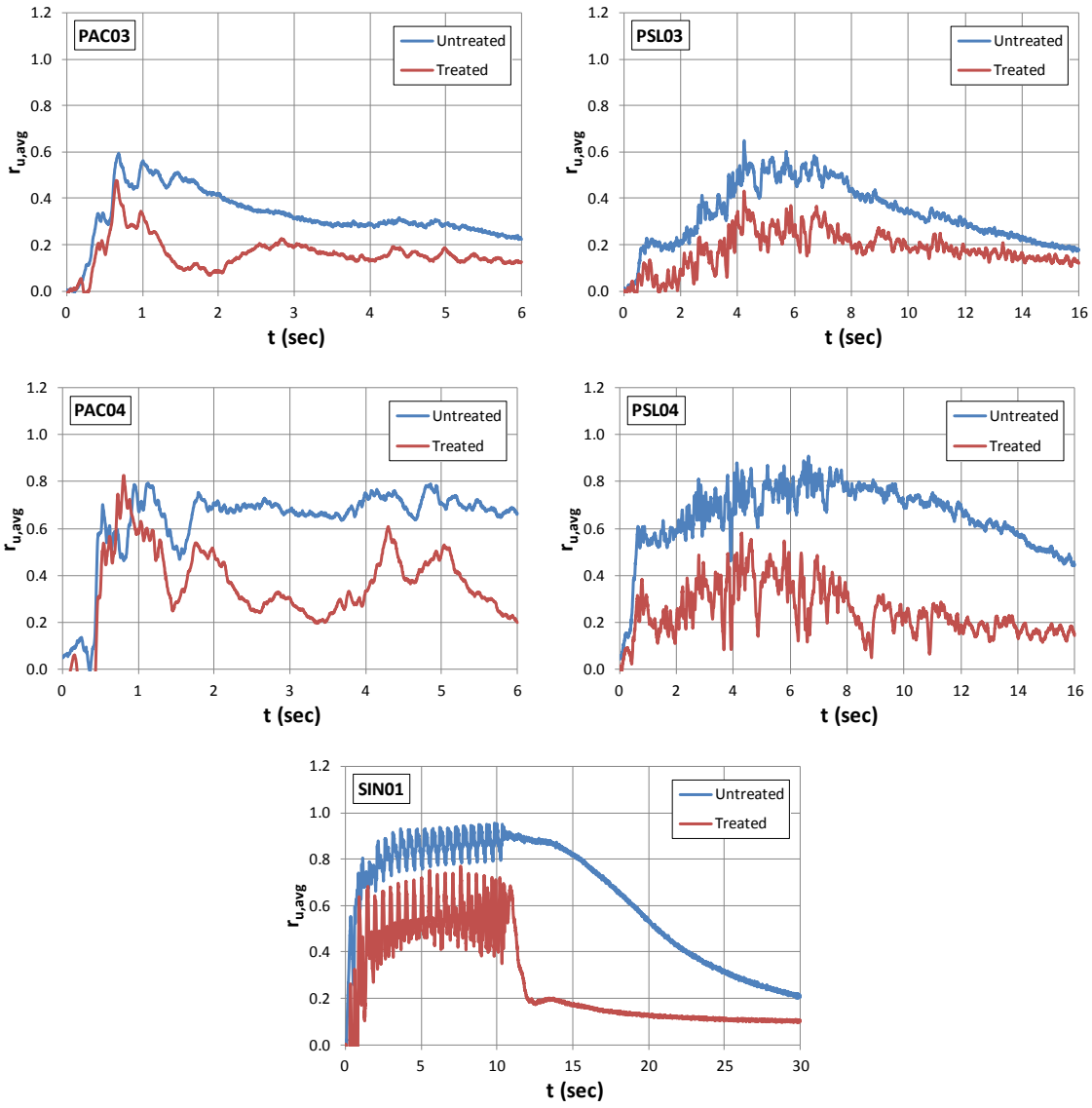

Figure 5.10: Average excess pore pressure ratio ($r_{u,avg}$) - time histories in the vertical arrays of the untreated and treated zones for (a) PAC03, (b) PSL03, (c) PAC04, (d)PSL04, (e) SIN01

To perform the FEQDrain analyses, three parameters need to be determined for each shaking event: the duration of shaking "t_d", the equivalent number of cycles "N_{EQ}" and the required number of cycles to cause liquefaction "N_L". For the earthquake motions, these parameters cannot be directly determined from the acceleration – time histories because they are not harmonic motions, but they can

be estimated using methods that convert earthquake motions into equivalent numbers of uniform cycles. For the sine event (SIN01), the first two parameters are easily determined (t_d = 10 sec and N_{EQ} = 20) as the model was subjected to 20 harmonic cycles at a frequency of 2 Hz. To estimate the value of N_L the same graphical procedure used in Section 4.3 is followed (Figure 5.11) and leads to N_L = 4.5 (N_{EQ}/N_L = 4.4). In addition, Figure 5.12 illustrates that the value A = 2.0 provides the best fitting of the experimental $r_{u,avg}$ versus N/N_L curve on the untreated side for the sine event.

For the earthquake shaking events, the duration of shaking is assumed to be equal to the time interval between the 5% and the 75% of the Arias intensity (D_{5-75}), which leads to t_d = 0.62 sec for the PAC events and t_d = 5.68 sec for the PSL events. The values of N_{EQ} and N_L were estimated by Howell et al. (2012) following the cycle conversion procedure of Seed et al. (1975). This procedure computes an equivalent number of uniform cycles for an earthquake motion given a selected fraction of the peak amplitude. Using this procedure N_{EQ} was computed as the equivalent number of cycles at 65% of the peak ground acceleration of the input motion. N_L was computed using the $r_{u,avg}$ response in the untreated zone. In this case, the time of initial liquefaction was identified and the equivalent number of uniform cycles of motion applied up to that time was taken as N_L. The value of exponent "A" cannot be estimated in the same way as in the SIN01 due to the difficulty in plotting $r_{u,avg}$ versus N/N_L. This value will be estimated and evaluated through the sensitivity analysis in FEQDrain. The estimated parameters for the five shaking events are summarized in Table 5.2.

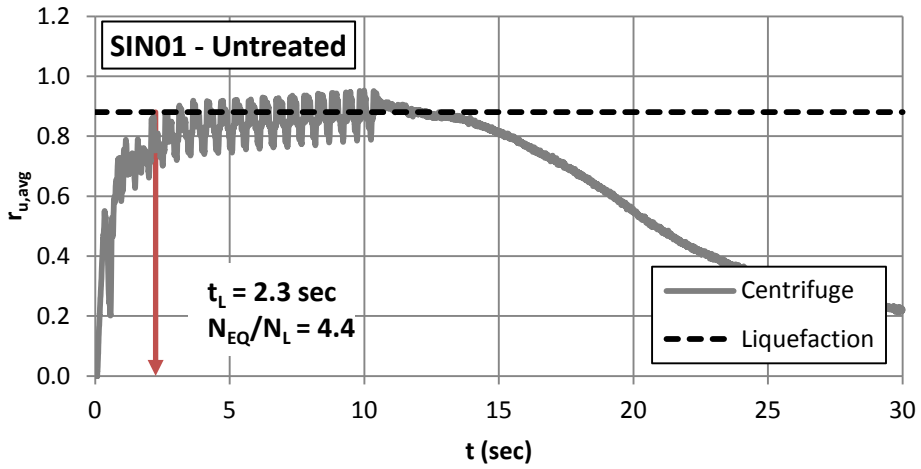

Figure 5.11: Determination of liquefaction time for SIN01 from the untreated $r_{u,avg}$-time histories

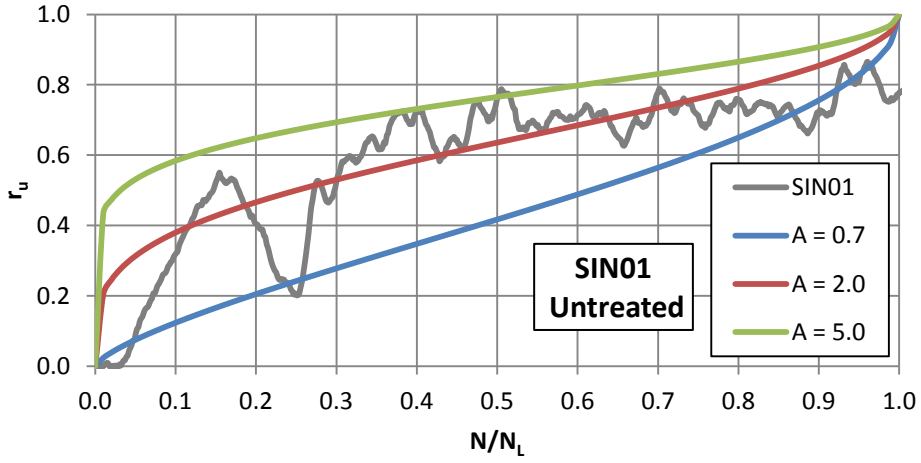

Figure 5.12: Determination of exponent A for SIN01 from the untreated $r_{u,avg}$ versus N/N_L

Table 5.2: Shaking duration and N_{EQ}/N_L ratio for the shaking events

Event	t_d (sec)	N_{EQ}	N_L	N_{EQ}/N_L
PAC03	0.62	2.3	2.3	1
PSL03	5.68	11	11	1
PAC04	0.62	4.3	4.1	1
PSL04	5.68	15.4	7.6	2
SIN01	10	20	4.5	4.4

Considering the estimated soil properties and ground motion characteristics (t_d and N_{EQ}/N_L), the FEQDrain analyses are performed for the untreated and drain – treated conditions for the shaking events PAC03, PSL03, PAC04, PSL04 and SIN01. Figure 5.13 illustrates the comparison between the numerical predictions of $r_{u,avg}$ – time histories and the experimental results on the untreated and the treated zones for the four earthquake shaking events. Having no additional information about the exponent "A" in the sand layer, the FEQDrain analyses are repeated for two different "A" values: A = 0.7 and A = 2.0, which represent the typical value (A=0.7) and the value that has been considered in the previous analyses for the same type of sand (A=2.0).

The numerical results on the untreated zone overestimate the peak value of $r_{u,avg}$ in all shaking events due to the presence of static shear stresses, which cannot be taken into account in FEQDrain. For the lower intensity events (PAC03 and PSL03), smaller values of the maximum $r_{u,avg}$ are predicted, compared to the high intensity ones (PAC04 and PSL04), which is consistent with the recorded values. The FEQDrain curves for A = 0.7 and A = 2.0 predict the same peak $r_{u,avg}$ value and overlap after the end of shaking. During shaking, it is observed that the use of A = 0.7 is more representative for the build – up in the pore pressure ratio for all shaking events. Similar to the results for SSK01, the excess pore pressures dissipate significantly slower in the numerical model due to the additional drainage that occurs through the channel and possible cracks in the clay cap.

In the treated zone, the numerical curves for A = 0.7 and A = 2.0 show differences in both the rate of build – up of excess pore pressures and also in the magnitude of the maximum $r_{u,avg}$. The A = 0.7 curve predicts noticeably smaller values of maximum $r_{u,avg}$ in all cases. For A = 0.7, the shape of the $r_{u,avg}$ – time

histories is more realistic and representative to the experimental curves and, for this reason, the value A = 0.7 is selected as the input exponent "A" for the earthquake events, despite the fact that in most of the events the maximum $r_{u,avg}$ values are closer to the recorded ones when A = 2.0. For A = 0.7, the maximum $r_{u,avg}$ predicted by FEQDrain is in good agreement with the experimental value only for PAC03, in which the peak numerical $r_{u,avg}$ value is slightly higher. In the other three events, FEQDrain underestimates the pore pressure response and the maximum values are 30 – 60 % lower than the experimental values. This inconsistency is mainly caused by the N_{EQ}/N_L values, which were estimated using the empirical procedure of Seed et al. (1975). Knowing that N_{EQ}/N_L is an indicator of the intensity of shaking and hence r_u increases with increasing N_{EQ}/N_L, the ratio needs to be increased for the results of PSL03, PAC04 and PSL04.

As for the sine event (SIN01), the $r_{u,avg}$ response of the centrifuge model is compared to the FEQDrain results in Figure 5.14 considering both untreated and treated conditions. In the untreated zone, the numerical curve has the same rate of excess pore pressure build – up as the experimental one, but the peak value is higher ($r_{u,avg}$ = 1) and the rate of dissipation of excess pore pressure to the drain is significantly smaller. In the treated zone, the FEQDrain curve is forming a plateau at $r_{u,avg}$ = 0.40 after 2 sec and until the end of shaking. This value is smaller than the recorded maximum of $r_{u,avg}$ = 0.75, but it is close to the mean value of the dilation spikes, which is almost constant at $r_{u,avg}$ = 0.50 for the same time interval, as the FEQDrain curve.

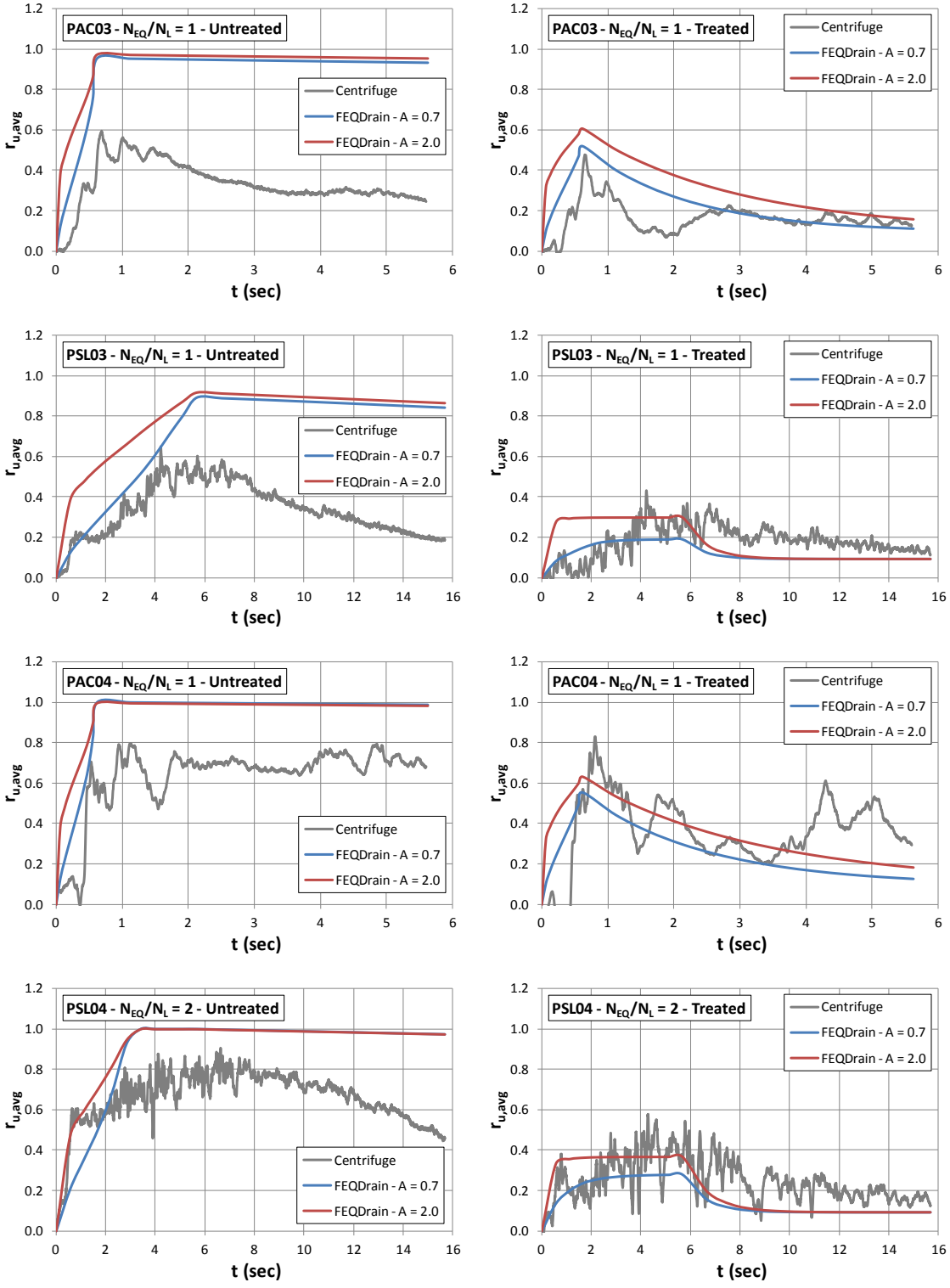

Figure 5.13: Comparison of experimental and numerical untreated and treated $r_{u,avg}$ – time histories of (a) PAC03, (b) PSL03, (c) PAC04, and (d) PSL04 for different A values

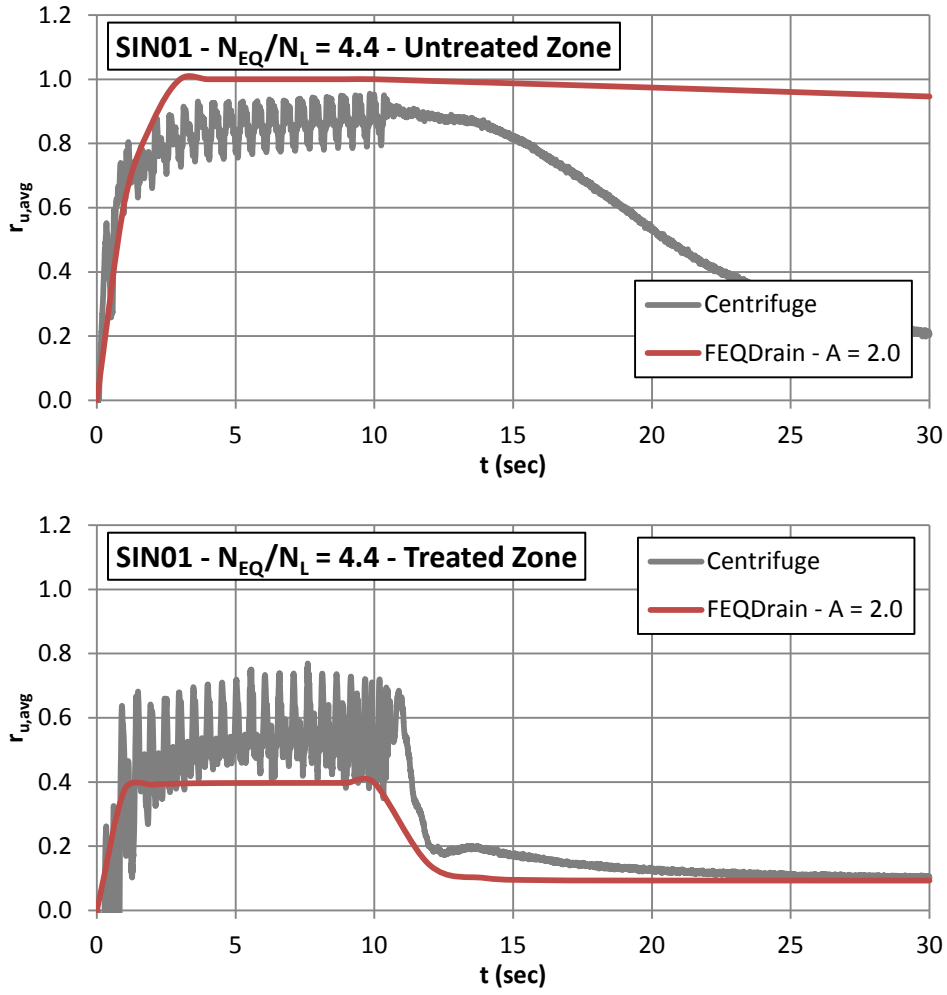

Figure 5.14: Experimental and numerical (a) untreated and (b) treated $r_{u,avg}$-time histories of SIN01

The comparison between the experimental and numerical results for the earthquake shaking events (Figure 5.13) indicates that the estimated values of N_{EQ}/N_L using the Seed et al. (1975) procedure may be inaccurate. For this reason, the appropriate N_{EQ}/N_L values that lead to the most satisfactory fitting of the centrifuge results are estimated by using a trial and error procedure. In particular, N_{EQ} is kept constant and N_L is altered until the maximum value and the shape of the FEQDrain $r_{u,avg}$ curve matches best with the recorded data. To obtain more insight about the effect of N_{EQ}/N_L and to estimate a range of N_{EQ}/N_L ratios for each shaking

event, comparisons are also made relative to the r_u – time histories measured at two different locations within the vertical array, one close to the top of the sand layer (depth = 2.2 m) and one at the bottom (depth = 5.8 m). Figures 5.15 through 5.17 illustrate the comparisons between the experimental results and the FEQDrain curves with the selected N_{EQ}/N_L ratios for PSL03, PAC04 and PSL04. It must be noted that PAC03 is excluded from this procedure, as the results match with the experimental data. The new N_{EQ}/N_L ratios are compared in Table 5.3 with the initial values that were estimated according to the procedure of Seed et al. (1975).

For PSL03 (Figure 5.15), the N_{EQ}/N_L ratio must be increased from N_{EQ}/N_L = 1 to N_{EQ}/N_L = 2.6, namely approximately 2.5 times, in order to fit the experimental results. It is observed that the response at the top of the layer is very sensitive to small changes in the ratio, as the peak of the N_{EQ}/N_L = 2.6 curve is more than 2 times bigger than the peak when N_{EQ}/N_L = 2 and about 4 times bugger when $N_{EQ}/N_L = 1$. On the contrary, the results at the bottom are essentially insensitive to the same changes in N_{EQ}/N_L. For PAC04 (Figure 5.16), the ratios for which the FEQDrain results are in good agreement with the experimental ones are: N_{EQ}/N_L = 1.3 for the average response and N_{EQ}/N_L = 2.0 for the top of layer. It is observed that $r_{u,avg}$ increases significantly when N_{EQ}/N_L just increases from 1 to 1.3. Finally, for PSL04 (Figure 5.17), the average experimental response is captured by FEQDrain when the ratio increases from N_{EQ}/N_L = 2.0 to N_{EQ}/N_L = 2.8. Unlike the previous event, where the ratio at the top was greater than at the bottom, in this case the results at the top fit when N_{EQ}/N_L = 2.8 and at the bottom when N_{EQ}/N_L = 3.2.

Three main observations can be made from the sensitivity analysis on the N_{EQ}/N_L ratio. The empirical procedure of Seed et al. (1975) seems to underestimate N_{EQ}/N_L values, which leads to the prediction of smaller excess pore pressures. In

particular, the N_{EQ}/N_L ratio from FEQDrain was 30% – 40% bigger for the high intensity events (PAC04 and PSL04), and it was increased 2.5 times in order to fit the results of PSL03. Additionally, the comparisons indicated that, with the exception of PSL04, the response on the upper part of the liquefiable layer fits with experimental results for higher values of N_{EQ}/N_L than on the lower part. For this reason, the use of the average response is suggested, as it compromises any differences with depth. Finally, the excess pore pressure response is very sensitive to small changes in N_{EQ}/N_L when $r_{u,avg}$ ranges from 0.5 to 0.8, but practically insensitive for smaller $r_{u,avg}$ values. Similarly to the observations of the previous chapters, a consideration of a design threshold of $r_{u,avg}$ lower than 0.4 covers any uncertainty on the ground motion characteristics.

Table 5.3: N_{EQ}/N_L ratios estimated by FEQDrain and Seed et al. (1975)

Shaking Event	**N_{EQ}/N_L**	
	Seed et al.	***FEQDrain***
PSL03	1	2.6
PAC04	1	1.3
PSL04	2	2.8

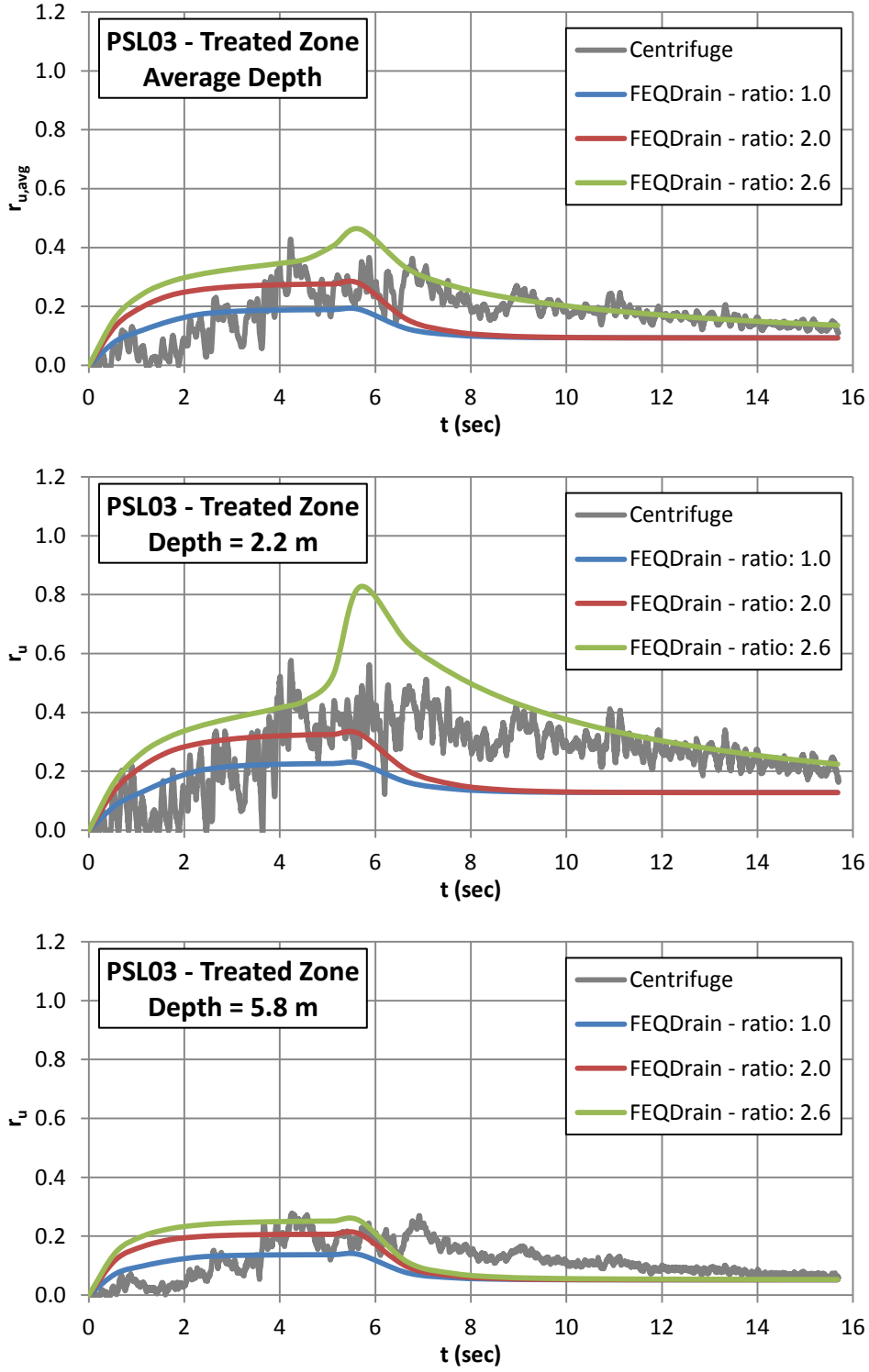

Figure 5.15: Comparison of experimental and numerical treated (a) $r_{u,avg}$ – time histories and (b) r_u – time histories at different depths of PSL03 for different N_{EQ}/N_L ratios

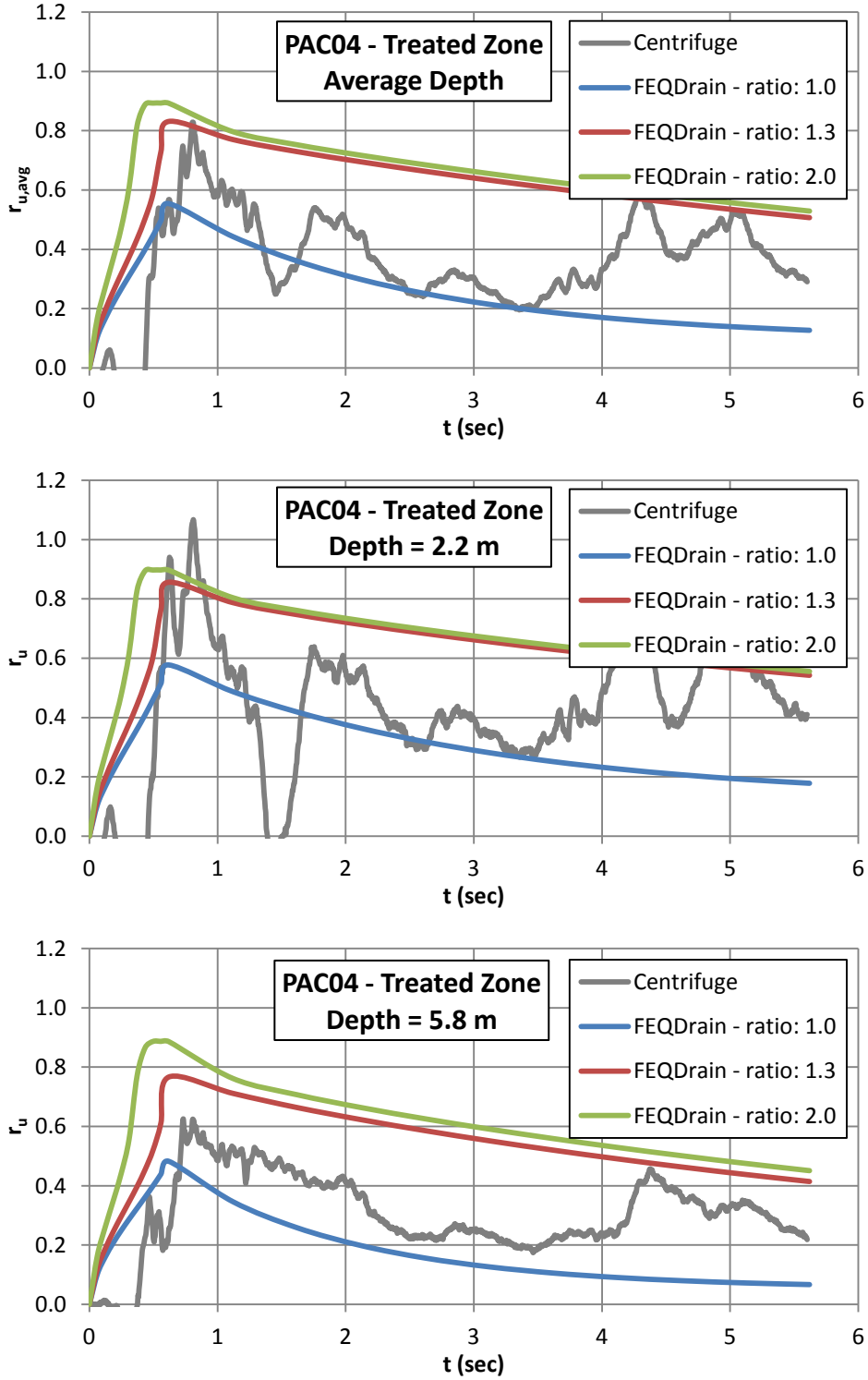

Figure 5.16: Comparison of experimental and numerical treated (a) $r_{u,avg}$ – time histories and (b) r_u – time histories at different depths of PAC04 for different N_{EQ}/N_L ratios

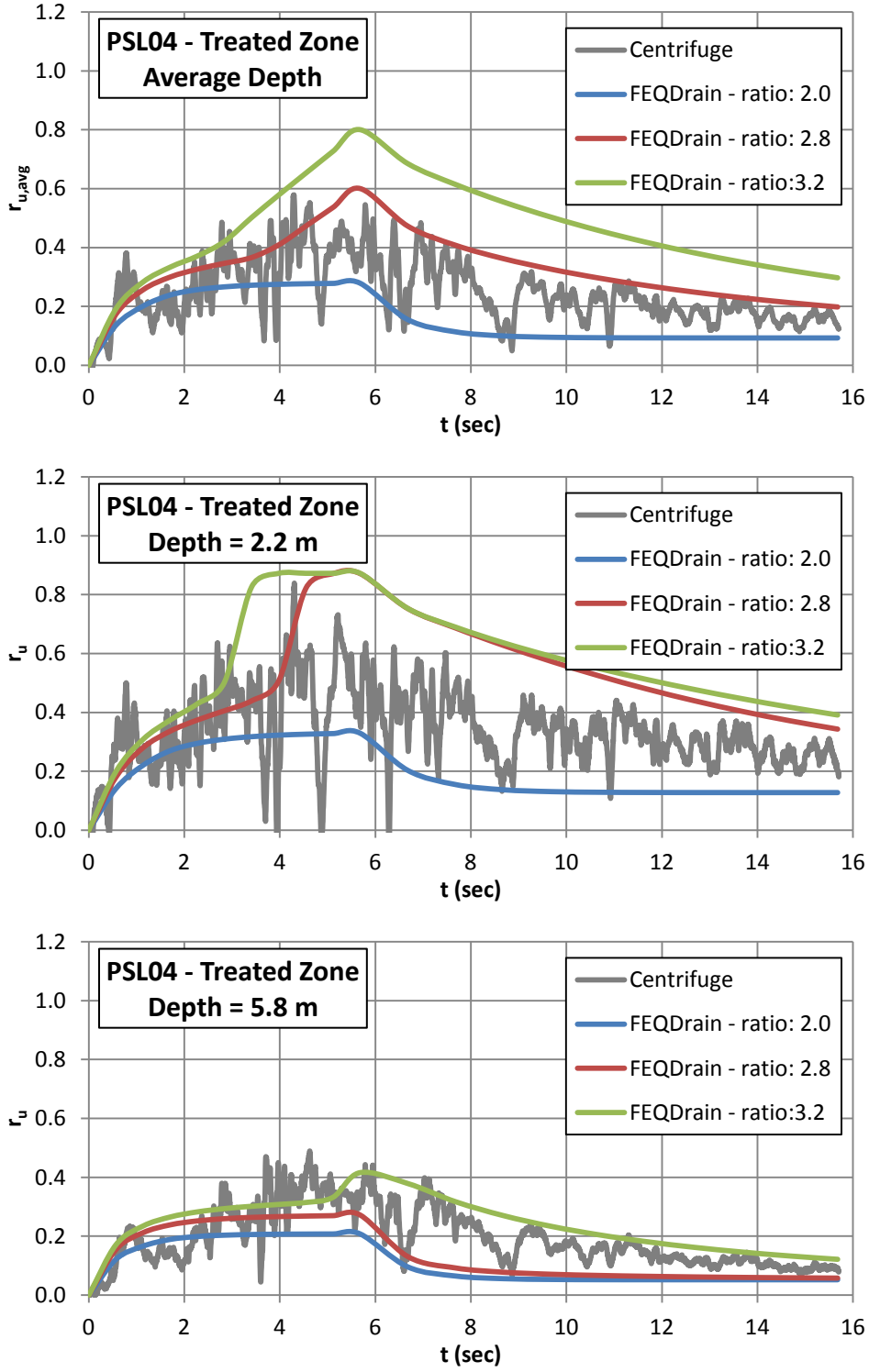

Figure 5.17: Comparison of experimental and numerical treated (a) $r_{u,avg}$ – time histories and (b) r_u – time histories at different depths of PSL04 for different N_{EQ}/N_L ratios

5.4 Summary

In this chapter, the experimental results of the centrifuge test conducted by Howell (2008) were compared to the numerical predictions of FEQDrain. The centrifuge model was subjected to four earthquake shaking events and one sinusoidal ground motion. For the earthquake events, the equivalent number of uniform stress cycles of shaking "N_{EQ}" and the number of cycles required to cause liquefaction "N_L" has been estimated from Howell et al. (2012) using the empirical procedure of Seed et al. (1975). The comparison with the experimental $r_{u,avg}$ time – histories indicated that FEQDrain underestimates the excess pore pressure response for the given N_{EQ}/N_L ratios. The values of N_{EQ}/N_L were estimated again from a sensitivity analysis in the $r_{u,avg}$ response and in the r_u response at the top and the bottom of the liquefiable sand layer. The sensitivity analysis revealed that N_{EQ}/N_L ratio that fits the results is 30 – 40% bigger for the higher intensity events, compared to the initial estimation.

Finally, it was observed that the sine event (SIN01) produces larger excess pore pressure than the more intense earthquake motions (PAC04 or PSL04), despite the significantly lower PGA value (0.60 g versus 0.90 – 0.95 g). This fact is attributed to the differences in the shape of the input motions (more cycles in the sine event) and emphasizes the role of the input motion characteristics in the performance of vertical drains to mitigate liquefaction.

Chapter 6

Conclusions

6.1 Summary and Conclusions

Prefabricated vertical drains (PVD) represent a soil improvement technique that achieves liquefaction mitigation by decreasing the drainage path length and hence expediting the dissipation of excess pore pressures. Pestana et al. (1997) developed a finite element program "FEQDrain" to predict the pore pressure response in drain – treated ground. The effectiveness of prefabricated vertical drains for liquefaction mitigation has been recently evaluated via small – scale centrifuge testing performed on untreated soil deposits and on soil deposits treated with vertical drains. In particular, the performance of soil deposits subjected to sinusoidal motions and actual earthquake recordings was tested by Marinucci et al. (2008) and Howell (2008), respectively.

The main goal of this research is to compare the experimental observations of pore pressure response from the centrifuge experiments of Marinucci et al. (2008) and Howell (2008) with the numerical predictions of FEQDrain. The comparison focuses on the average excess pore pressure ratio ($r_{u,avg}$) that was developed in the location of the vertical array both on the untreated and drain – treated sides of the models. In parallel, a parametric study is performed in FEQDrain in order to study the effect of each input parameter that influences the pore pressure prediction, namely the effect of soil properties (i.e. hydraulic conductivity "k" and coefficient of

compressibility "m_v"), ground motion characteristics (i.e., duration of shaking and number of cycles of motion) and drain parameters.

The effect of hydraulic conductivity on the pore pressure response is directly related to the coefficient of compressibility of the soil (and vice versa) and consequently these parameters should always been examined together. The main soil parameter that drives the response is the coefficient of consolidation "c_v", which takes into account both k and m_v, as soils with c_v of the same order of magnitude exhibit similar development of excess pore pressure.

The depth of groundwater table plays a significant role in soil response as additional pore pressures are induced due to the head build up in the drain. The magnitude of the extra pore pressures is proportional to the head difference inside the drain (typically the water level is on the ground surface) and outside the drain (depth of ground water table) This detail is not taken into account in the design charts (Seed & Booker, 1977, and JGS, 1998), which are commonly used in practice, leading to the prediction of lower maximum pore pressures and hence to an unconservative drain design.

The comparison between the results of the centrifuge test conducted by Marinucci et al. (2008) and the predictions of FEQDrain indicated that the numerical $r_{u,avg}$ time – histories are generally in good agreement with the recorded values. On the treated side, the FEQDrain model managed, in most of the cases, to predict the same maximum $r_{u,avg}$, which is the parameter that is used in drain design. Inconsistency was only observed in the rate of dissipation of excess pore pressures and in the maximum $r_{u,avg}$ of the untreated side. The first observation is attributed to the additional drainage through the main channel and through any cracks in the clay cap of the centrifuge model caused by the laterally spreading ground.

FEQDrain can only model soil profiles with leveled ground surface and hence it cannot take into account the existence of static shear stresses in sloping grounds, the presence of which limits the maximum possible decrease in effective stress and consequently the maximum r_u. The inability of FEQDrain to incorporate sloped soil profiles affects mainly the results on the untreated side and specifically it over – predicts $r_{u,avg}$ close to liquefaction.

The numerical predictions for the earthquake events in the centrifuge test conducted by Howell (2008) depend on the value of the N_{EQ}/N_L ratio, namely the equivalent number of uniform stress cycles of shaking "N_{EQ}" over the number of cycles required to cause liquefaction "N_L", that is used in the analysis. When these values are estimated using the empirical procedure of Seed et al. (1975), FEQDrain underestimates the excess pore pressure response. To fit the results, the N_{EQ}/N_L ratio must be increased 30 – 40% for the higher intensity events, compared to Seed et al. (1975).

For the same centrifuge test, the harmonic shaking event produces larger excess pore pressure than the more intense earthquake motions despite the significantly lower PGA value (0.60 g versus 0.90 – 0.95 g). This fact is attributed to the differences in the shape of the input motions (more cycles in the sine event) and emphasizes the role of the input motion characteristics in the performance of vertical drains to mitigate liquefaction.

FEQDrain provides a more adequate fitting with the centrifuge results when the $r_{u,avg}$ time – histories are compared, rather than the pore pressure response at specified depths. For this reason, the use of the average response in design is suggested, as it compromises any differences with depth.

The sensitivity analyses of the computed pore pressure response to either the input soil properties (i.e., k and m_v) or the ground motion characteristics (i.e., N_{EQ}/N_L) is more significant when the predicted pore pressures are in the range of $r_{u,avg}$ equal to 0.5 to 0.8. When the predicted $r_{u,avg}$ is less than about 0.5 or greater than 0.8 the results are less sensitive to the specified parameter. This observation supports the use of a smaller pore pressure threshold for drain design.

In conclusion, FEQDrain is found to be a reliable program to predict the pore pressure response and to design prefabricated vertical drains for liquefaction mitigation despite the simplicity of the constitutive model that it uses and the limitations in analysis. From a practical standpoint, the consideration of drain design value of $r_{u,avg}$ smaller than 0.4 is recommended in order to incorporate any uncertainty on the soil properties or on the characteristics of shaking.

Bibliography

Bouckovalas, G., Papadimitriou, A., Niarchos, D., Tsiapas Y. (2011). "Sand Fabric Evolution Effects on Drain Design for Liquefaction Mitigation" *Journal of Soil Dynamics and Earthquake Engineering*, Vol. 31, No. 10, pp. 1426-1439

De Alba, P., Chan, C.K. and Seed, H.B. (1975). "Determination of Soil Liquefaction Characteristics by Large-Scale Laboratory Tests" *Report No. EERC 75-14*, Earthquake Engineering Research Center, University of California, Berkeley

Howell, R. (2008). "Effectiveness of Prefabricated Vertical Drains for Liquefaction Remediation" Master Thesis, University of Texas at Austin

Howell, R., Kamai, R., Conlee, C., Rathje, E.M., Boulanger, R.W., Marinucci, A. and Rix, G. (2009). "Evaluation of the Effectiveness of Prefabricated Vertical Drains for Liquefaction Remediation – Centrifuge Data Report for RLH01" Center for Geotechnical Modeling Data Report UCD/CGMDR. University of California, Davis

Howell, R., Rathje, E., Kamai, R. and Boulanger, R. (2012). "Centrifuge Modeling of Prefabricated Vertical Drains for Liquefaction Remediation" ASCE, *Journal of Geotechnical and Geoenvironmental Engineering*, Vol. 138,No. 3, pp. 262-271

Japanese Geotechnical Society, (1998). Remedial Measures against Soil Liquefaction: From Investigation to Implementation. A.A. Balkema, Rotterdam, Netherlands

Kamai, R., Kano, S., Conlee, C. Marinucci, A., Rathje, E., Boulanger, R. and Rix, G. (2007). "Evaluation of the Effectiveness of Prefabricated Vertical Drains for Liquefaction Remediation – Centrifuge Data Report for SSK01," Center for Geotechnical Modeling Data Report UCD/CGMDR. University of California, Davis

Kramer, L.S. (1996). Geotechnical Earthquake Engineering, Prentice-Hall, New Jersey, 653p.

Kulasingam, R. (2003). "Effects of Void Redistribution on Liquefaction-Induced Deformations" Ph.D. dissertation, University of California, Davis

Lee, K.L. and Albaisa, A. (1974). "Earthquake induced settlements in saturated sands" ASCE, *Journal of the Geotechnical Engineering Division*, Vol. 100 (GT 4): 387-406

Marinucci, A. (2010). "Effectiveness of prefabricated vertical drains on pore water pressure generation and dissipation in liquefiable sand" Ph.D. dissertation, University of Texas at Austin

Marinucci, A., Rathje, E., Kano, S., Kamai, R., Conlee, C., Howell, R., Boulanger, R., and Gallagher, P. (2008). "Centrifuge Testing of Prefabricated Vertical Drains for Liquefaction Remediation" In Geotechnical Earthquake Engineering and Soil Dynamics IV, ASCE Geotechnical Special Publication No. 181. D. Zeng, M. Manzari, and D. Hiltunen, editors

Onoue, A., Mori, N. and Takano, J. (1987). "In Situ Experiment and Analysis on Well Resistance of Gravel Drains" Japanese Society of Soil Mechanics and Foundation Engineering, *Soils and Foundations*, Vol. 27, No. 2, pp. 42-60

Onoue, A. (1988). "Diagrams Considering Well Resistance for Designing Spacing Ratio of Gravel Drains" Japanese Society of Soil Mechanics and Foundation Engineering, *Soils and Foundations*, Vol. 28, No. 3, pp. 160-168

Pestana, J.M., Hunt, C.E. and Goughnour, R.R. (1997). "FEQDrain: A Finite Element Computer Program for the Analysis of the Earthquake Generation and Dissipation of Pore Water Pressure in Layered Sand Deposits with Vertical Drains" *Report No. EERC 97-17*, Earthquake Engineering Research Center, University of California at Berkeley, CA

Seed, H.B. and Booker, J.R. (1977). "Stabilization of Potentially Liquefiable Sand Deposits Using Gravel Drains" ASCE, *Journal of the Geotechnical Engineering Division*, Vol. 103, No. GT7, p 757-768

Seed, H.B., Martin, K. and Lysmer, J. (1975). "The Generation and Dissipation of Pore Water Pressures during Soil Liquefaction" *Report No. EERC 75-26*, Earthquake Engineering Research Center, University of California, Berkeley

Seed, H.B., Mori, P.P. and Chan, C.K. (1975). "Influence of Seismic History on the Liquefaction Characteristics of Sands" *Report No. EERC 75-25*, Earthquake Engineering Research Center, University of California, Berkeley

Seed, H.B., Idriss, I.M., Makdisi, F. and Banerjee, N. (1975). "Representation of Irregular Stress Time Histories by Equivalent Uniform Stress Series in Liquefaction Analyses" *Report No. EERC 75-29*, Earthquake Engineering Research Center, University of California, Berkeley

Vita

Ioannis Tsiapas was born in Athens, Greece on July 7th, 1986, the son of Zikos Tsiapas and Georgia Kostara. After completing his studies at Third Lyceum of Ilioupolis, Athens, Greece, in 2004 he entered National Technical University of Athens (NTUA). He received the degree of Diploma in Civil Engineering in November 2009. In August 2010, he entered the Graduate Program of the Cockrell College of Engineering at The University of Texas at Austin.

e-mail: tsiapas@utexas.edu

This thesis was typed by the author.